NAVAL POSTGRADUATE SCHOOL
MONTEREY, CALIFORNIA

THESIS

FORCE FEEDBACK FOR ANTHROPOMORPHIC TELEOPERATED MECHANISMS

by

James A. Chatfield, II

June 1995

Thesis Advisor: **Morris Driels**

Approved for public release; distribution is unlimited.

REPORT DOCUMENTATION PAGE

Form Approved OMB No. 0704-0188

1. AGENCY USE ONLY *(Leave blank)*	2. REPORT DATE June 1995	3. REPORT TYPE AND DATES COVERED Master's Thesis

4. TITLE AND SUBTITLE FORCE FEEDBACK FOR ANTHROPOMORPHIC TELEOPERATED MECHANISMS

FUNDING NUMBERS

6. AUTHOR(S) Chatfield, James A. II

7. PERFORMING ORGANIZATION NAME(S) AND ADDRESS(ES)
Naval Postgraduate School
Monterey CA 93943-5000

8. PERFORMING ORGANIZATION REPORT NUMBER

9. SPONSORING/MONITORING AGENCY NAME(S) AND ADDRESS(ES)

10. SPONSORING/MONITORING AGENCY REPORT NUMBER

11. SUPPLEMENTARY NOTES The views expressed in this thesis are those of the author and do not reflect the official policy or position of the Department of Defense or the U.S. Government.

12a. DISTRIBUTION/AVAILABILITY STATEMENT
Approved for public release; distribution is unlimited.

12b. DISTRIBUTION CODE

13. ABSTRACT *(maximum 200 words)*

The use of anthropomorphic teleoperated mechanisms has gained considerable attention as a means of performing tasks that require human-like control, but due to the nature of the environment, would be optimally accomplished without direct human contact in the particular workspace. These tasks include mine clearance, space operations, hazardous waste cleanup, and even surgery. In order to continue research into this method of remote, manual supervisory control, an anthropomorphic robot was monitored and tested with the results formulated into an operating manual intended to standardize system control. Further experimentation was conducted to examine various methods of implementing bilateral force feedback on the robot using a durable and cost effective system.

14. SUBJECT TERMS Force Feedback, Anthropomorphic, Teleoperatation, Robotics, Solenoid, Servomotor, Remote Supervisory Control

15. NUMBER OF PAGES 146

16. PRICE CODE

17. SECURITY CLASSIFICATION OF REPORT	18. SECURITY CLASSIFICATION OF THIS PAGE	19. SECURITY CLASSIFICATION OF ABSTRACT	20. LIMITATION OF ABSTRACT
Unclassified	Unclassified	Unclassified	UL

NSN 7540-01-280-5500

Standard Form 298 (Rev. 2-89)
Prescribed by ANSI Std. 239-18 298-102

Approved for public release; distribution is unlimited.

FORCE FEEDBACK FOR ANTHROPOMORPHIC TELEOPERATED MECHANISMS

James A. Chatfield, II
Lieutenant, United States Navy
B.S., United States Naval Academy, 1989

Submitted in partial fulfillment
of the requirements for the degree of

MASTER OF SCIENCE IN MECHANICAL ENGINEERING
from the
NAVAL POSTGRADUATE SCHOOL
June 1995

Author: 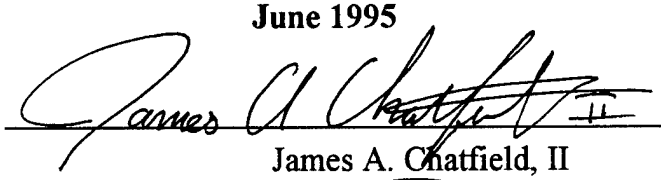
James A. Chatfield, II

Approved by: 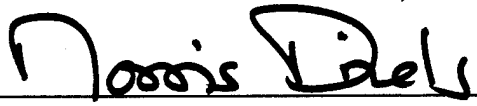
Morris Driels, Thesis Advisor

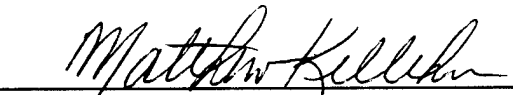
Matthew D. Kelleher, Chairman
Department of Mechanical Engineering

ABSTRACT

The use of anthropomorphic teleoperated mechanisms has gained considerable attention as a means of performing tasks that require human-like control, but due to the nature of the environment, would be optimally accomplished without direct human contact in the particular workspace. These tasks include mine clearance, space operations, hazardous waste cleanup, and even surgery. In order to continue research into this method of remote, manual supervisory control, an anthromorphic robot was monitored and tested with the results formulated into an operating manual intended to standardize system control. Further experimentation was conducted to examine various methods of implementing bilateral force feedback on the robot using a durable and cost effective system.

TABLE OF CONTENTS

LIST OF FIGURES

List of Tables

ACKNOWLEDGMENT

I would like to thank the Naval Ocean Systems Command for their excellent work in building the Green Man anthropomorphic robot, and their assistance in bringing the system to the Naval Postgraduate School (NPS). In my analysis, it was obvious that the system's creators put a great deal of time and energy into this project, and it is a tribute to their work that Green Man is still functioning today.

I would also like to thank Professor Morris Driels for his guidance, assistance, and support during the entire thesis process. Professor Driels is an outstanding example of how to conduct business of learning in a professional, down to earth manner.

Additionally, I would never have reached this point at NPS without the friendship and academic assistance from LT Brian Eckerle and LT Robert Jones. Their patience in continually pounding the fundamentals of mechanical engineering into my head led to many fun times and long study sessions.

To my mother and father, thank you for the constant support, words of wisdom, and faith in my ability. My accomplishments would be much fewer without you both.

Finally, to my bride to be Denisia, your positive and loving support kept me going through many rough days. I will always appreciate your understanding and assistance in helping me achieve this educational goal.

I. INTRODUCTION

A. PURPOSE

The purpose of this thesis centers around an anthropomorphic teleoperated robot that was donated to the Naval Postgraduate School (NPS) in the spring of 1994. This particular robot, formally labeled by it's creators as Green Man, came to NPS with very little supporting documentation. Due to the lack of technical documentation and operational instruction, the process of testing, tracing, and monitoring the system was done in order to fully understand Green Man's capabilities and operating parameters. This information, which has been documented in the form of an "operating manual" for Green Man, encompasses the first part of this thesis. Upon gaining a firm understanding of Green Man's abilities, research moved toward adapting Green Man with a cost effective, light weight bilateral force feedback system from the slave back to the master human operator. After sufficient investigation, the idea of using a band brake system triggered by a pulse width modulated signal was decided upon as the optimal configuration. Testing was then conducted to evaluate and compare two possible band brake activation subsystems in order to make a recommendation for implementation to the joints of the master unit. This research and experimentation process comprise the second part of the thesis.

B. GREEN MAN

1. Background

"Green Man" was designed as an anthropomorphic teleoperated robot for the Army by the Naval Ocean Systems Command (NOSC) in Kaneoe, Hawaii. In building Green Man, NOSC began to investigate the use of robots in such areas as mine clearance, hazardous waste cleanup, and underwater drilling. In 1992, following the closure of NOSC, Green Man was placed in a crate and shipped to San Diego for storage. After learning of the termination of the Green Man program, Professor Morris Driels began the process of obtaining Green Man as an addition to the NPS robotics laboratory in order to continue further research in the field of human supervisory control. Specifically, study would focus on the completion of tasks that required human-like control, but due to the nature of the work environment, could optimally be completed without direct human interface. These tasks encompass numerous technologically advanced arenas, from space to surgery. Thus in fall of 1993, the first examination of the Green Man anthropomorphic robot was conducted in the Mechanical Engineering department at the Naval Postgraduate School. An actual picture of the Green Man slave assembly is included as Figure 1, with an overall schematic that will be the basis of the slave description added as Figure 2.

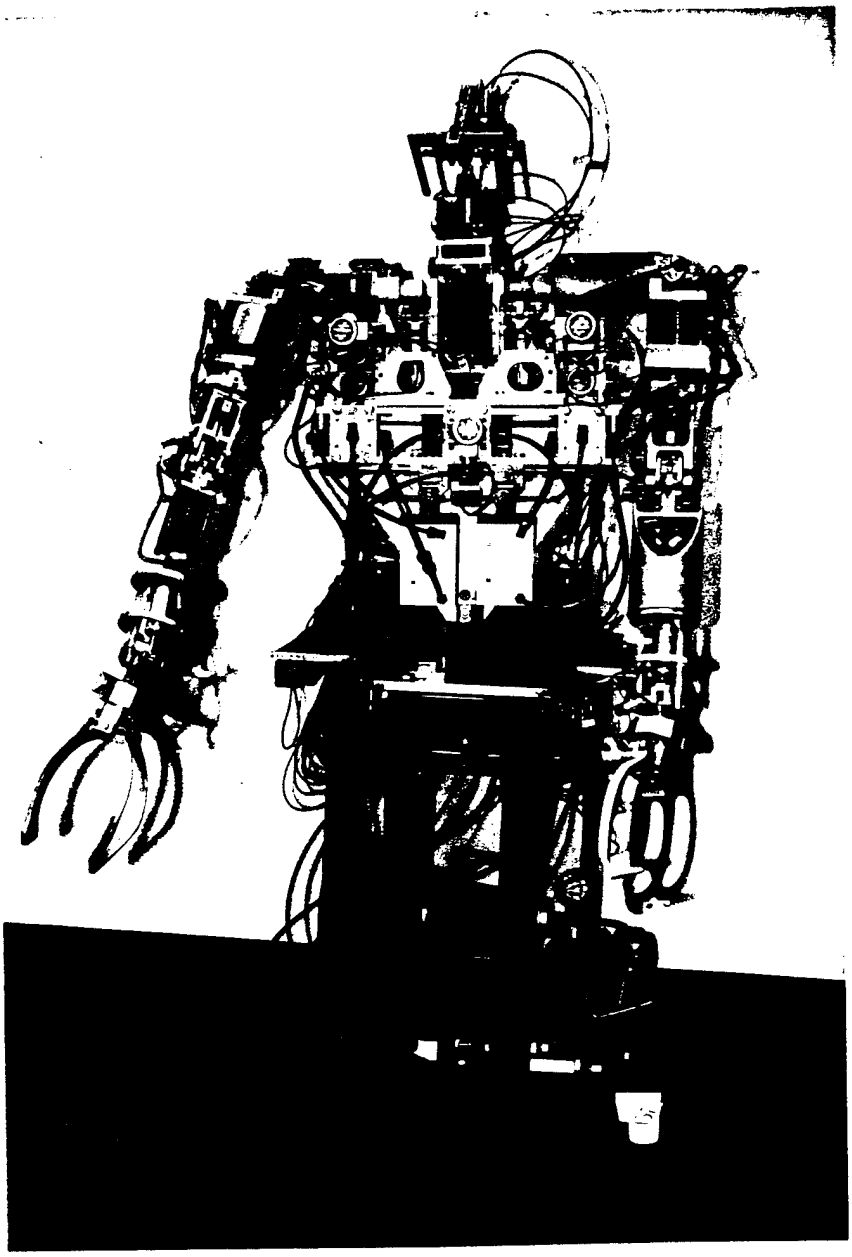

Figure 1: Actual Picture of the Green Man Slave Assembly

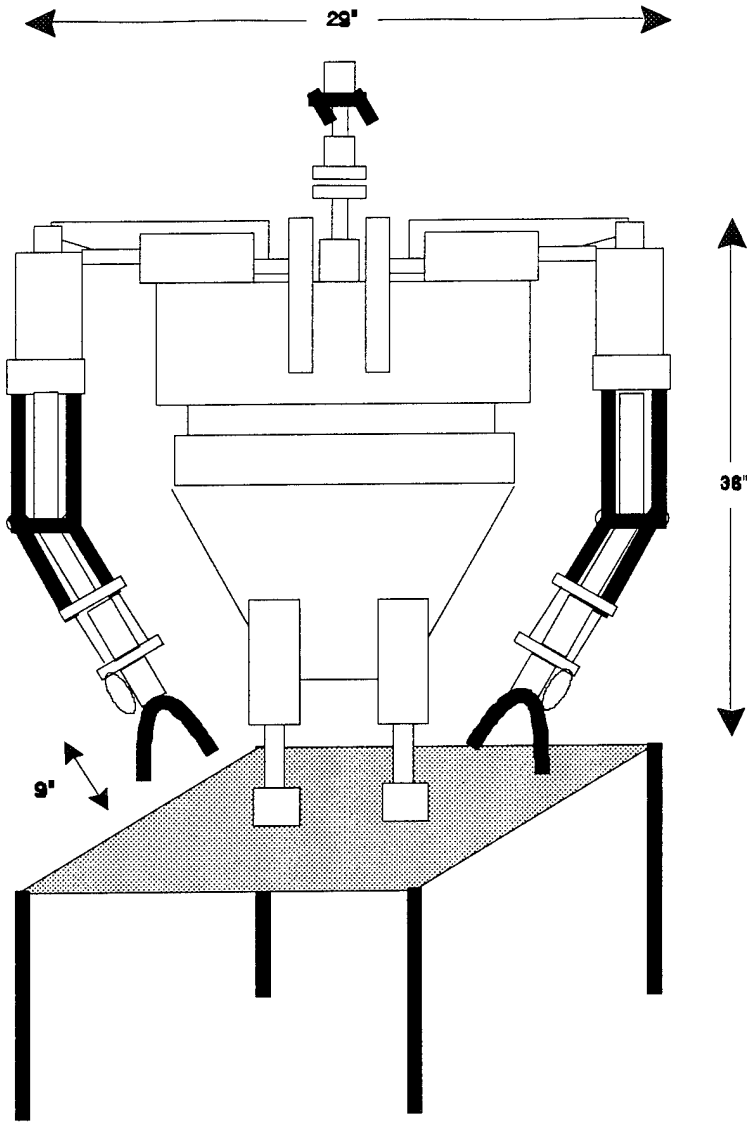

Figure 2: Green Man Slave

2. Definitions

Before proceeding into the details of this research, it is important that the reader have a general understanding of some of the definitions that will prove as a benchmark in achieving this type of robotic control. First, the Robot Institute of America has defined a

robot as a reprogramable multi-function manipulator designed to move material, parts, tools, or specialized devices through variable programmable motions for the performance of various tasks. Green Man is labeled a teleoperated anthropomorphic robot, where anthropomorphic means human-like, with mechanical objects that resemble arms and hands, a description which Green Man easily fits. The term teleoperated though, implies direct and continuous human control of a teleoperator (Green Man) that extends a person's sensing and/or manipulating capability to locations remote from that individual. In order to achieve full teleoperation and the corresponding extension of one's sense of touch, feedback from the slave must occur. Because Green Man was not equipped with such a feedback system, research focused on finding and testing an optimal feedback system for implementation on the Master Control Apparatus [Ref. 1: p15-17].

3. System Requirements

a. Control Mode Objective

In order to properly understanding the choice of feedback system, one must first look at Green Man's mode of control and corresponding system requirements. Green Man's strength and movements are controlled by the flow of hydraulic oil, which is regulated utilizing manual supervisory control. In this system, a human operator stimulates a controller which, through a computer interface, activates an actuator (servovalve), enabling the positive or negative flow of hydraulic oil into Green Man's appendages, which result in an array of movements. However, Green Man is not

equipped with the feedback control path that returns a signal from a sensor on the slave to the human operator based on forces acting on the slave. This signal is necessary in allowing the operator to "feel" any obstruction to the slave, thus truly extending the operator's senses and completing the system of supervisory control. This system is illustrated in block diagram form in Figure 3, with the deficient feedback path shown in bold.

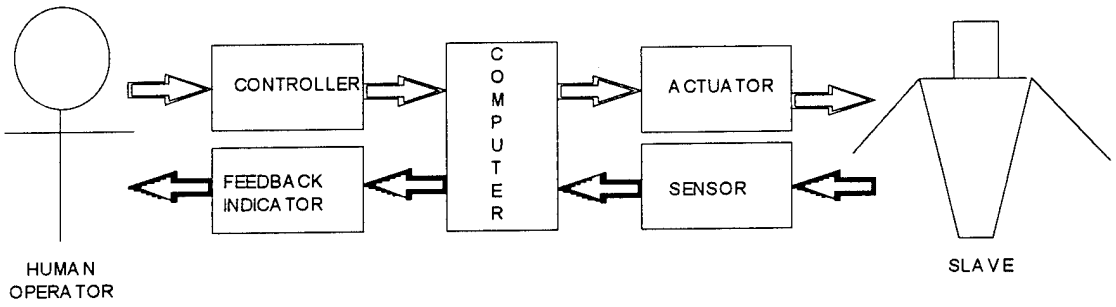

Figure 3: System Control Mode

b. Feedback Requirements

The only feedback system Green Man utilizes is the comparison of potentiometers on each joint of the master and slave, which is used to control the servovalves and flow of hydraulic oil to specific appendages. When the difference in potentiometer readings of the slave elbow and master elbow, for example, is zero, the servovalve restricts the flow of oil, holding the slave appendage at the same approximate position as the master. To fully complete the loop in gaining supervisory control, the operator must have direct feedback that the telerobot has accomplished its assigned task or that it has met an obstacle preventing the robot from achieving the task. One method

of feedback is bilateral force feedback, which measures the force applied to the particular appendage and transmits a proportional force back to the operator. Under the guidelines of this experiment, it shall be assumed that the slave could be outfitted with strain gauges at each appendage that would measure the strain absorbed by the component, with a corresponding signal transmitted back to the master control apparatus. With this assumption, a device had to be found that could transmit physical feedback to the operator in order to adjust his or her movement corresponding to the movement available, and opposition felt by the slave. Additionally, this device had to be light weight, small in size, cost efficient, durable, and adaptable to the various joints of the Master Control Apparatus (see Figures 4 and 5). Following an extensive investigation of various pneumatic, hydraulic, motor driven, and disk brake mechanisms, the band brake appeared to match the overall feedback system objectives. Figure 6 illustrates the implementation of the band brake system on one joint on the Master Control Apparatus.

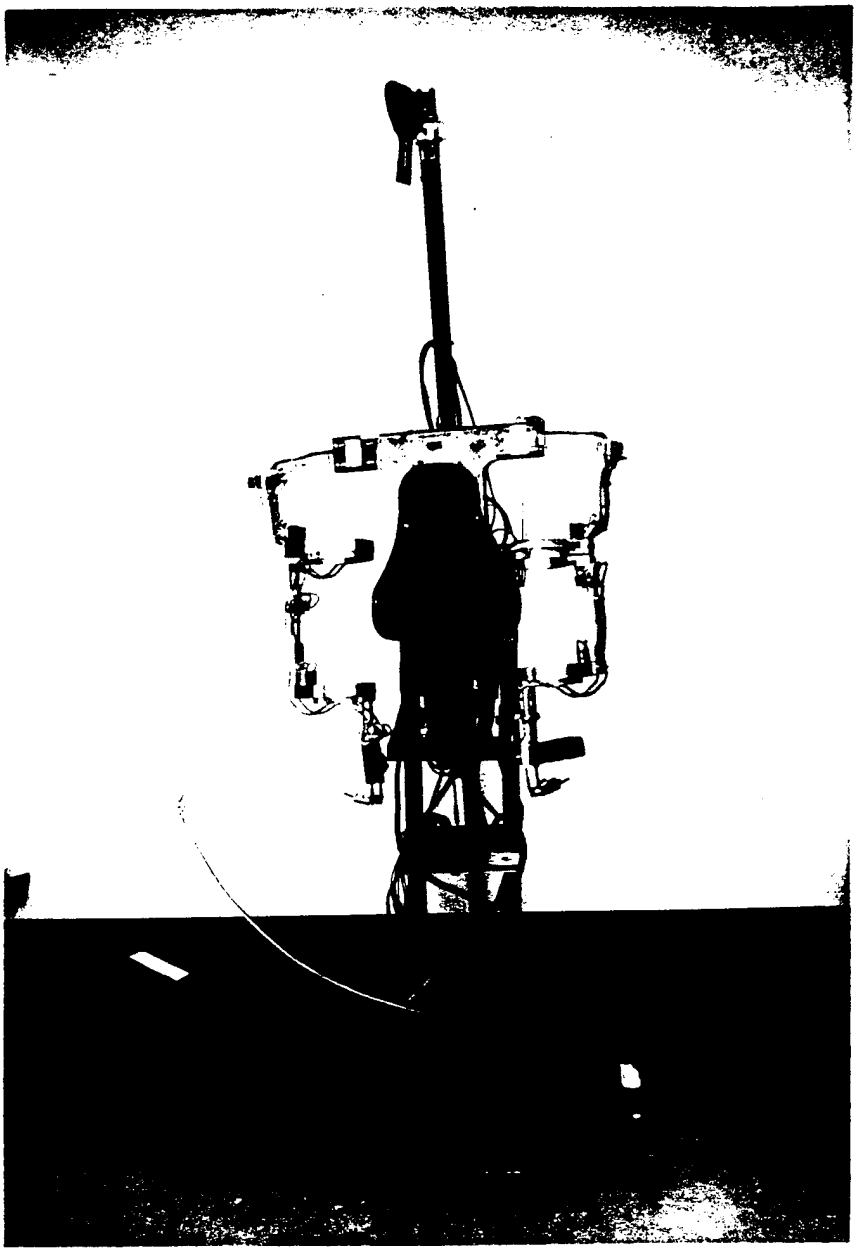

Figure 4: Actual Picture of the Master Control Apparatus

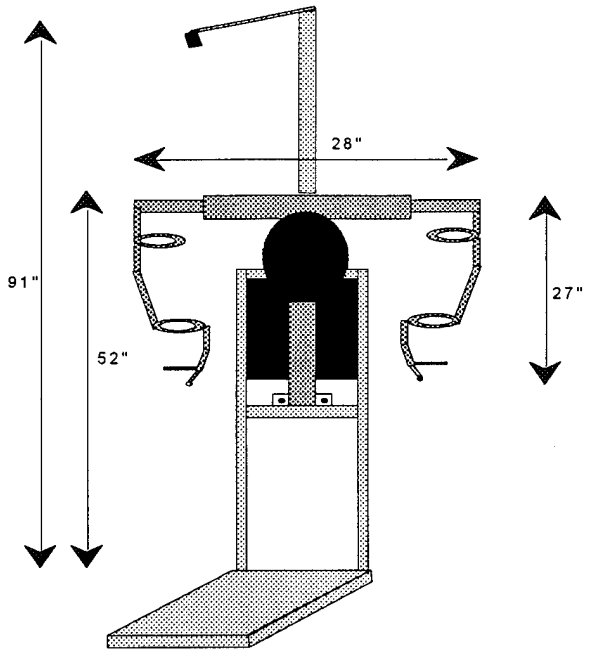

Figure 5. Master Control Apparatus

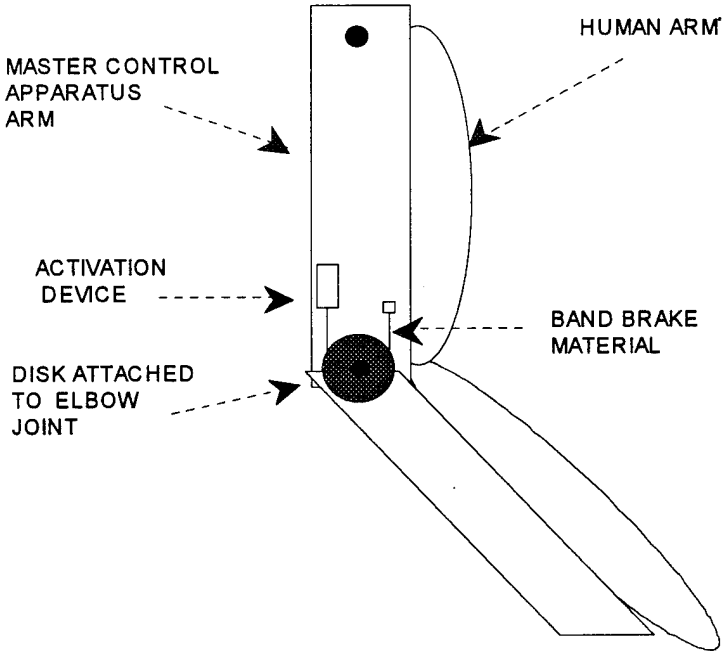

Figure 6: Band Brake System on the Master Control Apparatus

c. Band Materials

Realizing that an equally important facet of a band brake is the band material, three different materials will be tested. Due to the abrasive nature associated with the high frequency activation of each band brake, materials were chosen based on the criterion of coefficient of friction, elasticity, strength, durability, and heat dissipation. The materials utilized for testing were a synthetic shoe lace, leather band, and a two millimeter diameter steel chord. Although the characteristics of these materials were not analyzed in great detail, testing displayed their obvious traits, and the advantages and disadvantages associated with utilizing each material.

d. Test Model

In order to isolate on the behavior of each band brake system, and the expected response of the master, a test model was developed to emulate a joint on the master control apparatus. A disk was attached to a direct current (DC) motor to emulate the movement and resultant torque expected by a human joint. With the motor driven at a constant voltage, PWM signals were applied to the servomotor/solenoid activation subsystems. The results of these tests yielded a correlation of duty cycle versus speed differential for each activation device and band material in order to conclude which setup produced the optimal performance.

Thus, the format for this research will be to fully characterize the Green Man system, and then conduct tests in order to make a recommendation for implementation of the optimal force feedback system.

II. GREEN MAN

A. OVERVIEW

The idea behind the movement of the Green Man anthropomorphic teleoperated robot is relatively simple, but requires the coordination of numerous hydraulic actuators. The human teleoperator straps on the master control apparatus, placing his or her hands into the hand grips and begins movement of the shoulders, arms, and hands. By disconnecting the back plate from the support post, the operator may also gain control of Green Man's torso by rotating about the fixed pivot support. Although not analyzed during system checks, operator head movements can be monitored by the Polhemus Sensor located directly above (refer to Figure 4 and 5) to direct slave head movements in the events the slave is equipped with a video camera. In analyzing the master movements, Green Man uses a rack of circuit cards that basically compares the potentiometers of corresponding appendages on the master and slave. Based on the difference of the potentiometer voltages, servovalves are activated which transfer hydraulic oil to and from specific hydraulic actuators on the slave to produce movement. This system is represented in simple block diagram form in Figure 7.

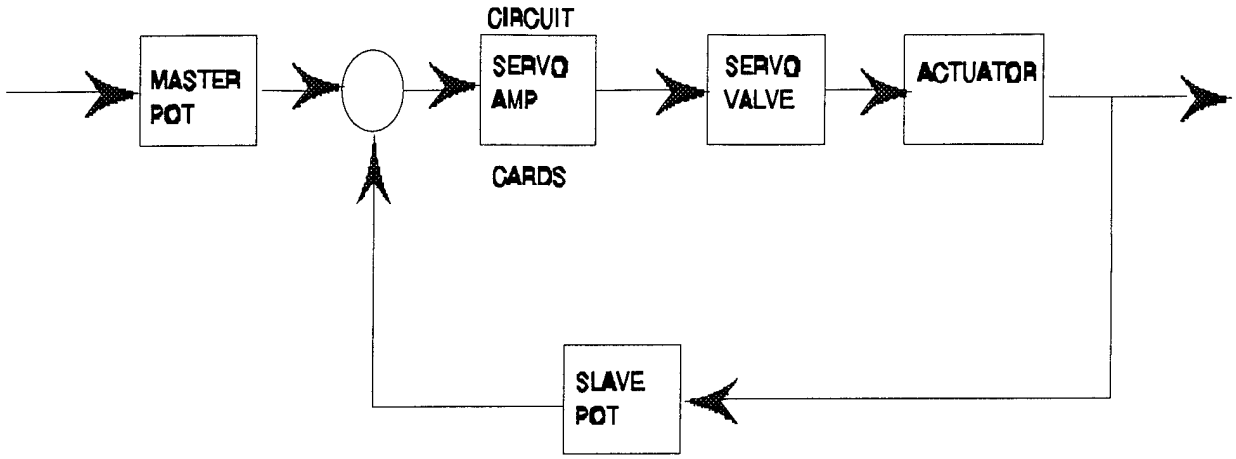

Figure 7. System Block Diagram

B. MASTER ELECTRONIC CONTROL STATION

1. Operation

a. Components

The master control exoskeleton is a light weight aluminum frame, adaptable to the operator's upper body, which allows for the translation and rotation of the arms and shoulders along multiple axis. Additionally, a hand operated mechanism allows for the manipulation of the slave's end effectors. All master control movements are monitored by various types of potentiometers (listed in Appendix A), with output voltages sent to the Servo Control Circuit Rack via the Master Electronic Input Transfer Cage (MEIOTIC). Other major components of the Master Electronic Control Station include:

- Master Servo Transmitter (SERVO XMIT)-a differential amplifier/buffer used to improve the signal to noise ratio and transmitted signal.

- Video/Audio Receiver-provides the power for the video/audio system, which includes the audio pre-amp, video cameras, and electronics, as well as the distribution of individual signals to the appropriate connections.
- Polhemus Processor-provides the head orientation signal to the servo system.
- Video/Audio Power Distribution System-provides power to all video/audio components and the Polhemus Processor with a single 120VAC power line with a local on/off switch.

Input: 120VAC, 60 Hz Output: 12VDC; 120VAC, 60 Hz

Further details of these components are included in Reference 2, page 5. Figure 8 illustrates the system in block diagram form.

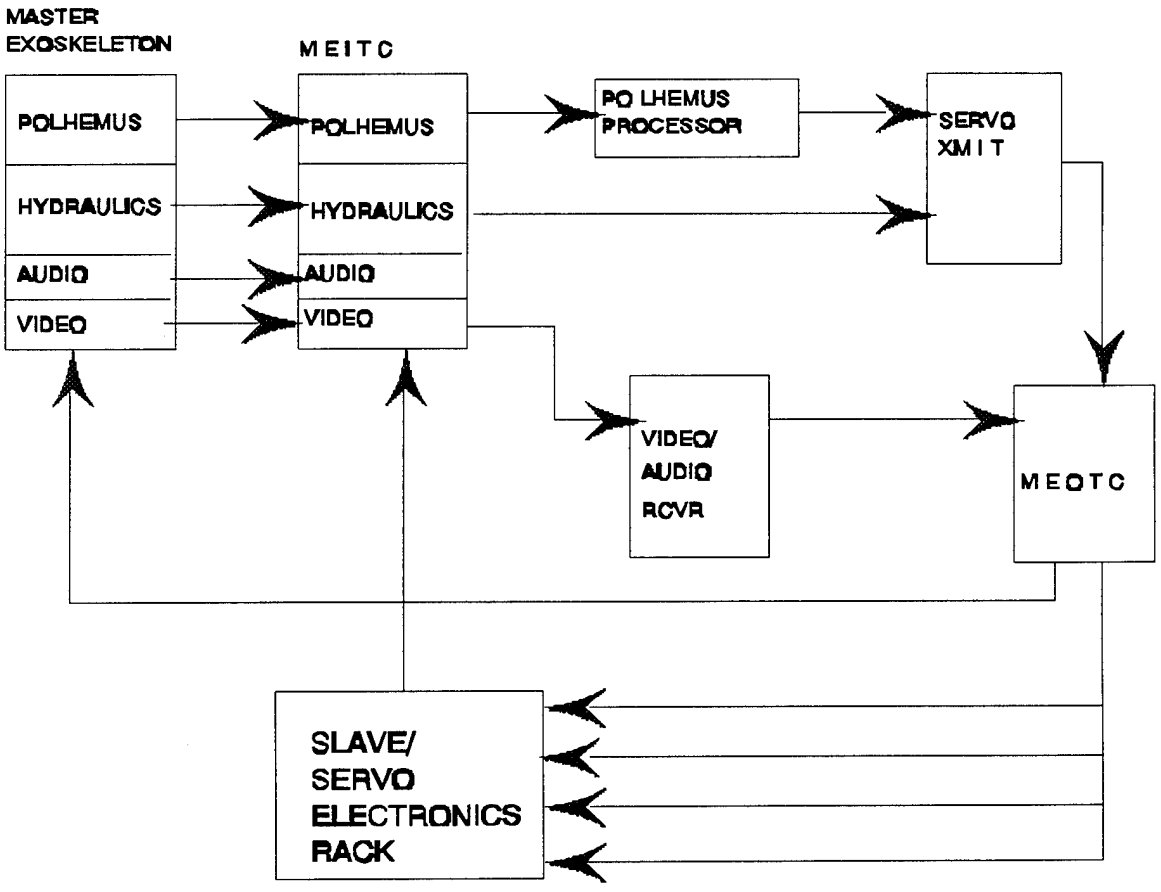

Figure 8: Master Electronic Station Block Diagram

b. Degrees of Motion

To accurately describe the motions available to the operator, a three dimensional coordinate system will be used (X positive right, Y positive up, and Z positive out of the paper), with motions summarized in Table 1 and shown in Figure 9.

POSITION	NUMBER	DEGREES OF MOTION
Shoulder Pitch	1	-80° to +45°
Shoulder	2	0° to +45°
Upper Arm Rot	3	0° to +90°
Elbow	4	-80° to +35°
Lower Arm Rot	5	0° to +180°
Wrist Pitch	6	-80° to +45°
Grip	7	-80° to +45°

Table 1 . Summary of Master Motions

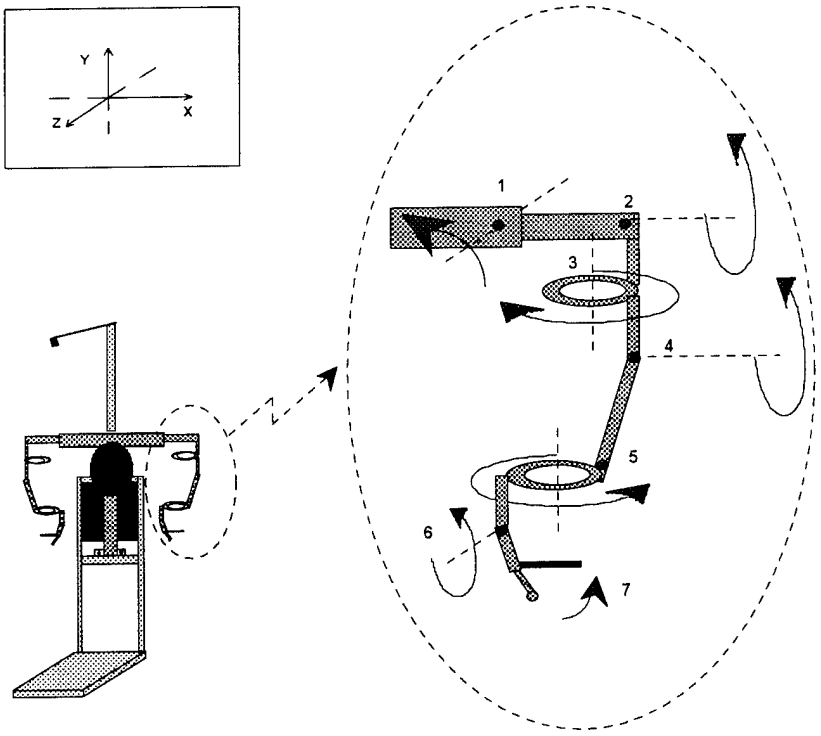

Figure 9: Master Control Station Movements

C. SLAVE UNIT

1. Operation

a. Component Integration

The slave unit is an anthropomorphic robot torso mounted on a moveable, two level cart, with the motor/pump and all servo valves located on the lower level. The torso is connected to allow for tilting and rotation of the slave unit. Additionally, numerous hydraulic actuators are interconnected to allow for rotation and translation of Green Man's appendages as well as operation of the end effectors. Similar to the master unit, all movements are monitored by potentiometers (listed in Appendix A) at each joint, with output voltages transmitted to the Servo Electronics Rack via the Slave Electronic Input Transfer Cage (SEITC). This transmission path controls the flow of hydraulic oil to the specific appendages. Other major components of the Slave Control Unit include:

- Video/Audio Processor-provides the interface between the video camera, microphone and speakers, and the single video/audio transmission cable.
- Servo Receiver (RCVR)-decodes the servo commands transmitted from the Servo Transmitter and outputs the proper signal to each servo card. The Transmitter/Receiver pair is used to increase operating distance and decrease noise interference.
- Servo Control Circuit Rack-a 19 inch STD bus card rack that holds all the closed loop servo cards.
- Servo Control Power Distribution System-provides power to all the servo control components from a single 120 VAC, 60 Hz power line with a +/- 15 VDC output, controlled by a local on/off switch

Further details of these components are located in Reference 2, page 6. Figure 10 illustrates the system in block diagram form.

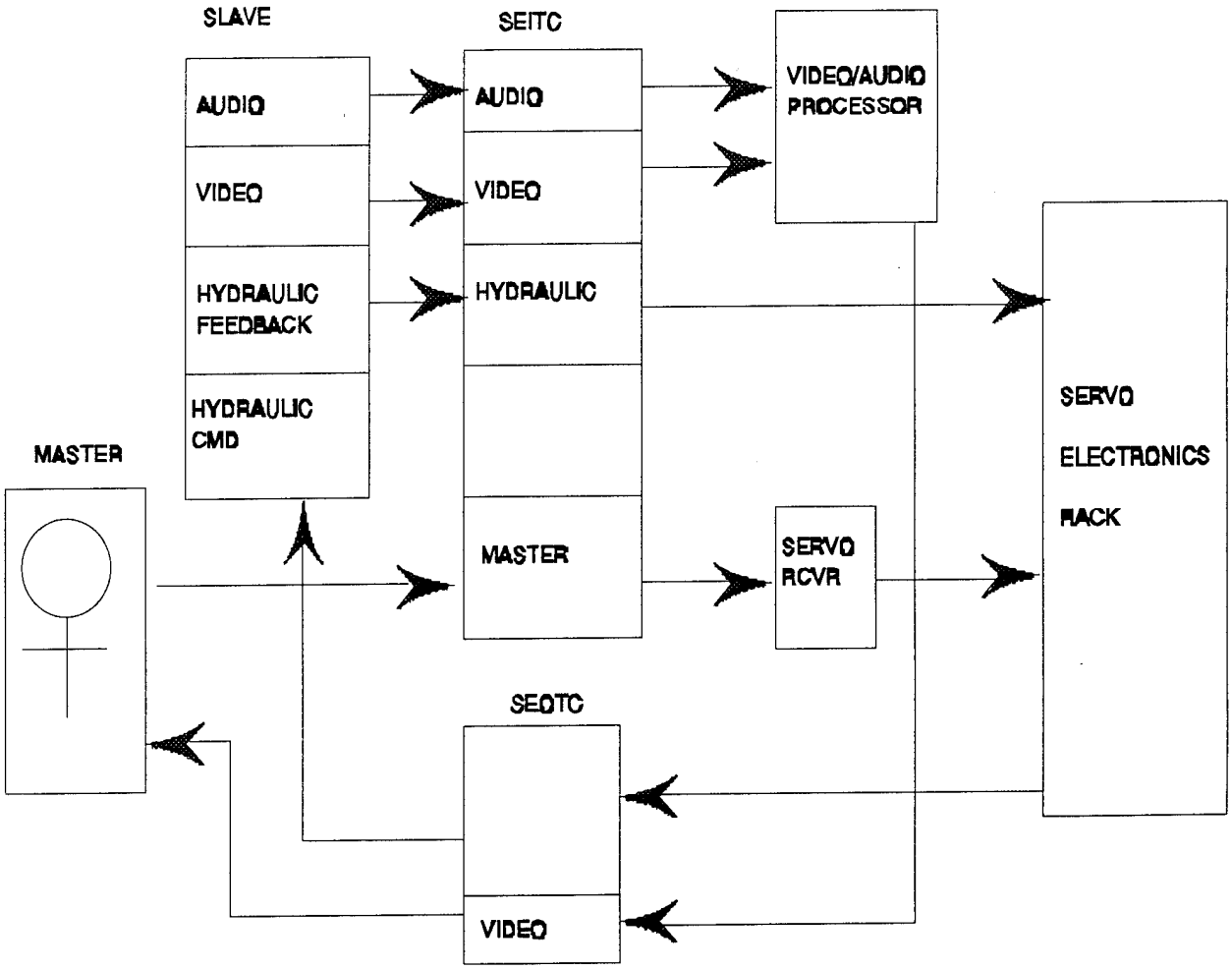

Figure 10: Slave Control Block Diagram

b. Degrees of Motion

Green Man has a wide range of movements that are best summarized in Table 2, and illustrated in Figure 11.

POSITION	NUMBER	DEGREES OF MOTION
Shoulder Pitch	1	-80° to +45°
Shoulder	2	0° to +45°
Upper Arm Rot	3	0° to +90°
Elbow	4	-80° to +35°
Lower Arm Rot	5	0° to +180°
Wrist Pitch	6	-80° to +45°
Grip	7	-80° to +45°
Torso Rotation	8	-45° to +45°
Torso Tilt	9	0° to +60°
Neck Tilt	10	0°....to -45°
Head Yaw	11	-45° to +45°
Head Tilt	12	0° to -45°

Table 2 . Summary of Slave Motions

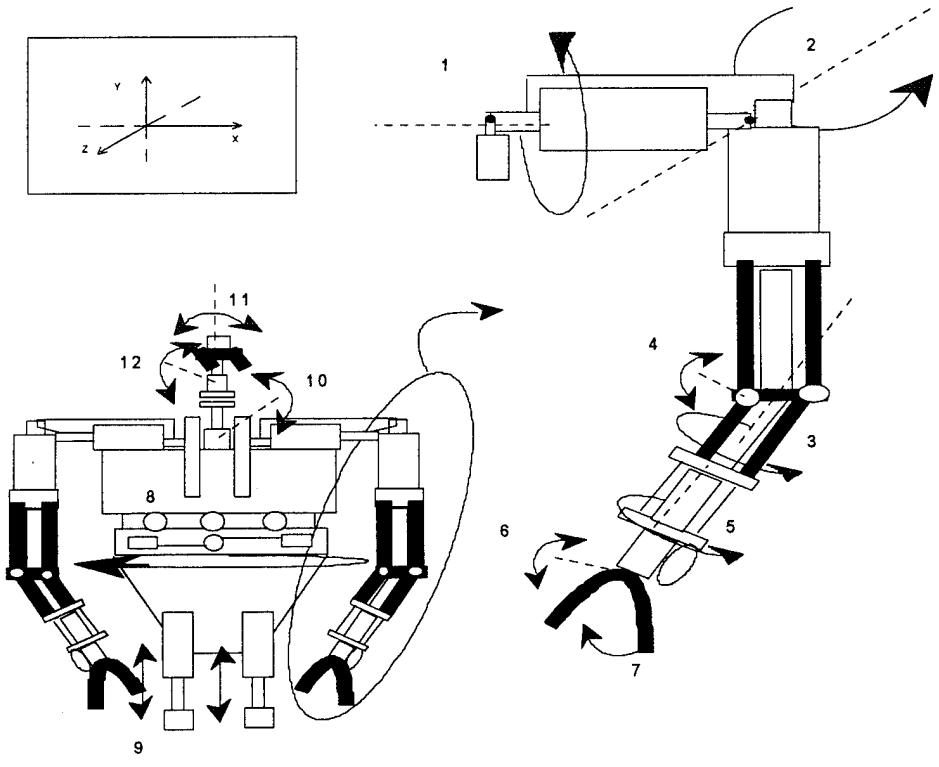

Figure 11: Slave Degrees of Motion

2. Motor/Hydrailic Pump

a. Hydraulic Oil Supply System

As previously stated, the majority of all hydraulic oil supply system components are located on the bottom level of the moveable cart (see Figure 12). To assist in understanding the hydraulic oil supply distribution, a block diagram of the system is illustrated in Figure 13.

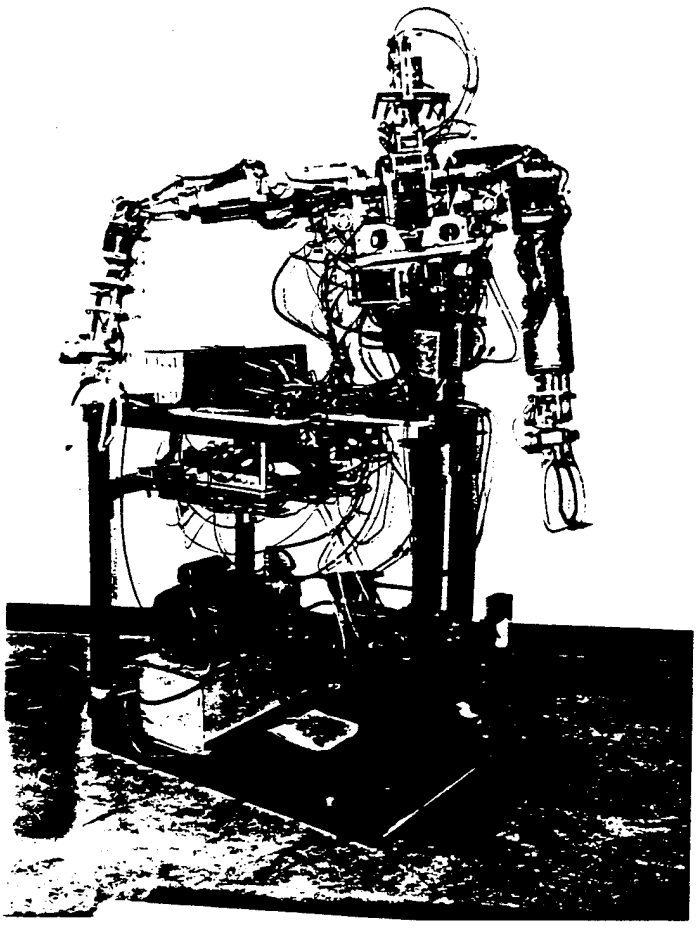

Figure 12: Actual Picture Illustrating the Major Components of the Hydraulic Oil Supply System

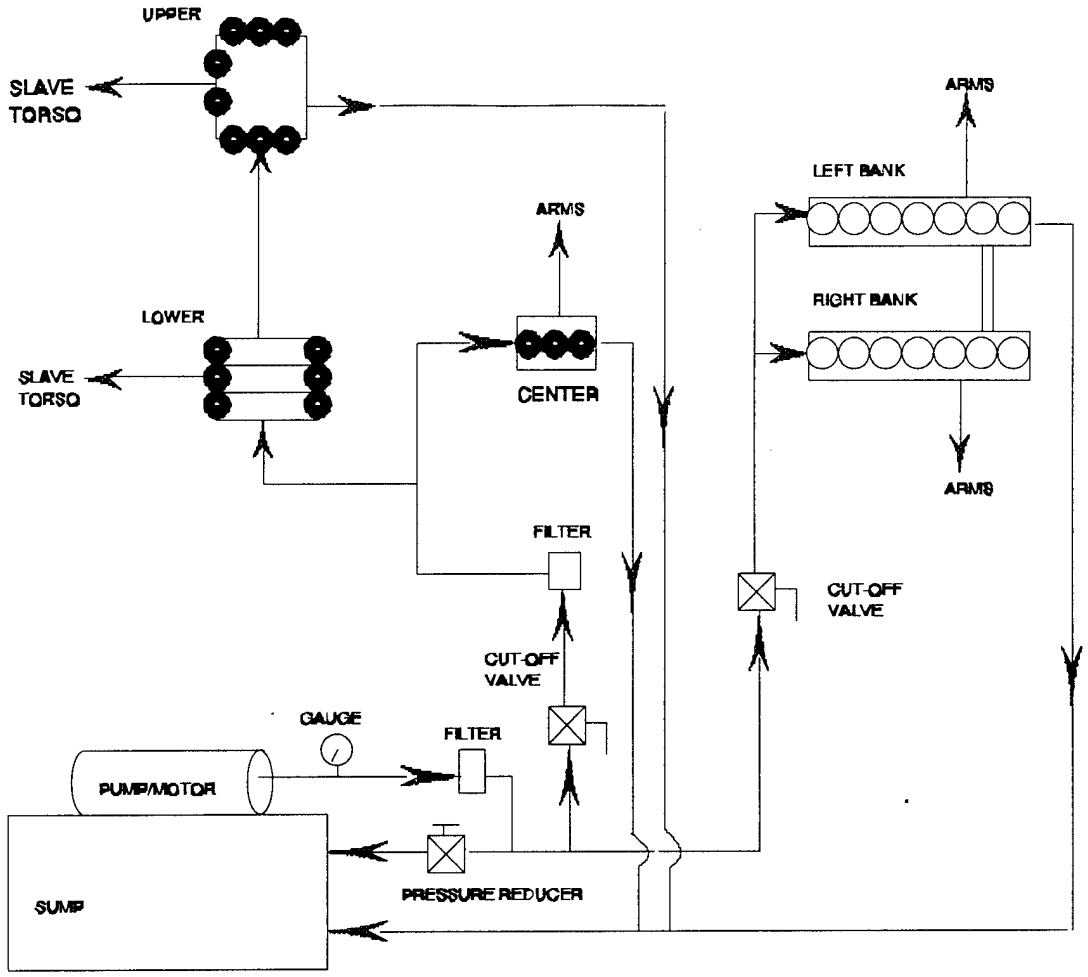

Figure 13: Hydraulic Oil Supply System

Brayco 762 oil is drawn from a four gallon sump and supplied to the system by way of a 115 volt Radial Piston pump. System pressure is controlled by a manual pressure reducer valve that varies the amount of oil that by passes the system and flows directly back into the sump. System pressure should be approximately 230-260 PSI during normal operation. As oil leaves the pump, it proceeds through a filter, then through one of two ports that are controlled by manual cut off valves. These valves enable flow into

either the left, right, or center hydraulic servo control valve banks, or the upper or lower distribution blocks, which controls arm or torso, respectively. Each servo valve is controlled by an output from the Servo Electronics Rack via the Slave Electronic Output Transfer Cage (SEOTC) as illustrated in Figure 8. Once hydraulic oil is utilized by the specific actuator, it is recirculated back to the sump.

b. System Startup

In order to enable the total Green Man anthropomorphic teleoperated system, the following steps should be read in full, then completed in sequential order:

1. Free Green Man slave from secured position, disconnecting arm constraints
2. Plug in Master Electronic Control Station (MECS) to a conventional 110 volt, 20 amp power supply outlet
3. Plug in Slave Electronic Control Box to surge protector strip located on back support of MECS
4. Plug in pump to surge protector. Ensure pump is in the "off" position
5. Connect master and slave transmission cable (R-1, L-2, H-3, T-4)
6. Connect Polhemus Sensor (if operational)
7. Plug in and turn on the surge protector
8. Ensure pressure relief valve is open (turned fully in the counterclockwise direction), allowing maximum oil to recirculate back to the sump.
9. Ensure both cut out valves are open (open according to the arrow)
10. Turn on pump at the local on/off switch. Oil will begin to flow throughout the slave, but at a very small pressure. There should be little or no movement of the slave.
11. Slowly begin to close the pressure relief valve until pressure reaches approximately 100 psi. Slave should start to rise to a vertically erect position. Ensure appendages and hydraulic lines are unobstructed.

12. Check system for any apparent major leakage.
13. Close relief valve until system achieves the desired operating pressure, nominally 230-260 PSI.
14. Begin system operational checks

c. System Shut Down

Green Man can be shut down and secured to various levels depending on the frequency of usage. If operating Green Man at regular intervals, it is safe to leave the unit fully energized at full pressure for a few hours, however reducing the pressure during the non-operational times is optimal if the situation permits. If Green Man is being secured for an elongated time (i.e., the end of a work day), it is recommended that at a minimum, the operator shut down the hydraulics (steps 1 - 6). For extended period of down time or for transport, ensure both the hydraulics and electronic components are properly secured by following all the steps below.

1. Slowly reduce the pressure to approximately 50 PSI by rotating the pressure relief valve clockwise. The slave arms (if extended) will begin to fall; slowly guide them to a rest position adjacent to the torso.
2. Continue to reduce the pressure by fully rotating the pressure relief valve clockwise until the minimum pressure is obtained and all supply oil is being recirculated back to the sump. As the hydraulic oil exits the torso, slowly guide the torso to a position flat on it's "back."
3. Turn off the pump at the local on/off switch
4. Secure the slave arms at the wrists
5. Close both cut off valves by rotating according to the arrow on the handle
6. Turn off the power at the surge protector strip
7. Disconnect the pump from the surge protector strip
8. Disconnect the Slave Electronic Control Box from the surge protector strip

9. Disconnect the Master Electronic Control Station (MECS)
10. Disconnect master and slave transmission cable
11. Disconnect the Polhemus Sensor (if operational)

3. Slave Hydraulics

a. Oil Flow Path to Appendages-Overview

As indicated in Section II.2.a, the Brayco 762 oil proceeds from the pump to either the upper/lower hydraulic oil distribution blocks or the left/right/center hydraulic servo control valve banks, then to the respective appendages or torso area (see Figure 13). The intricate web of hydraulic lines feeding multiple hydraulic actuators is configured to give Green Man the appearance of a human torso with the similar multiple degrees of motion. The trace of each flow line from flow control servo valve to hydraulic actuator is essential in understanding the slave dynamics, and can be a valuable aid in troubleshooting.

b. Hydraulic Servo Control Valve Banks

There are three Hydraulic Servo Control Valve banks (right, left, and center) located on the lower level of the Slave Control Unit which control flow to the arm and neck/head support actuators. The right and left banks comprise of MOOG type flow control valves (as listed in Appendix B) which have been labeled with a number system corresponding to the number affixed to the actuator it supplies. Figures 14 and

15 are provided as an aid in identifying the flow paths from the Hydraulic Servo Control Valve banks.

c. Hydraulic Oil Distribution Blocks

The two primary components that disperse hydraulic oil to the slave torso are the upper and lower distribution blocks. These blocks allow oil to be transferred to flow control servo valves that are located directly on the torso (vice on the lower level of the Slave Control unit). Figures 16 and 17 illustrate the flow path from the distribution blocks.

4. Servo Systems

a. Hydraulic Actuators

The motion of the slave is controlled by a configuration of multiple hydraulic actuators. The actuators for the arm movements, particularly the shoulder, end effector, and upper and lower arm rotation, were specifically developed for robotic use and add to the anthropomorphic appearance of Green Man. These and all actuators are listed in Appendix C. Although not drawn to be component specific for each actuator, Figure 11 exemplifies the various degrees of motion that are possible to the operator for remote control.

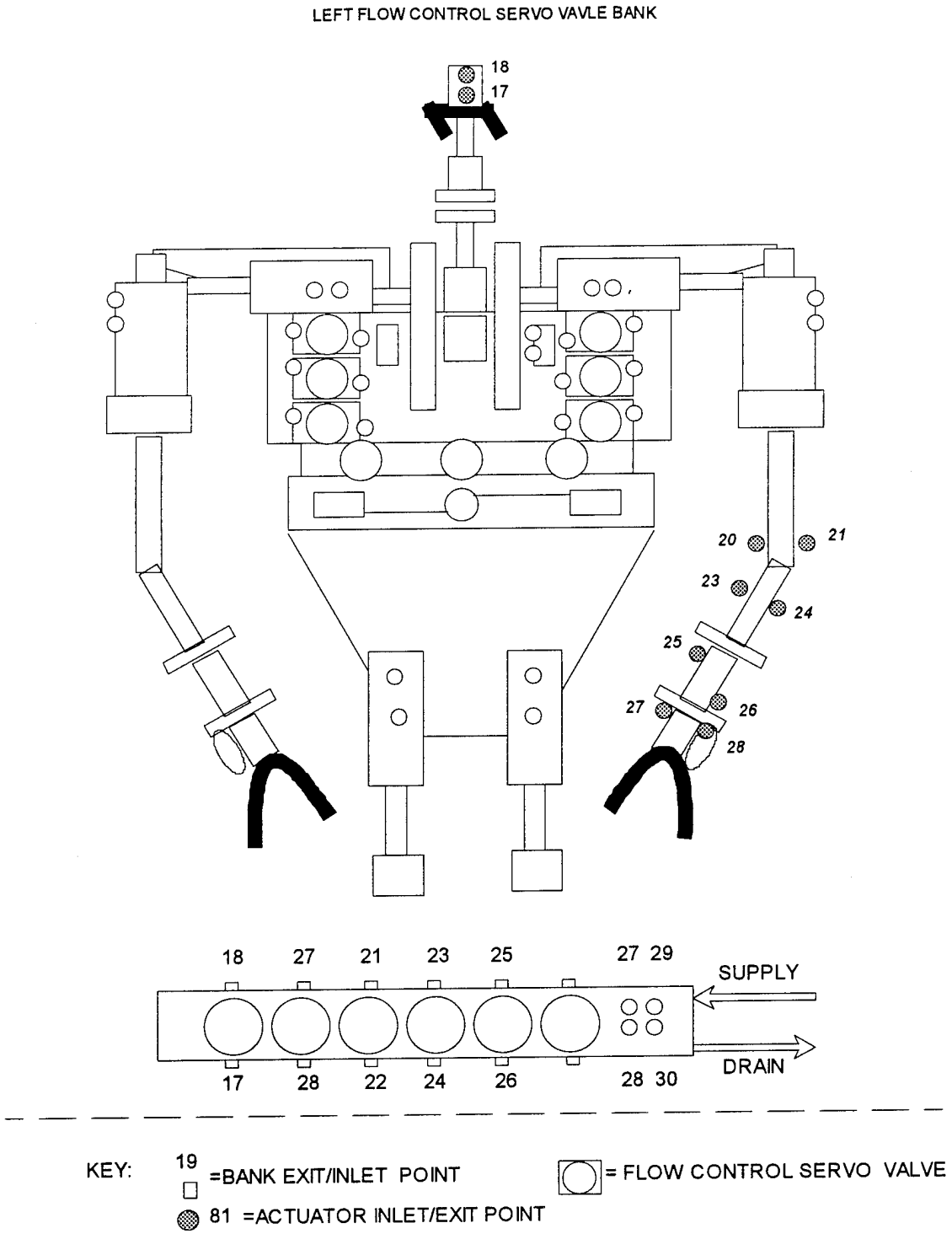

Figure 14: Flow Path of Left Servo Valve Bank

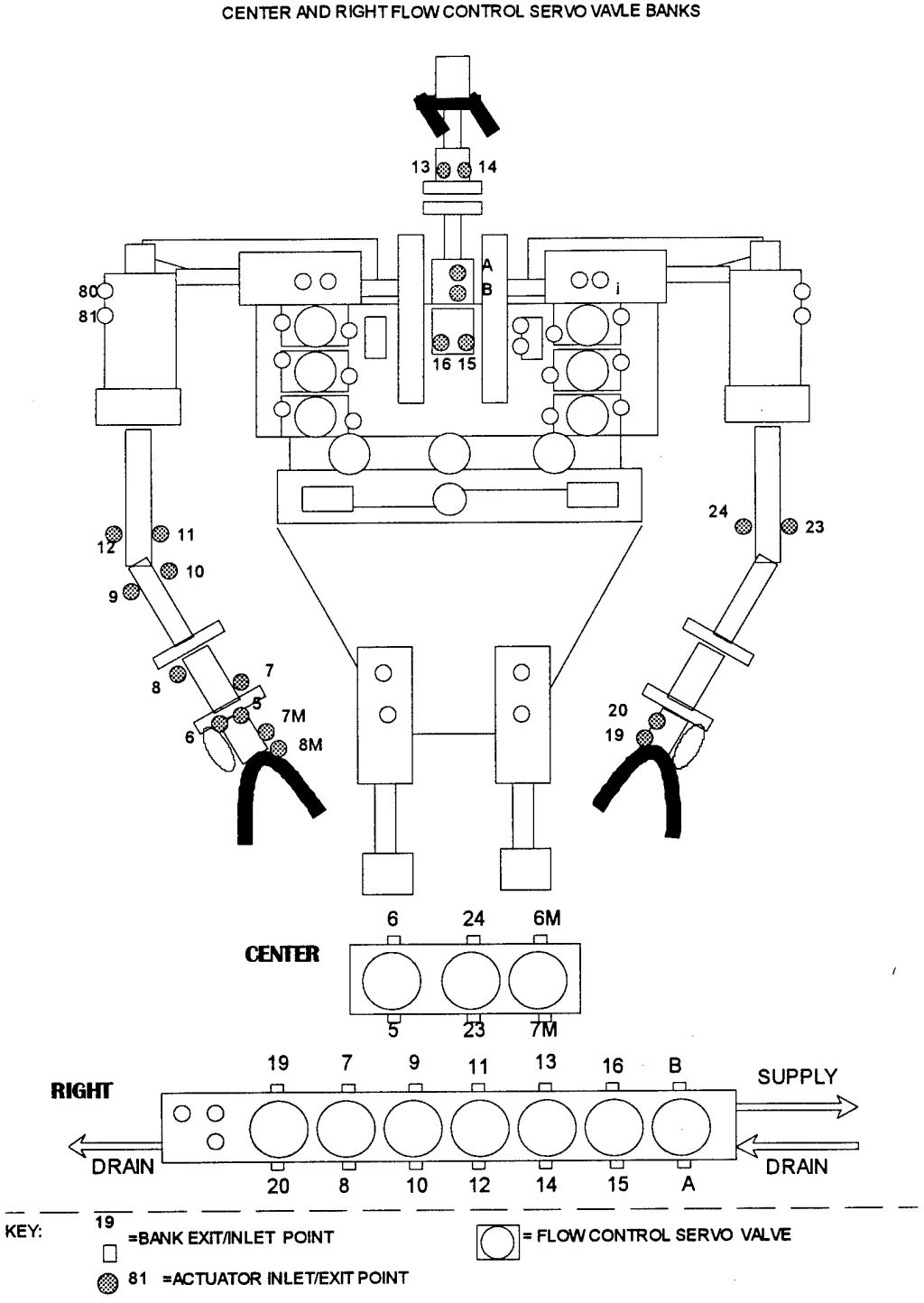

Figure 15: Flow Path of Center and Right Flow Control Servo Banks

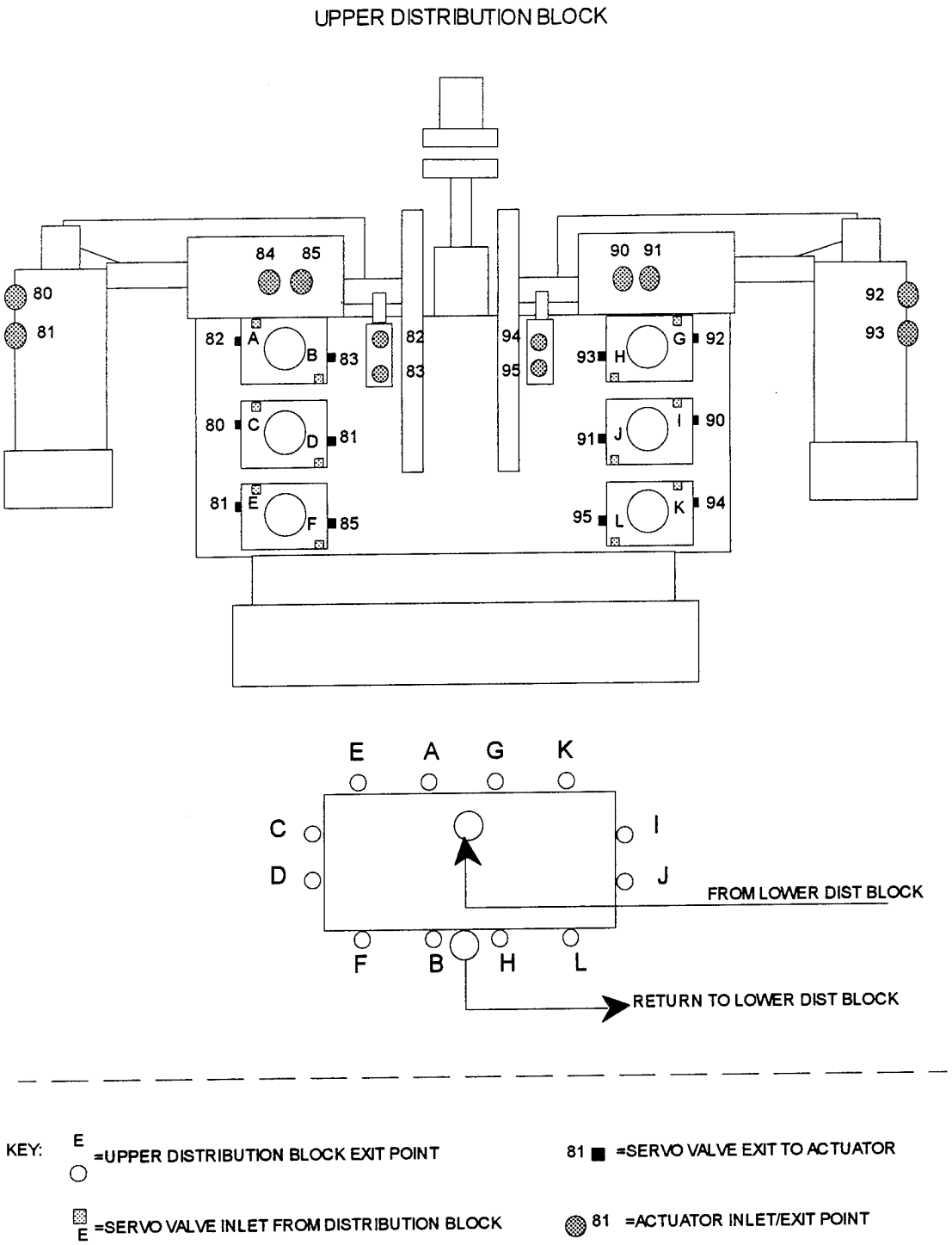

Figure 16: Flow Path for Upper Distribution Block

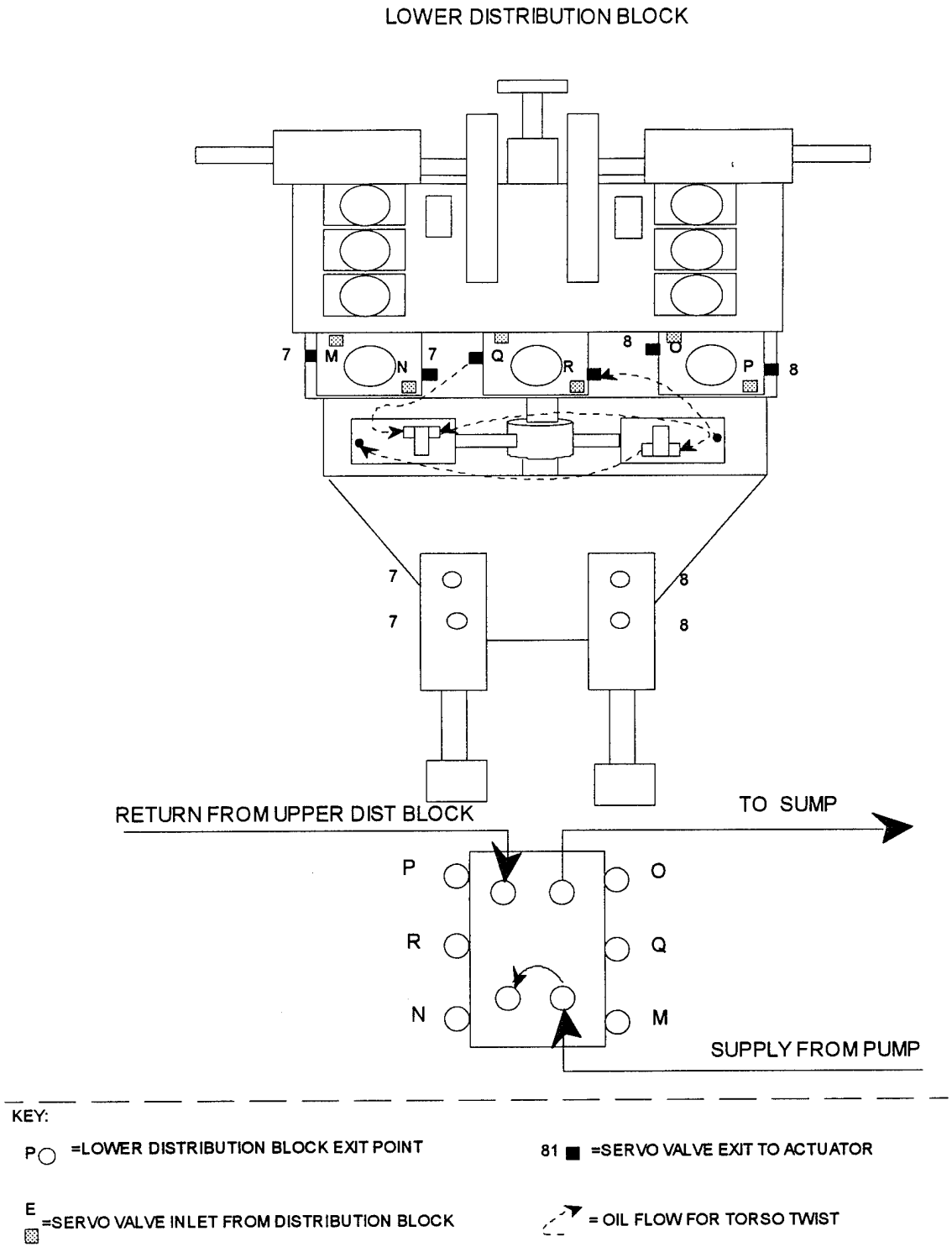

Figure 17: Flow Path For Lower Distribution Block

b. Potentiometers

The Green Man master and slave systems are equipped with potentiometers at each of the various joints. These potentiometers consist of numerous single turn, helical, and linear types, supplied mainly from the New England Instrument Company or Bournes. Each potentiometer serves as a device that outputs a voltage according to the position of the particular master or slave appendage. These potentiometer voltages are compared in the Servo Electronics Rack in order to control the amount and rate of hydraulic oil flow to specific appendages on the slave. As the master operator moves a specific joint from, for example, 0 degrees to 45 degrees, the potentiometer voltage goes from perhaps 0 volts to +3 volts. As the particular circuit card monitoring the joint senses a difference in potentiometer readings, it orders the flow control servo valve to pump more hydraulic oil to the specific hydraulic actuator until the joint moves to a position corresponding to +3 volts. When the potentiometer voltage difference between master and slave is zero, flow is ceased and the slave appendage is held at a position corresponding to that of the master. This system is represented in block diagram form in Figure 7. Figure 18 is provided to aid in identifying the type and location of each potentiometer. The numbering system is designed to coincide with the potentiometer listing in Appendix A. Additionally Appendix A contains potentiometer specifications and ordering information in the event of future procurement.

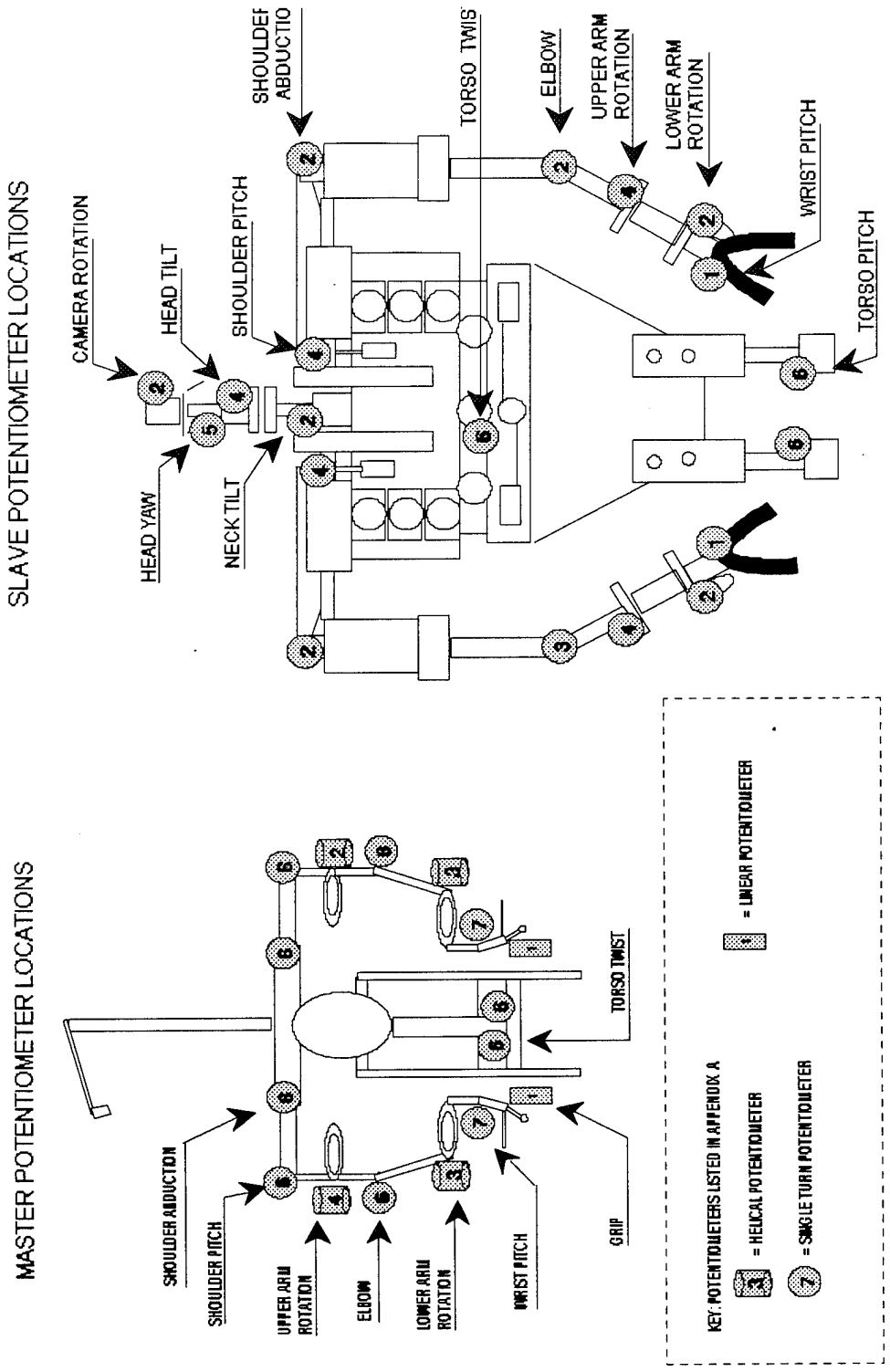

Figure 18: Potentiometer Locations for Master and Slave

5. Servo Electronics Rack Circuitry

a. Overview

The majority of electronic circuitry used by Green Man is contained in the circuit cards of the Servo Electronics Rack. These circuit cards compare the potentiometer voltages of the master and slave, and output a voltage to the appropriate servo valve to regulate hydraulic oil flow. The signal path linking the master to the slave travels through the transmission cable (wiring harness). Each potentiometer wire on the master is segregated into one of four bound wire runs labeled "R" for right arm appendages, "L" for left arm appendages, "T" for voltages from the torso, and "H" for signals from the head. These male DB 25 pin connectors are attached to the female ends accompanying the slave control unit in the following order: R to 1, L to 2, H to 3, T to 4. From the transmission cable the signals (containing the command position voltage) enter the Servo Electronics Rack through the DB 25 pin ports labeled E, F, G, and H, respectively. These signals from the master are compared in each circuit card with in slave potentiometer voltage signals, which enter through ports A, B, C, and D.

b. Circuit Cards

Contained in the in the Servo Electronics Rack are eleven virtually identical circuit cards. Due to lack of equipment necessary to properly analyze the head

motions, testing focused on the circuit cards controlling the shoulder, arm, and hand motions. Each of these cards serves as dual channel amplifiers with one card per appendage movement, and two channels per card (for the left and right sides). Because each actuator requires a different robustness, the gains for each appendage can be varied in a centralized location on each circuit card. Each card uniformly receives input from the master at pins 3 and 20 and from the slave at pins 5 and 18, where pins 3 and 5 control the right side and 18 and 20 control the left. Table 3 summarizes each circuit card's control appendage and Figure 19 illustrates a typical card. Cards 8, 9, and 10 control all head and neck movements, while Card 11 controls torso twist and tilt.

CARD	CONTROL	CARD	CONTROL
1	SHOULDER ABDUCTION	7	GRIP
2	SHOULDER PITCH	8	HEAD 1,2
3	UPPER ARM	9	HEAD 3,4
4	ELBOW	10	HEAD 5,
5	LOWER ARM ROTATION	11	WAIST 1,2
6	WRIST PITCH		

Table 3: Numbering of Servo Electronics Rack Circuit Cards

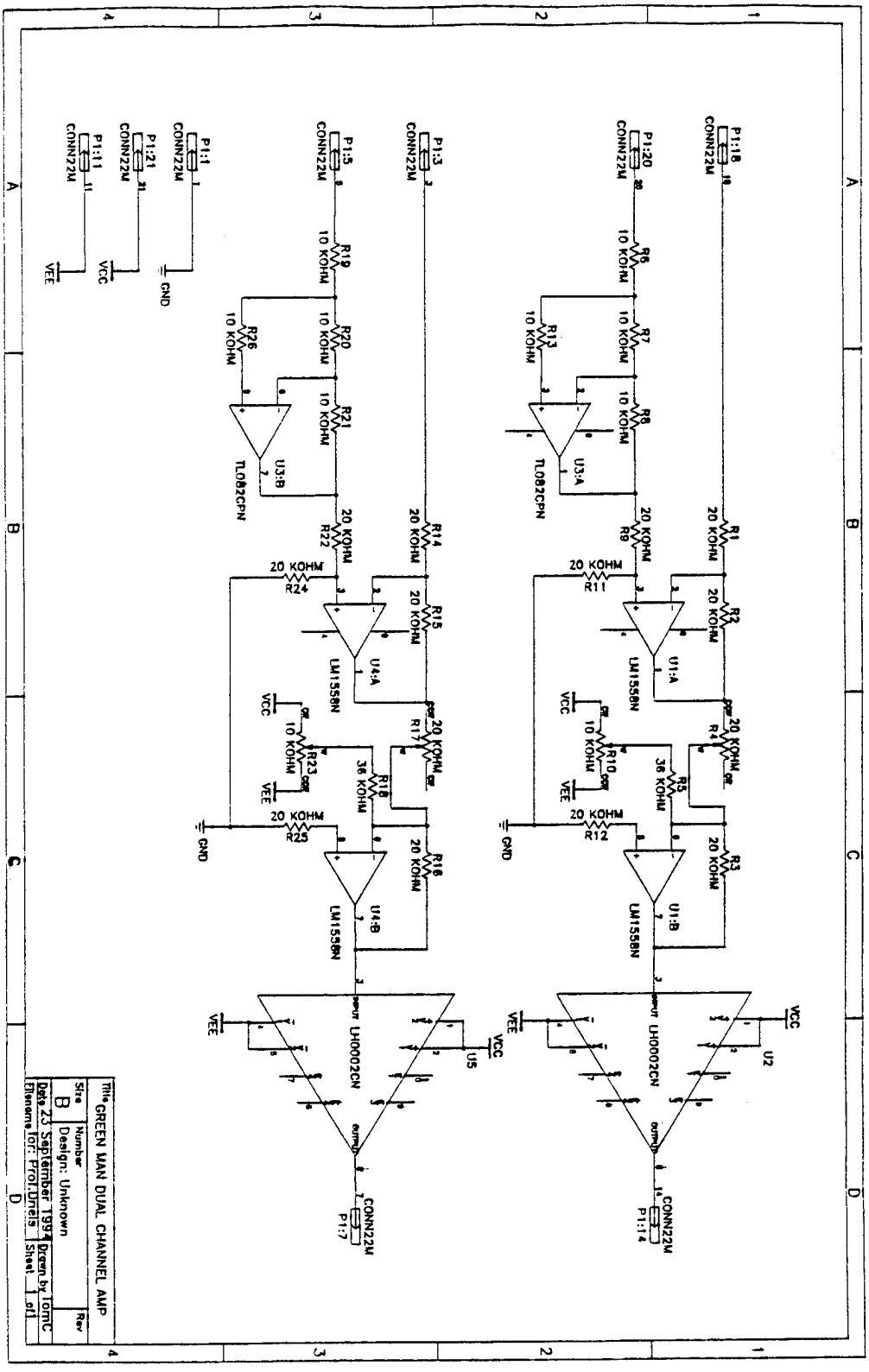

Figure 19: Dual Channel Amplifier Circuit Card from Servo Electronics Rack

III. FORCE FEEDBACK -THEORY

A. THEORY

1. Background

When researching possible bilateral feedback systems for implementation on the Master Control Apparatus, many factors contributed to the decision to test a band brake force feedback system. The system was chosen over other pneumatic, hydraulic, and motor driven mechanisms due to added advantages in cost, weight, size, part and component availability, and simplicity of implementation. Once this method was decided upon, there was still a question of the optimal activation technique, thus analysis was based on the exact goals that this system must achieve.

2. Goals of the Feedback System

To envision the goals of the bilateral force feedback system, one must examine the method of operation and objectives necessary in completing a remote manual supervisory controlled task. As the master teleoperator begins to move a particular appendage, the slave will react and move corresponding to the master (minus a small dynamic lag). If the slave should encounter an obstacle, the operator must immediately be notified of this obstruction, and gain a sense for the type of obstruction that a particular limb has met. For example, if the operator is conducting a curl movement with the right arm/elbow, and the slave curling movement is obstructed by a solid table or

wall, the operator should sense a force that stops his or her motion as well. Similarly, if the obstruction is a spring or movement of the arm through a liquid, completion of the curl will be more "difficult" and slowed by the obstacle or work environment. In this case, the master arm should also feel the resistance in the form of a damping effect proportional to the force felt by the slave. Thus for the purpose of this experimental research, a feedback system will be considered satisfactory if it can transmit to the master appendage, a "one-to-one" replication of the obstruction encountered by the slave appendage. This criterion means that there must be tight, robust control of the specific joint as well as the ability to stop the movement of that joint on the Master Control Apparatus if necessary.

3. Assumptions

To continue with the requirements of the bilateral force feedback, the following assumptions were made:

- Signal is available from the slave (i.e., a strain gauge) indicating the amount of strain in a particular member
- The operator would make movements slowly i.e., similar to the dynamics of the slave
- When the feedback system gives indications that the slave has encountered opposition that would terminate movement along the intended path, the operator will cease movement and move in the opposite direction until the feedback system indicates freedom of movement and/or a relief in strain on the slave.

4. Band Brake System Feedback Signal Conversion

Beginning with the assumed voltage signal from the strain gauge of a particular appendage, this voltage would be converted into a pulse width modulated (PWM) signal that would be used to control band brake activation device, either a servomotor or solenoid. This activation device would alternate the tension on a band material wrapped around a disk that would be fastened to the particular joint on the Master Control Apparatus. Activation of the brake system will serve as a damper for the particular joint on the slave, with resistance proportional to the duty cycle of the PWM signal. In the case of the servomotor, the position of the servomotor arm is controlled by the duty cycle of the PWM signal. As the duty cycle increases, the servomotor rotates, thus increasing the tension on the band brake and slowing the rotational motion of the joint in accordance with the tension and coefficient of friction of the band material. The solenoid, on the other hand, is a cylinder wrapped in coils whose magnetic field pulls a plunger into the cylinder at a certain force. In this feedback system configuration, the solenoid will be directly "pulsed" at a frequency corresponding to the duty cycle of the PWM signal. This will cause the solenoid to exert a pulling force on the plunger in an alternating fashion, resulting in activation of the band brake in an "on/off" manner proportional to the duty cycle of the PWM signal (see Figure 20). Thus, the solenoid configuration should allow for control of the rotational speed of the joint by varying the frequency of activation with more dependence on band brake tension and less

dependence on the material's coefficient of friction. In both cases, as the duty cycle increases with increased slave strain, the band brake will correspondingly slow or dampen the movement of the master. This system would be relatively simple to integrate into the existing system, requiring minor changes to the circuit boards and the addition of minimal wiring on the Master Control Apparatus.

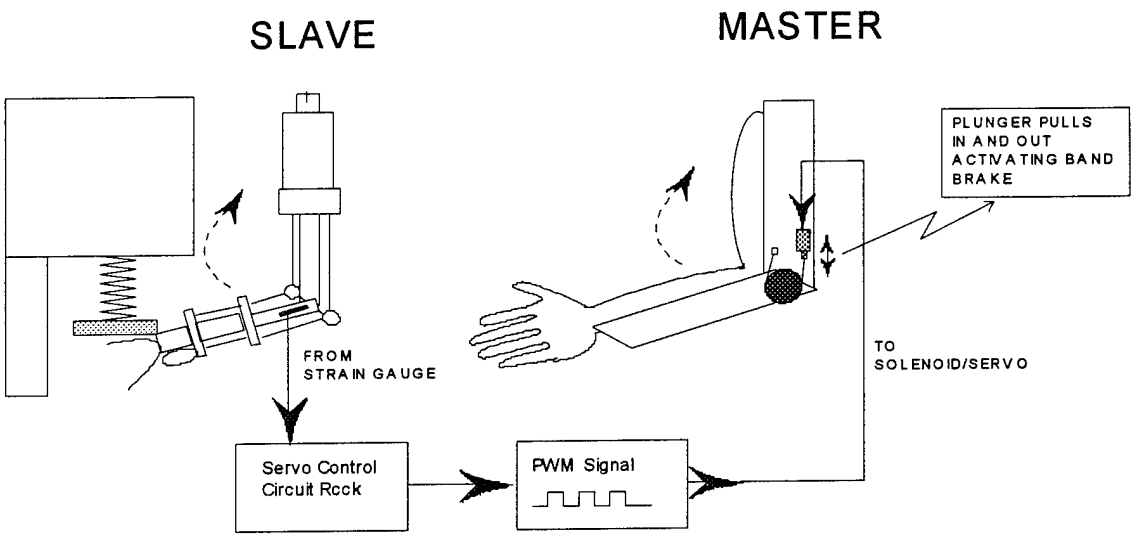

Figure 20. Feedback Signal Conversion

B. THEORETICAL MODEL

1. Background

Rather than attempt to test the band brake activation systems directly on the Master Control Apparatus, the decision was made to model a specific joint on the master and isolate the performance of each activation configuration in a controlled manner.

Realizing that rotation of a particular joint on the Master Control Apparatus was dependent upon a continuous torque applied by the teleoperator, the idea of using a motor to simulate this torque seemed logical. Thus, a motor was chosen as the basis of the test model due to it's ability to offer the ideal simulation of the torque applied by an operator at a joint, and control of the motor speed by the band brake activation system would indicate the ability to control a human's motion. Once the test motor was obtained and analyzed (Section IV.C) the theoretical model of the testing apparatus was formulated and evaluated. This testing apparatus would include the motor, with a disk attached in a manner that would allow for interchanging of the multiple activation configurations, and a tachometer that could monitor rotational speed of the system. The goal in analyzing the theoretical model would be to prove that the speed of the system could be controlled by varying the inputs to the various activation configurations. The sketch of the theoretical model is as shown in Figure 21.

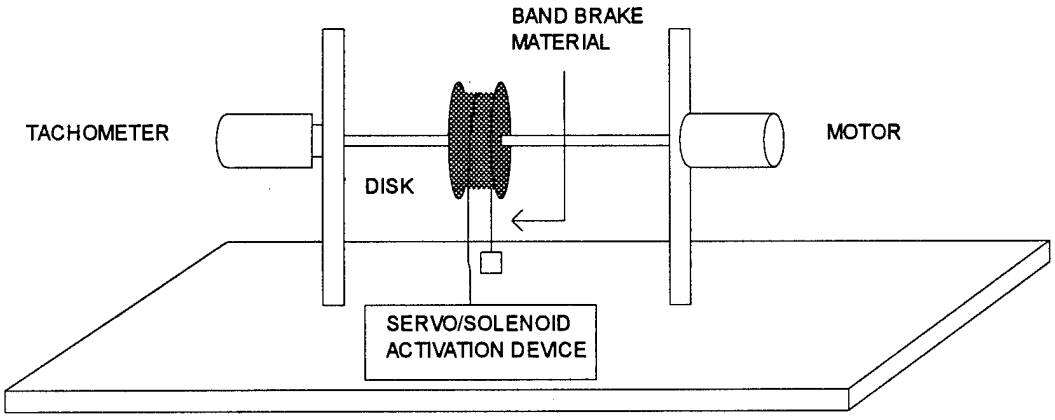

Figure 21: Theoretical Test Model

2. Assumptions

In order to properly analyze the theoretical model, the following assumptions were made:

- The motor would be operated at constant voltage
- All motor characteristics are in accordance with those obtained in Section IV.C
- Upon activation of the brake, and opposition of disk rotation, the motor torque would increase in a linear fashion in accordance with the motor characteristics (Section IV.C)
- Band brake materials possess coefficients of friction (μ_k) in accordance with Section IV.D
- The band brake is in continuous contact with 180 degrees of the circular disk

3. Solenoid

a. Equations of Motion

In analyzing the equations of motion for the solenoid, it is assumed that the solenoid will be supplied a PWM signal with a duty cycle proportional to the strain guage signal from the slave. This duty cycle will control the interval of time that the solenoid (and band brake system) is on or off. For example, a duty cycle of 75% corresponds to an activation voltage of 5 volts "on" for 0.3 seconds and "off" for 0.1 seconds. Thus over a time, the solenoid will be cycled through activation for 0.3 seconds, then deactivation for 0.1 seconds until the PWM signal is updated or changed. The result should be a change in speed proportional to the duty cycle i.e., the greater the duty cycle, the greater the decrease in speed. The response of the theoretical model will

be monitored for the ability of the band brake system to control the change in speed of the motor for various materials and duty cycles. The experimental trials will be conducted over a specific time interval, with the motor initially running at a constant rotational speed. To represent the dynamics of the system in equation format, the test apparatus is drawn in Free Body Diagram form in Figure 22.

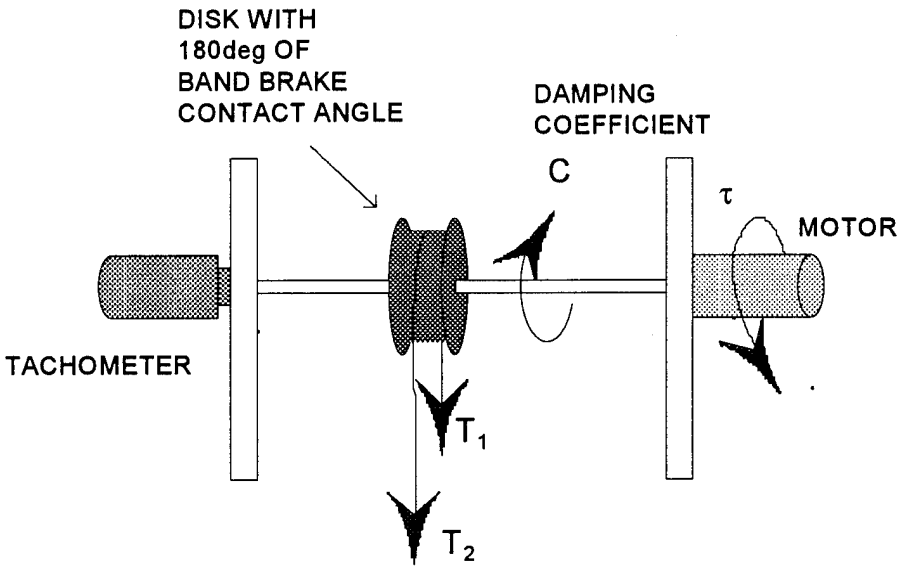

Figure 22: Test Apparatus Free Body Diagram

From the Free Body Diagram, the following equation of motion can be written:

$$\sum \tau = J\dot{\omega} \tag{1}$$

$$J\dot{\omega} + C\omega = \tau + r(T_2 - T_1) \tag{2}$$

With the following equation applicable for the relationship between T_1 and T_2 for a band brake:

$$\frac{T_1}{T_2} = e^{\mu_k \beta} \tag{3}$$

where: μ_k=band brake material coefficient of friction

β=band brake contact angle

Incorporating the motor torque as a function of rotational speed (ω), armature voltage (V_a), armature resistance (R_a), and proportionality constant (K_V) from Section IV.D.2. yields the following equation:

$$\tau = \frac{K_V V_a - K_V^2 \omega}{R_a} = Q_1 + Q_\omega \omega \tag{4}$$

Additionally, the system damping coefficient (C) and system inertia (J) were estimated according to Section IV.C.3:

$$C = \frac{\tau_m}{\omega} = 0.54 N \cdot m \cdot \sec \tag{5}$$

$$(t) = 0.784(1 - e^{\frac{-0.605t}{J}}) \Rightarrow J = 0.076 kg \cdot m^2 \tag{6}$$

Substituting equations (3), (4), (5), and (6) into equation (2) and letting $\beta=\pi$ produces:

$$\dot{\omega} + X\omega = \frac{Q_1 + rT_1(e^{-\mu_k \pi} - 1)}{J} \tag{7}$$

Where

$$X = \frac{C + Q_\omega}{J} \tag{8}$$

For the solenoid, there are two possible values for T_1, one with the brake on, and one with the brake off. In the case of the brake off, the solenoid cylinder does not exert a force on the plunger, thus T_1 equals to the weight of the plunger only.

$$T_1 = mg = 0.0657N \tag{9}$$

Since the entire "forcing function" is constant for the brake off interval, let the entire left side of equation (7) equal the constant "Brakeoff":

$$Brakeoff = \frac{Q_1 + rmg(e^{-\mu_k \pi} - 1)}{J} \tag{10}$$

After solving for the particular solution and an equation for $\omega(t)$, initial conditions were applied to each interval of the PWM signal. The first initial condition was $\omega(0)=0$, then each progressive increment used the final speed of the subsequent increment as its initial condition, yielding the following general equation for the "brake off" situation:

$$\omega(t) = [\omega(0) - \frac{Brakeoff}{X}]e^{-Xt} + \frac{Brakeoff}{X} \tag{11}$$

Similarly, with the solenoid activated, the maximum pull of the solenoid when the plunger is fully emersed in the cylinder is 80 ounces or 22.24 Newtons, thus the value of T_1 is changes for the "brake on" condition:

$$T_1=22.24\ \text{N} \tag{12}$$

Again, the forcing function for the "brake on" situation is a constant, thus the entire right side of equation (7) can now be represented by:

$$Brakeon = \frac{Q_1 + T_1 r\left(e^{-\mu_k \pi} - 1\right.}{J} \tag{13}$$

with the following equation for $\omega(t)$ for the "brake on":

$$\omega(t) = \left[\omega(0) - \frac{Brakeon}{X}\right] e^{-Xt} + \frac{Brakeon}{X} \tag{14}$$

It is important to emphasize that the "brake off" and "brake on" equations will be applied in an alternating fashion, at intervals corresponding to the PWM signal duty cycle.

b. Utilization of Matlab

To access the validity of the equations of motion, equations (11) and (17) were formatted into a Matlab program. The program was executed four times while varying the duty cycle and the coefficient of friction (μ_k) according to the expected values during actual testing. Each run started with an initial rotational speed of 4 rad/sec (38.2 RPM) that would simulate the movement of a human elbow joint. Although this

speed represents the upper end of speed expected by a human elbow, it was the lowest speed that minimized the effects of the noise inherent to the test tachometer. Additionally, each particular test was conducted for 20 seconds to properly measure the change in speed. The program also used the values of damping coefficient (C) and system inertia (J) from equations (5) and (6), respectively. In all, four runs were executed with two separate duty cycles (33% DC and 75% DC) and two different coefficients of friction (μ_k=0.25 for steel on aluminum disk and μ_k=0.4 for leather on aluminum disk).[Ref. 4: p. Z7] Table 4 summarizes the results of the four runs.

	33% DC μ_k=0.4	75% DC μ_k=0.4	33% DC μ_k=0.25	75% DC μ_k=0.25
Mean Speed (rad/sec)	0.6734	0.4632	0.6753	0.4640

Table 4: Theoretical Final Mean Speed Due to Solenoid Activation

As expected, using the brake material with the higher coefficient of friction resulted in a slightly greater speed decrease. But the most notable result is that for a given band brake material, a higher duty cycle produced a greater decrease in speed with little dependence on the coefficient of friction, which could be important in gaining consistent control even through long periods of wear. These theoretical results indicate the possibility for control of speed reduction for the motor driven test apparatus, and ultimately a joint on the Master Control Unit using the solenoid activated system. Figures 23 through 26 show the plots of theoretical speed versus time for each of the four trails, with the Matlab program included in Appendix D.

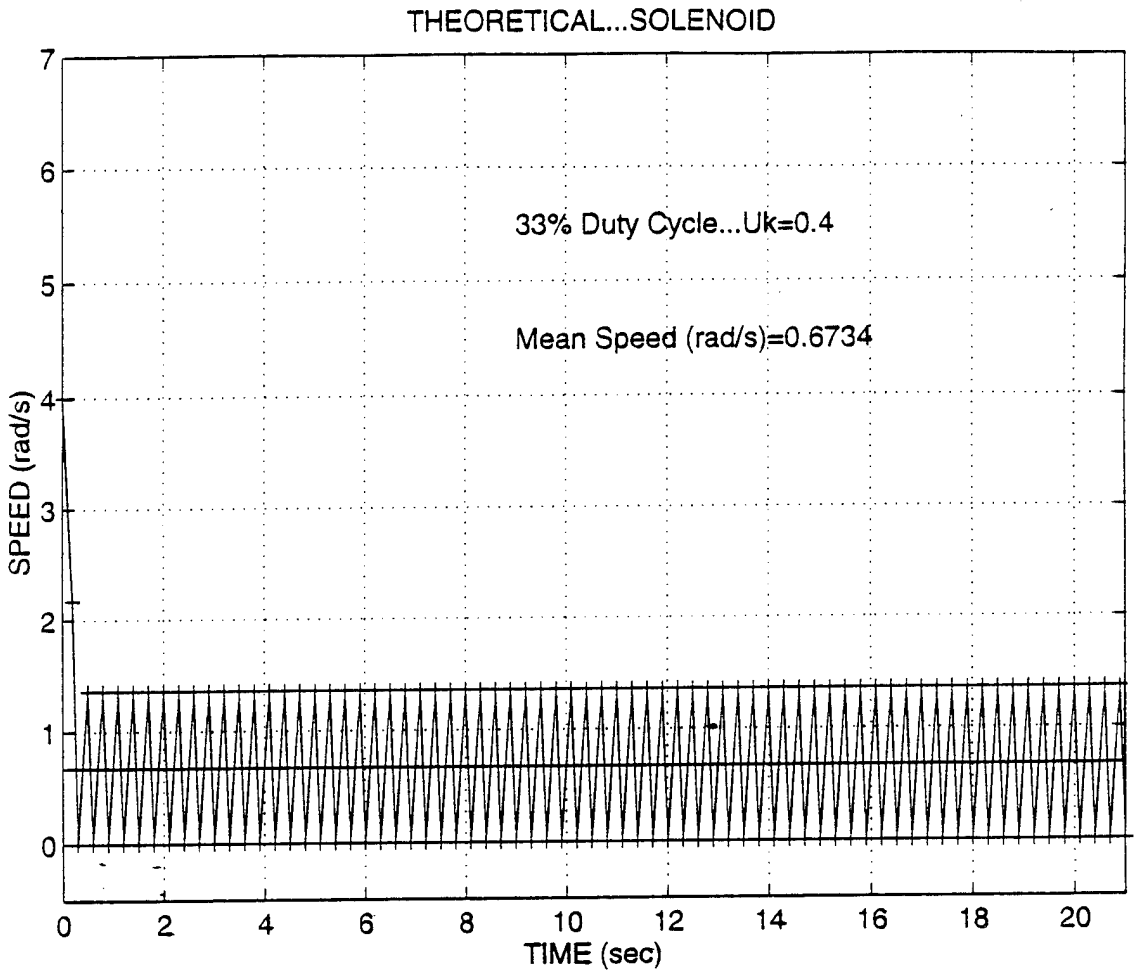

Figure 23: Theoretical Model of Solenoid Activation with Band Brake Material μ_k=0.4 and 33% Duty Cycle

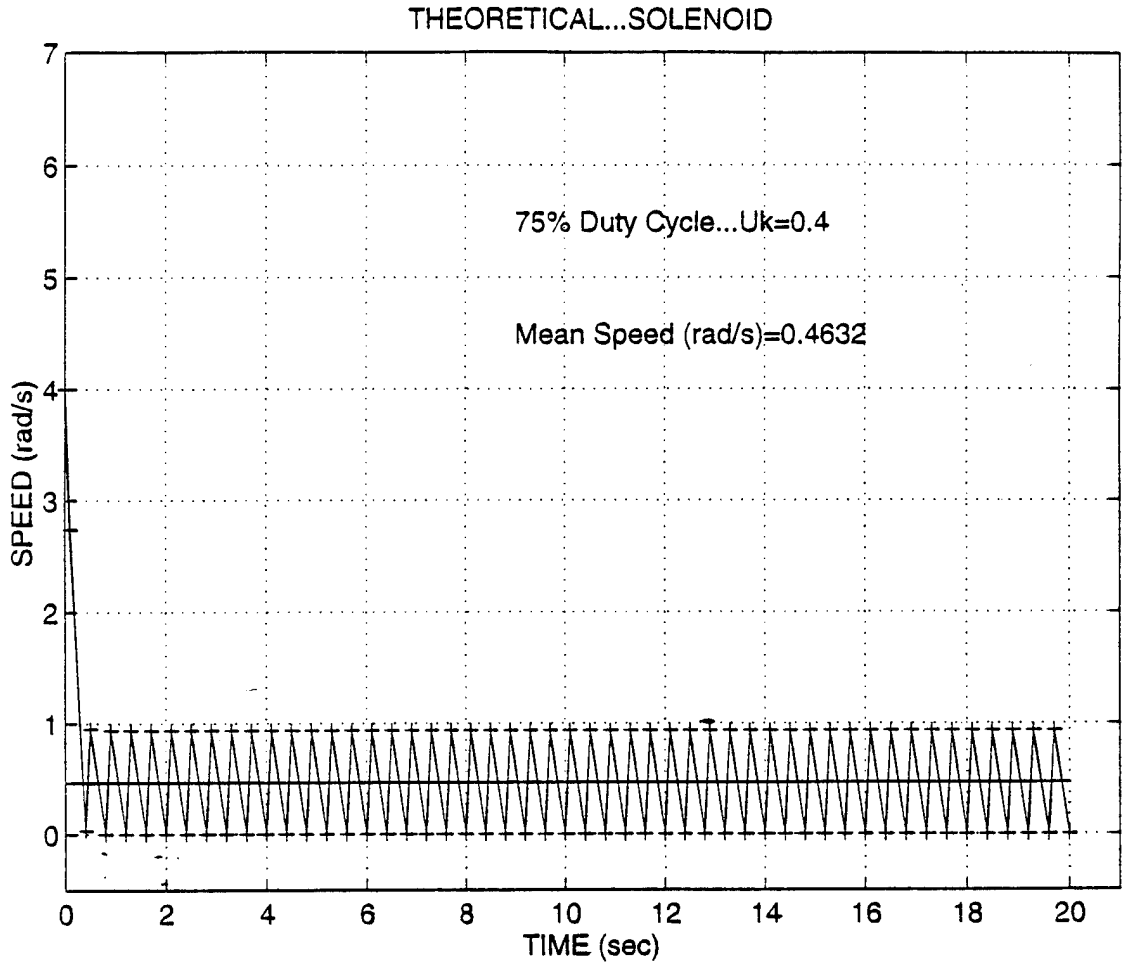

Figure 24: Theoretical Model of Solenoid Activation with Band Brake Material μ_k=0.4 and 75% Duty Cycle

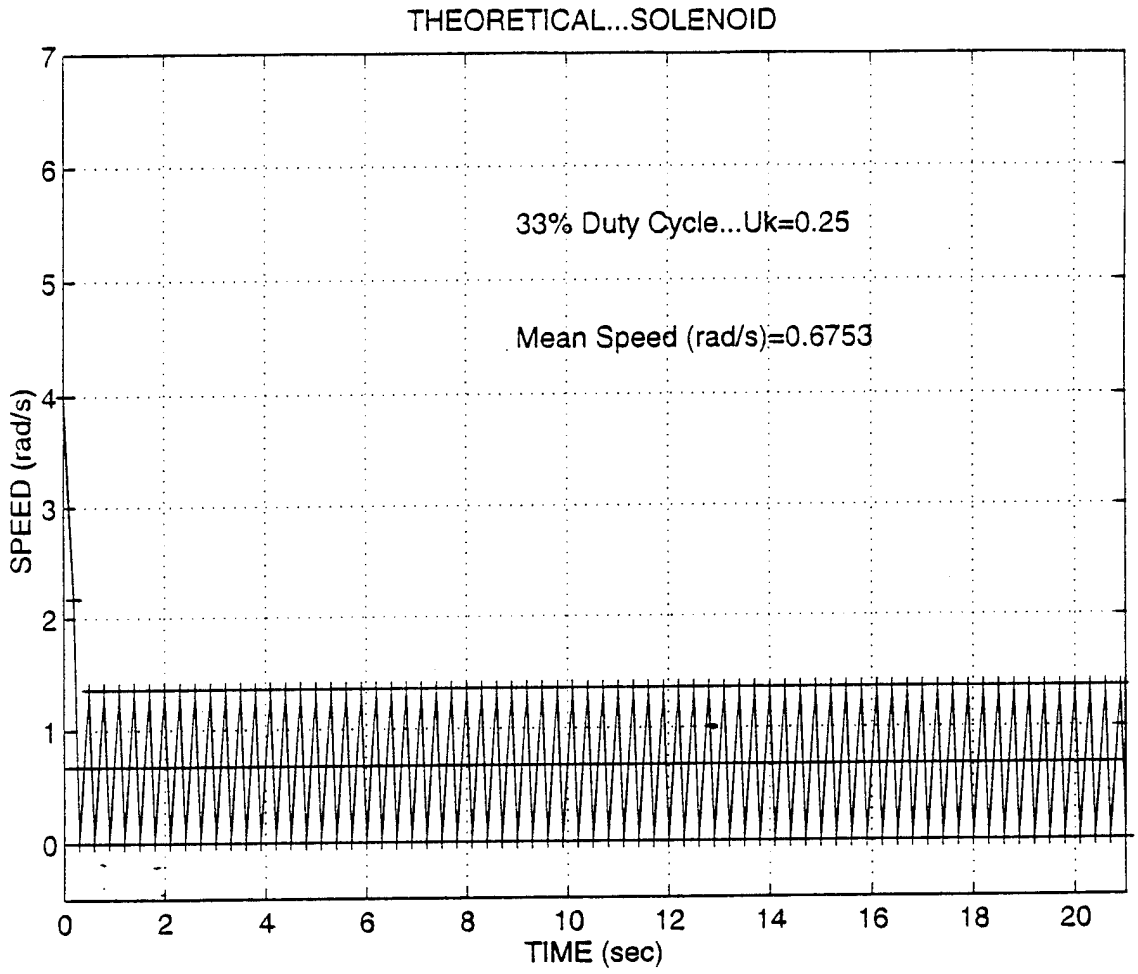

Figure 25: Theoretical Model of Solenoid Activation with Band Brake Material μ_k=0.25 and 33% Duty Cycle

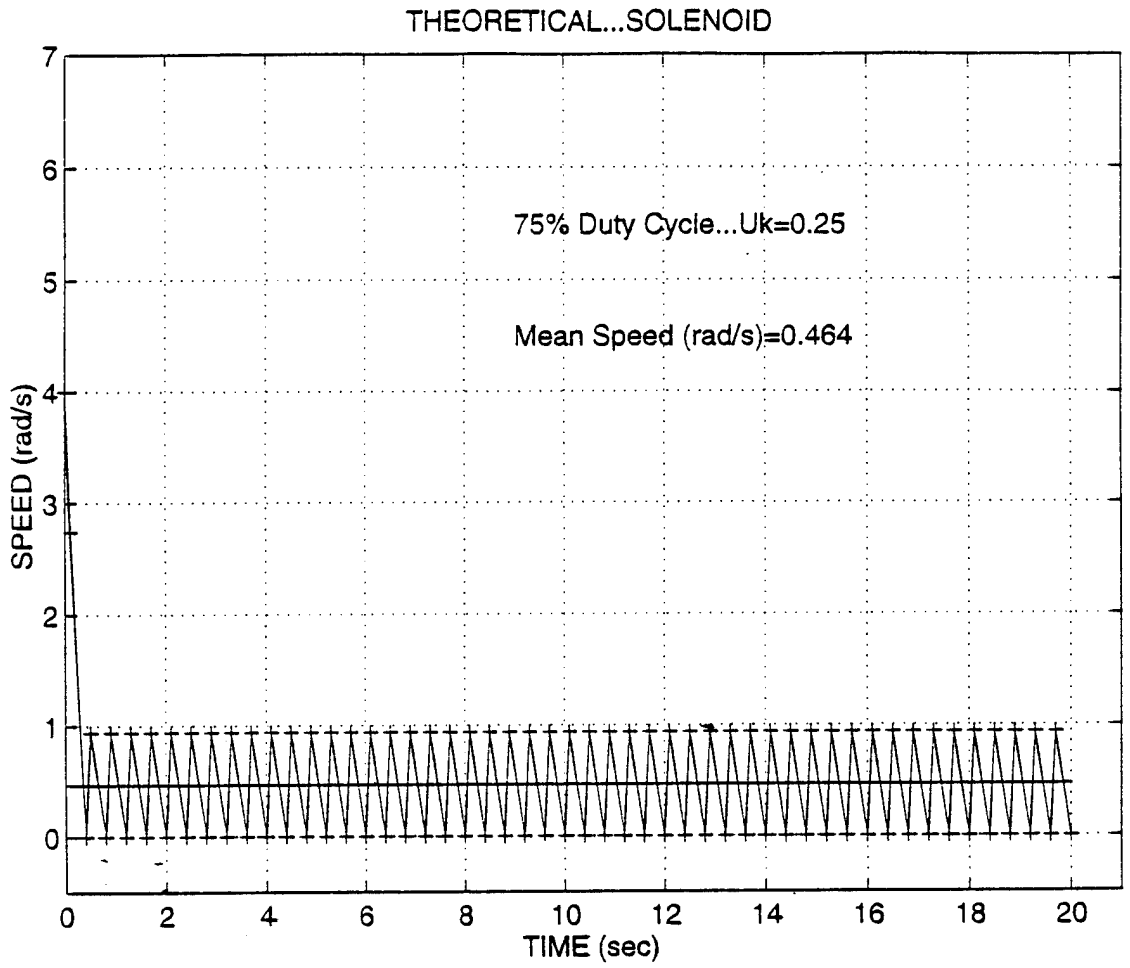

Figure 26: Theoretical Model of Solenoid Activation with Band Brake Material μ_k=0.25 and 75% Duty Cycle

4. Servomotor

a. Equations of Motion

The equation of motion for the servomotor, when activated is nearly identical to that of the solenoid except that the servomotor tension (T_1) can be varied by rotating the servomotor arm as indicated in Figure 27.

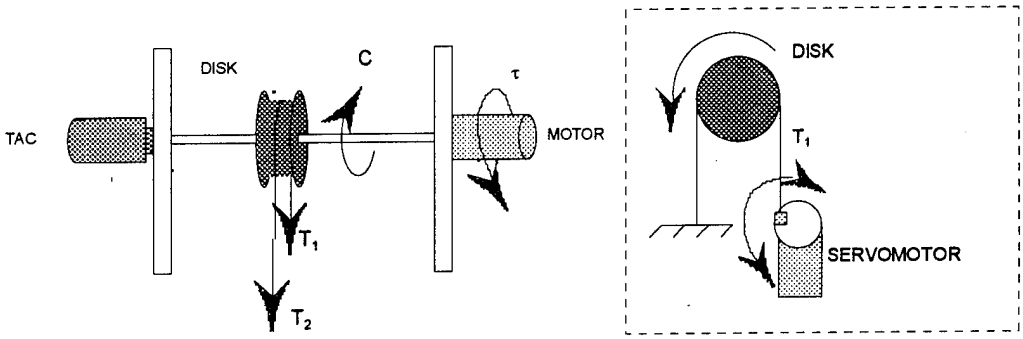

Figure 27: Theoretical Servomotor Free Body Diagram

When the servomotor is off (i.e., the arm is fully rotated upward to the 12 o'clock position) the tension is zero and the equation for $\omega(t)$ is:

$$J\dot{\omega} + C\omega = \tau \tag{15}$$

Once again using equations (4), (5), and (6) produces the following equation for $\omega(t)$:

$$\dot{\omega} + X\omega = \frac{Q_1}{J} \tag{16}$$

$$\omega(t) = \left[\omega(0) - \frac{Q_1}{XJ}\right]e^{-Xt} + \frac{Q_1}{XJ} \tag{17}$$

As stated above, when the band brake is activated, the equation is the same as equation (14), but with a variable tension (T_1) according to the band brake material used and the position of the servomotor arm. Tabulated values for the tensions (T_1) associated with the three expected band brakes are included in Appendix E.

b. Utilization of Matlab

Utilizing Matlab once again, four runs were completed with two variables, the band material friction coefficient (μ_k) and the position of the servo arm, which changed the corresponding tension(T_1). Each test run was conducted over a 20 second interval with an initial speed of ω=4 rad/s, and utilizing the system inertia (J) and damping coefficient (C) from equations (5) and (6), respectively. The coefficients of friction were chosen for a leather band (μ_k=.4) and a steel cord (μ_k=.25) activated to a servo arm angle of 30 degrees(T_1=5 Newtons) and 70 degrees (T_1=25 Newtons) to allow for an adequate separation of expected operational conditions. The results of the experimental computer simulations are summarized in Table (5), with the graph of each trial included as Figures 28 through 31. It is clear that by varying the position of the servomotor arm, the speed reduction can be controlled for a given band brake material. Also, as μ_k is increased, there is a greater decrease in speed. Thus the theoretical models of the

	30 deg μ_k=0.4	70 deg μ_k=0.4	30 deg μ_k=0.25	70 deg μ_k=0.25
Mean Speed (rad/sec)	1.673	1.603	1.685	1.631

Table 5: Theoretical Final Mean Speed Due to Servomotor Activation

solenoid and servomotor have shown sufficient evidence of the capability to control speed reduction by varying the PWM signal supplied to the activation device. The experimental runs however, did not give any indication as to which activation device might prove optimal. By conducting detailed tests using an actual test apparatus, the data should point to an optimal band brake configuration. Additional data analysis should lead to a relationship that can be used to dampen Master Control Apparatus movements proportional to the strain gauge signal.

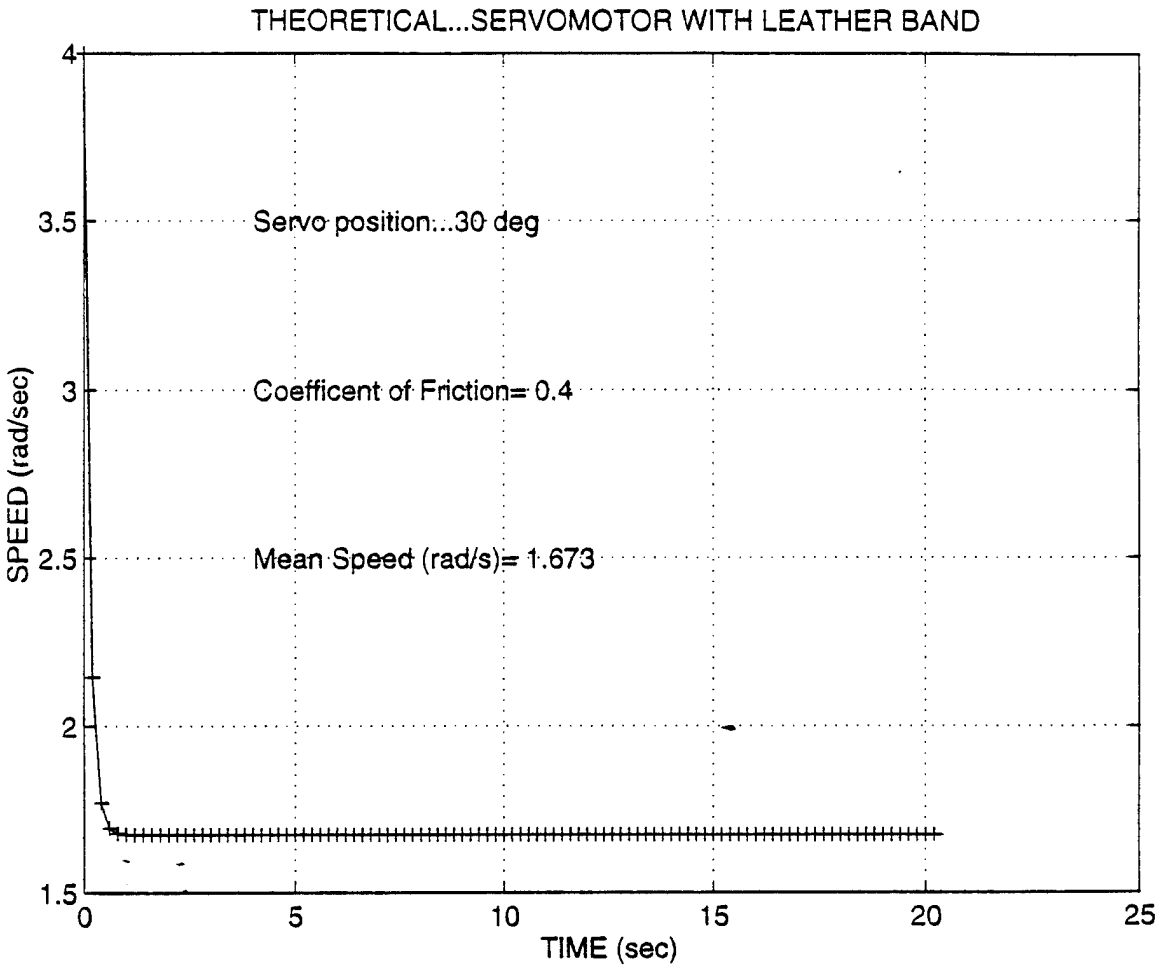

Figure 28: Theoretical Model of Servomotor Activation with Band Brake Material μ_k=0.4 and 30 Degree Arm Position

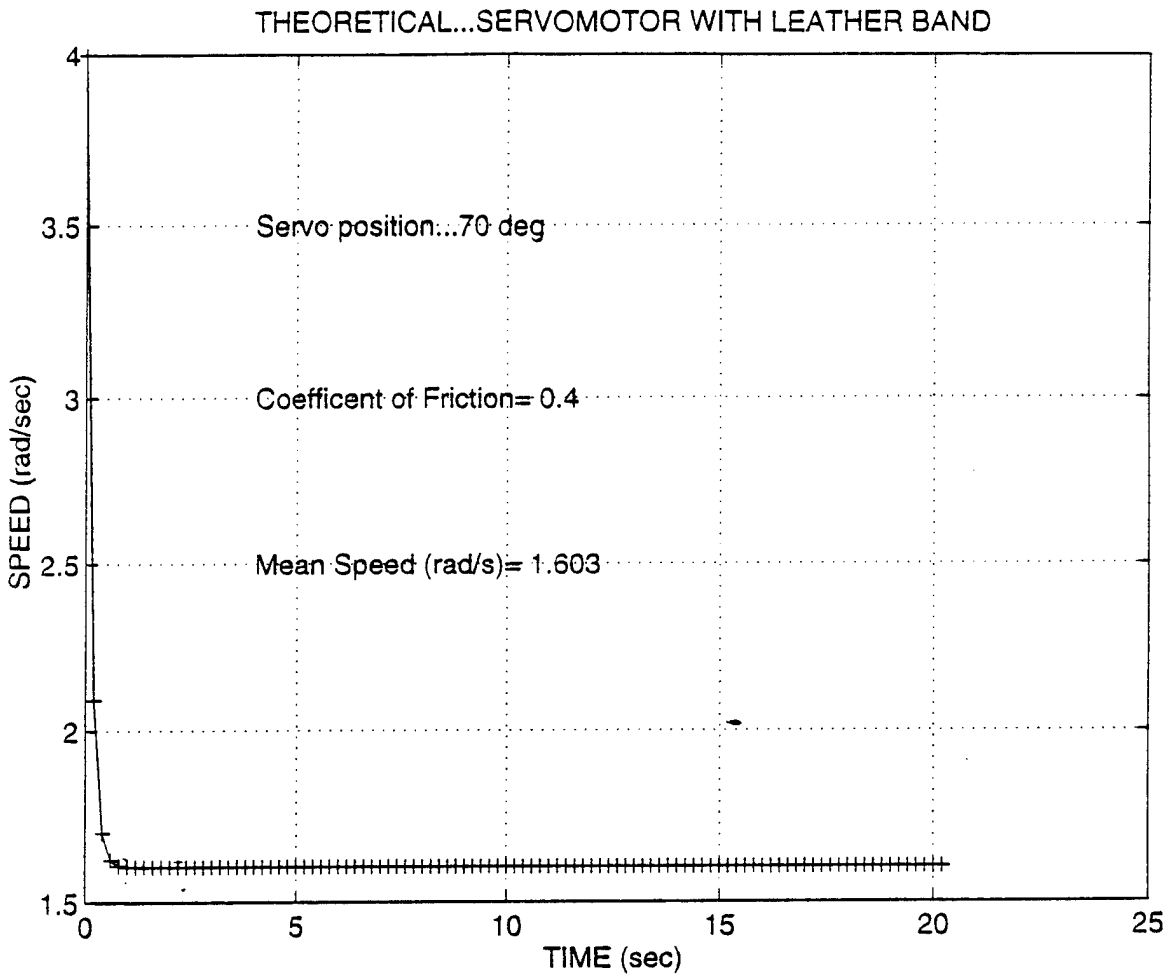

Figure 29: Theoretical Model of Servomotor Activation with Band Brake Material μ_k=0.4 and 70 Degree Arm Position

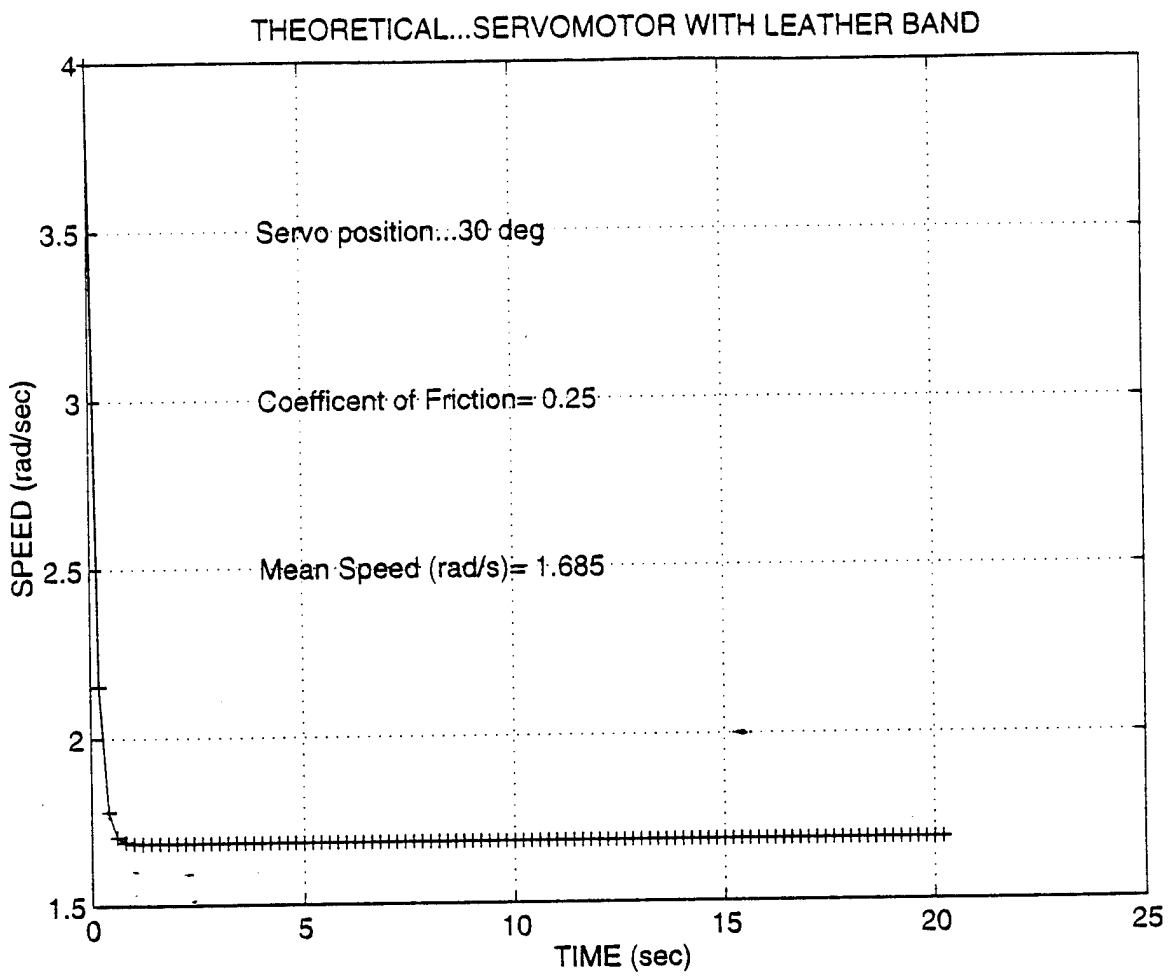

Figure 30: Theoretical Model of Servomotor Activation with Band Brake Material μ_k=0.25 and 30 Degree Arm Position

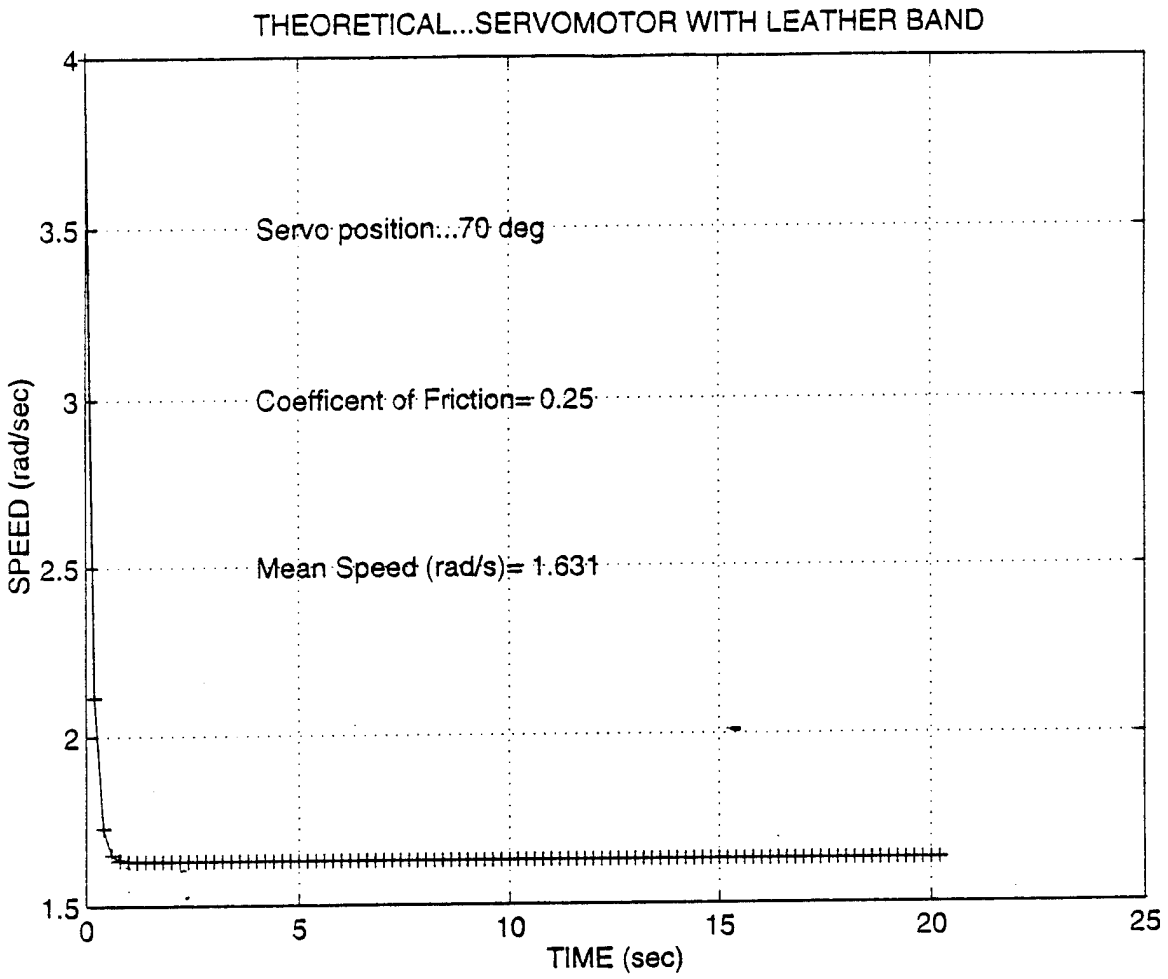

Figure 31: Theoretical Model of Servomotor Activation with Band Brake Material μ_k=025 and 70 Degree Arm Position

IV. EXPERIMENTAL TESTS

A. FORMAT FOR TESTS

In order to evaluate which band brake system meets the criterion as outlined in Section III.A.2., the test apparatus was constructed as hypothesized in the previous section, with the motor simulating the torque applied by a human operator on a particular joint. Care was taken to conduct all runs under identical conditions to ensure unbiased results, thus this experiment was completed in the following manner:

- Two activation devices were utilized: a 24 Volt DC solenoid and a 5 Volt DC Servomotor
- Each activation device was paired with one of three band brake materials: a 1/8 inch synthetic nylon band (Material 1), a 1/8 inch leather band (Material 2), or a 1/16 inch, 6 strand steel wire (Material 3).
- Six runs were conducted per configuration: one with the motor and disk rotating freely without any band attached, one with the band material attached to the disk, but in the "off" mode, and four runs at various settings to determine each configuration's speed controllability.
- The motor armature voltage, V_a=10.04 volts for all runs.
- Each run started with the same initial rotational speed throughout the tests for a given material configuration.
- Tachometer voltage data was recorded by the MacIntosh Data Acquisition System (every 50 millisecond to avoid biasing) and compiled using the MATLAB computer program.
- Due to the noise inherent to the tachometer/MacIntosh setup, speed data collected over the activation increment was averaged and compared to the average initial speed.

- Data will be presented in two graphs: Mean Speed versus Duty Cycle for the solenoid, and Mean Speed versus Servo Position for the servomotor. This data will be analyzed to obtain an optimal configuration that allows for a predictable and controllable speed reduction that can be related to a system damping.

B. TEST MODEL SETUP

1. Test Apparatus

Before proceeding to the details of the tests, a full description of the apparatus is necessary. The apparatus was constructed from aluminum and placed on a stand that would allow the various activation systems to be interchanged (see Figure 32). At one end of the shaft is a 27 volt DC Shunt motor that rotates the disk. The speed of the disk was monitored by the tachometer at the opposite end. Located directly under the disk is an attachment built to fix one end of the band material, and interchangeable supports for the solenoid/servomotor activation device.

1. Solenoid Setup

The solenoid chosen for the test runs was a 24 volt DC, 59 Ohms, continuous duty, pull type, tubular solenoid with a maximum pull of 80 ounces and an operating frequency ranging from 1 to 12 Hertz. Further operating characteristics are provided in Appendix E, along with ordering information for these and various other solenoid types.

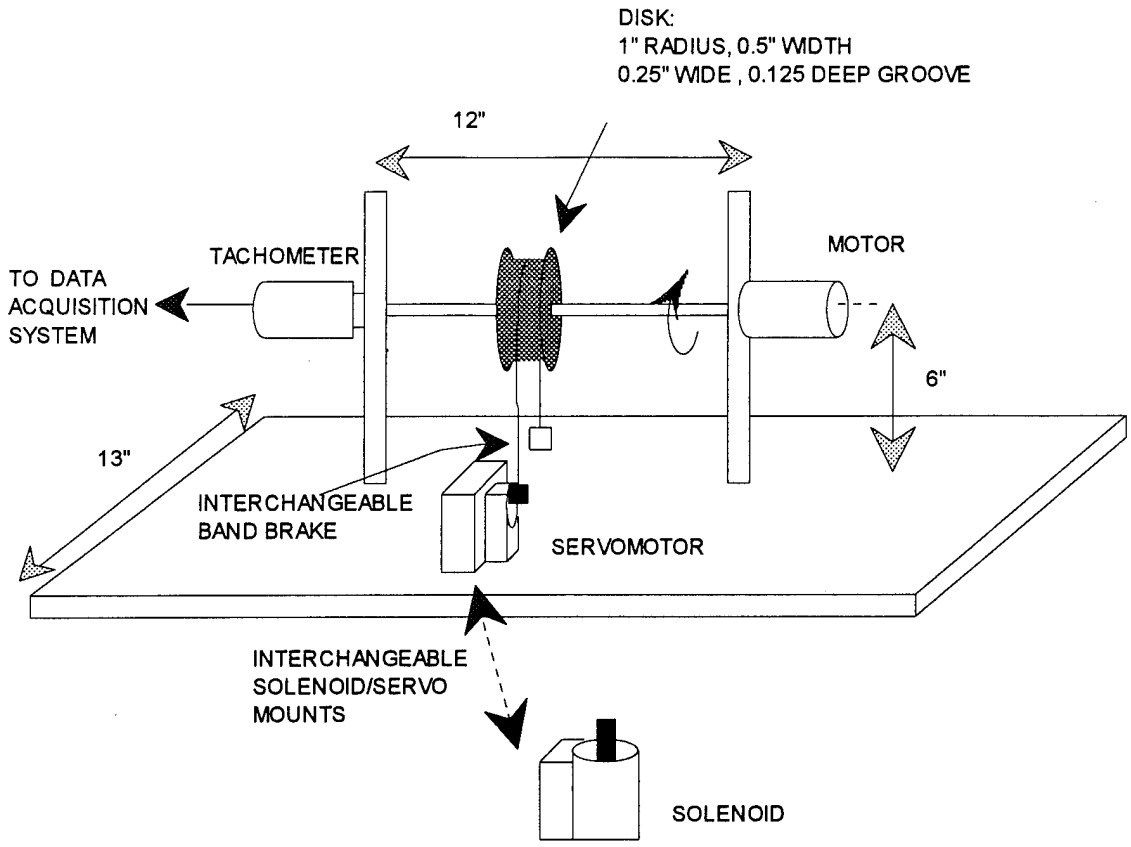

Figure 32: Model Test Apparatus

A 20 volt, 0.25 amp signal powers the solenoid, while it's activation rate is controlled by a relay that is triggered by in accordance with the duty cycle of a 5 volt square wave transmitted from a function generator or the MacIntosh computer. Each time the square wave reaches its peak value, the relay triggers the solenoid, activating the pulling force for the duration of the 5 volt square wave peak. Thus, as the duty cycle increases, the solenoid activates the brake for a greater portion of the period (see Figure 33).

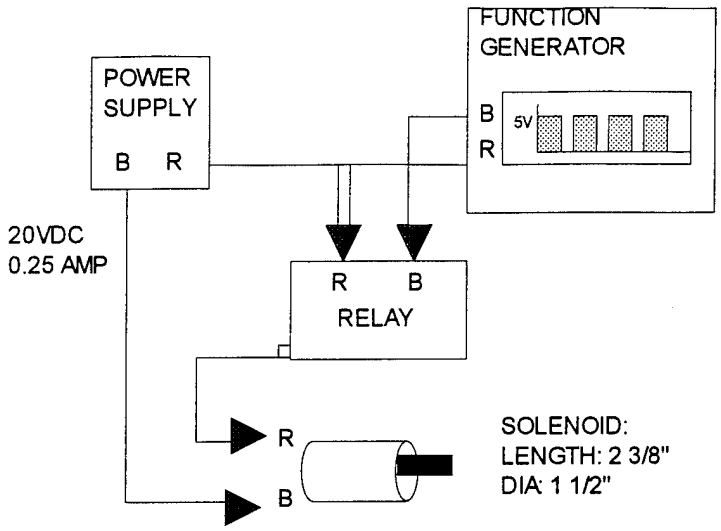

Figure 33: Solenoid Setup

3. Servomotor Setup

The servomotor setup is similar to the solenoid in that it is powered by a 5 volt DC power supply, with arm angle position controlled directly by the duty cycle of a 5 volt square wave from the function generator or MacIntosh computer. The servo simply takes the average voltage of the square wave and rotates the arm to any position, from 200 degrees clockwise through to 160 degrees. The servomotor setup is illustrated in Figure 34.

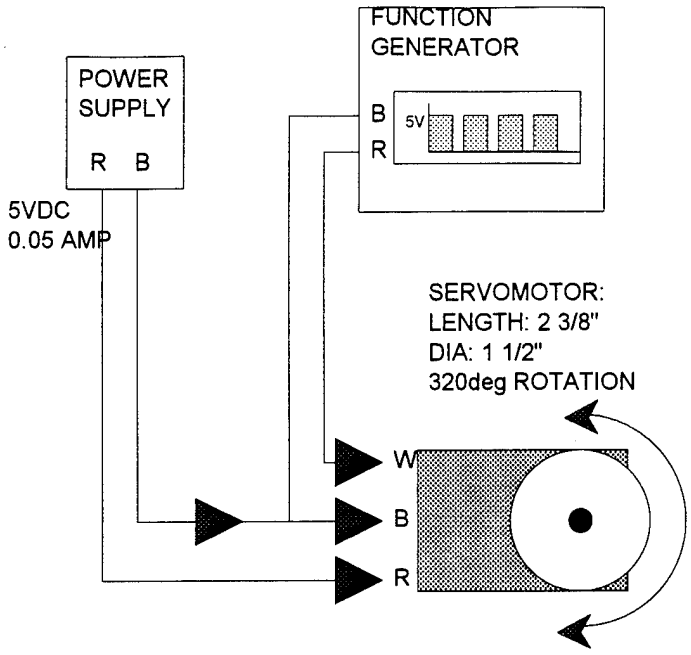

Figure 34: Servomotor Setup.

C. APPARATUS VERIFICATION

1. Overview

Prior to starting the experimental band brake activation runs, an examination of the apparatus was conducted in order to correctly characterize the system and it's components. For example, since the specific documentation on the motor and/or tachometer was unavailable, tests were conducted to calibrate the tachometer and define the speed-torque relationship for the motor. The information from these tests was used to refine the theoretical model, as well as gain a better understanding of the system response.

2. Tachometer Verification

Because the test tachometer provided only an output voltage, tests were conducted to calibrate the output voltage with the known shaft speed in order to obtain the tachometer constant K_T. Ten runs were conducted with the test apparatus performance parameters monitored with the following devices:

- Shaft RPM measured with a separate tachometer
- Motor armature current (i_a) measured with a current probe.
- Armature Resistance (r_a) measured using an ohmmeter.
- Armature voltage (V_a) as obtained from the motor with a voltmeter.
- Tachometer voltage (V_T) with an oscilloscope

Table 6 lists the data accumulated from the ten runs. For each run the shaft speed (radians/second) was divided by the tachometer voltage (volts) in order to obtain the tachometer voltage constant (K_T). Then the tachometer constants for each run were averaged to produce a final tachometer constant to be used throughout the testing process. This value was determined to equal:

$$K_T = 25.97 \text{ rad/s/volt.} \tag{18}$$

V_T	SHAFT RPM	SHAFT (RAD/S)	i_a	V_a	K_V (RAD/S/V)
1.66	413	43.23	0.480	30.04	26.04
1.45	360	37.70	0.470	26.23	26.00
1.29	308	32.20	0.470	23.30	24.96
1.14	282	29.53	0.456	21.08	25.90
0.99	248	25.97	0.456	18.36	26.23
0.85	210	21.99	0.448	16.08	25.87
0.68	170	17.80	0.448	13.75	26.18
0.47	122	12.76	0.434	9.65	27.15
0.30	72	7.54	0.424	6.72	25.13
0.20	50	5.24	0.416	5.30	26.20

Table 6: Apparatus Verification Data

3. Motor Characteristics

The motor utilized for all experiments was a 27 volt DC Shunt motor. To understand the dynamics of the system it was important to document the torque versus speed profile of the motor for any given armature voltage (V_a). A Shunt motor can be simplified into the following diagram, which when analyzed yields equation 19 [Ref. 5: p 444].

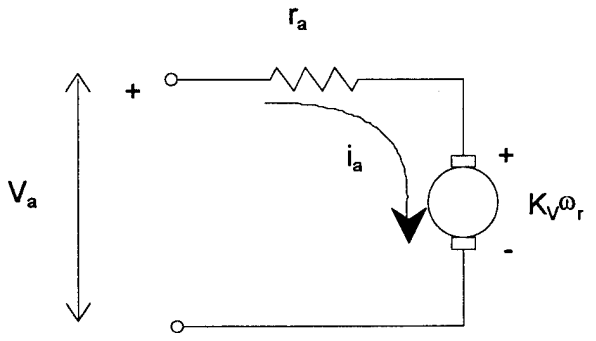

Figure 35: Simplified Circuit Analysis of a Shunt Motor

$$i_a = \frac{V_a - K_V r_a}{r_a} \tag{19}$$

Each value above could be measured, except for the motor proportionality constant (K_V). In evaluating this constant, it can also be written that:

$$\tau = K_V i_a \tag{20}$$

Thus, by substituting equation (19) into equation (20), K_V may be determined by the following relationship:

$$K_V = \frac{V_a - i_a r_a}{\omega_r} \tag{21}$$

Using the data from Table (6) and averaging the values of each calculated K_V, an overall motor proportionality constant (K_V) was determined:

$$K_V = 0.624 volts \cdot s / rad \tag{22}$$

Next, by supplying the motor a constant armature voltage while varying the resistance on the rotating disk, the armature current (i_a) and rotational speed (ω) were measured. A torque (τ) versus rotational speed (ω) graph was then obtained utilizing equation (20) and the following:

$$\tau = \frac{K_V V_a - K_V^2 \omega_r}{r_a} \tag{23}$$

The data for these tests is tabulated in Table 7 with the supporting graph illustrated as line (2) of Figure 36. These results can also be used to show that the performance of the motor can be predicted for any armature voltage. By letting V_a=30.04 volts in Equation 23 and plotting Torque versus Speed for two values ω_r=0, then τ=0, line (1) was obtained. Note that the line shifts, depending on the armature voltage, but the slope remains virtually the same. Thus these results reinforce our theoretical model and furnish a method of predicting the torque of the motor under various conditions.

RUN	RPM	ω (RAD/SEC)	$\tau = \frac{K_V V_a - K_V^2 \omega_r}{r_a}$	$\tau = K_V i_a$
1	175	18.33	0.235 Nm	0.272 Nm
2	170	17.8	0.270 Nm	0.301 Nm
3	160	16.76	0.330 Nm	0.351 Nm
4	151	15.80	0.399 Nm	0.386 Nm

Table 7: Torque Versus Rotational Speed Data. Armature Voltage V_A=13.7 volts

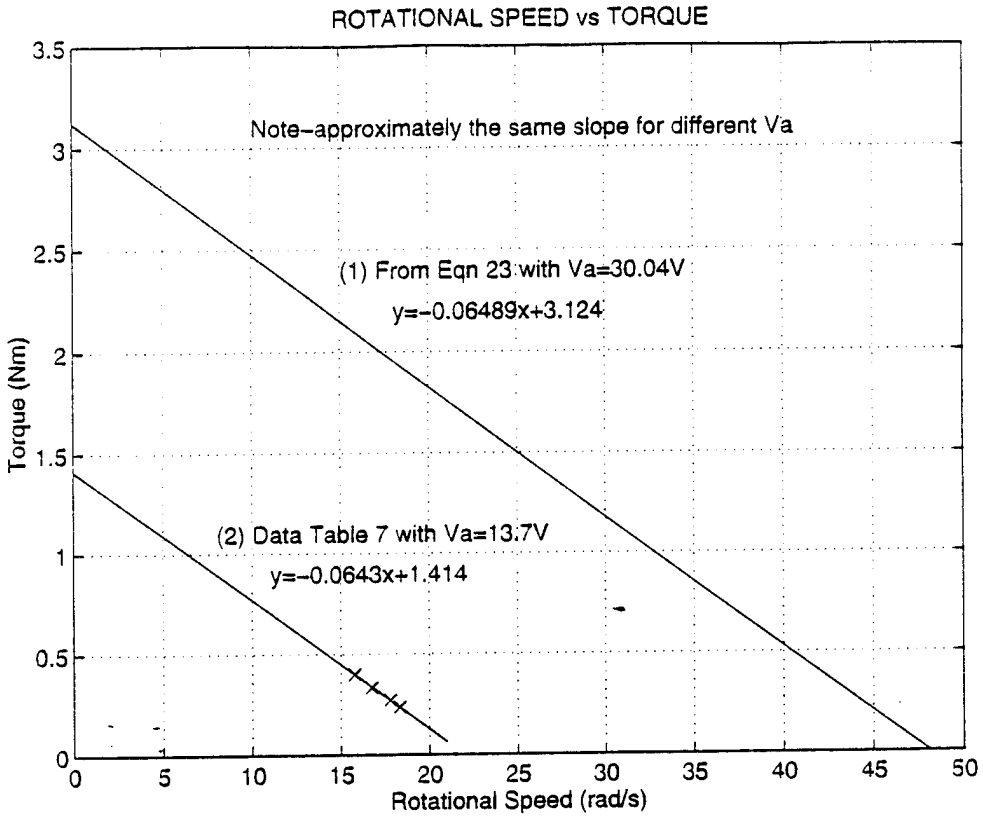

Figure 36: Torque versus Rotational Speed

4. Dynamics Tests

a. System Damping Coefficient (C)

For the dynamics tests, the motor was run with V_a=10.02 volts with the motor rotating the disk without any resistance. Under these conditions, the system can be represented by the following:

$$J\dot{\omega} + C\omega = \tau = \frac{K_V V_a - K_V^2 \omega}{r_a} \tag{24}$$

At steady state, the rotational acceleration $\dot{\omega} = 0$, thus from Figure 37 the steady state tachometer voltage (V_T) was averaged for two run resulting in the following value for ω:

$$= K_T V_T = (25.97 rad \cdot volt / s) \cdot (0.499 volts) = 12.96 rad / s \tag{25}$$

Thus from Equations 24 and 25:

$$\tau = 0.20 Nm \tag{26}$$

Which yields

$$C = \frac{\tau}{\omega} = \frac{0.20 Nm}{12.96 rad / s} = 0.016 N \cdot m \cdot s \tag{27}$$

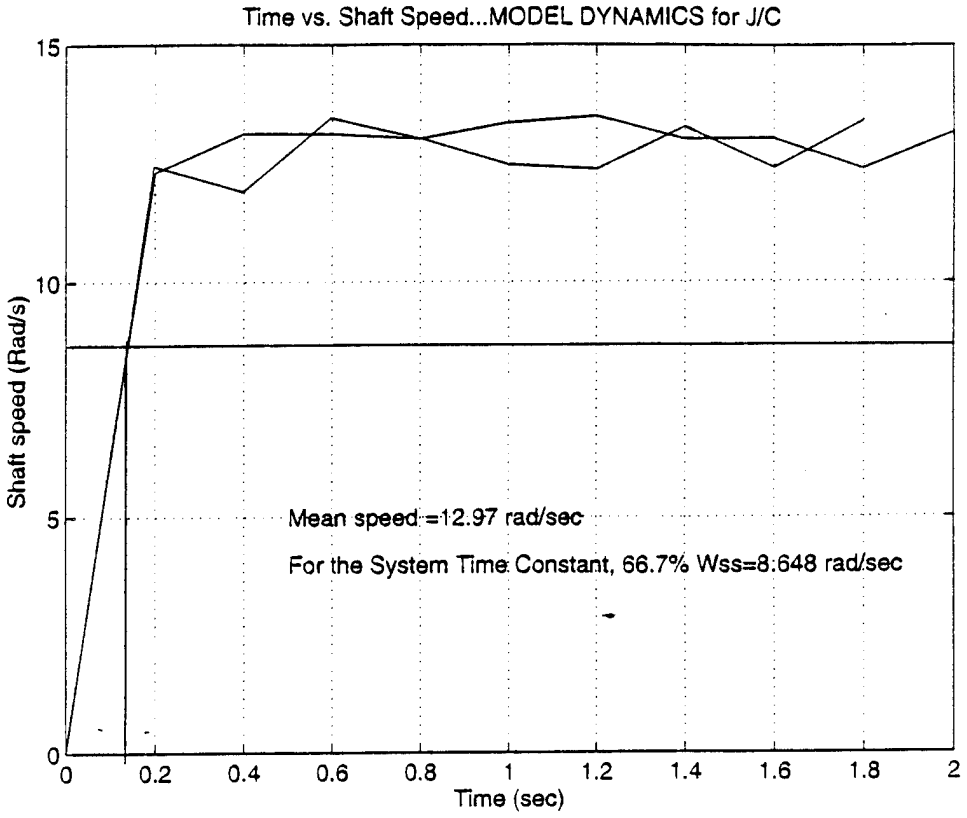

Figure 37: Motor Experimental Test Run for Model Verification

b. System Inertia (J) Estimate

In estimating the system inertia (J), the idea was to determine the system time constant from the experimental test runs that were used in the previous section. In modeling the system with the determined value of the damping coefficient (C), Equation 24 becomes:

$$J\dot{\omega} + C\omega = \frac{K_V V_a - K_V^2 \omega}{r_a} = 1.04 + 0.065\omega \tag{28}$$

Rearranging the equation yields the following ordinary differential equation (ODE):

$$\dot{\omega} + \frac{0.081\omega}{J} = \frac{1.04}{J} \tag{29}$$

By solving the ODE for the particular solution with initial condition $\omega(0)=0$, the following solution is obtained:

$$\omega(t) = 12.84(1 - e^{\frac{-0.081t}{J}}) \tag{30}$$

In evaluating the system time constant, the rotational speed at 66.7 percent of the steady state speed was determined from Figure 33. Utilizing the information that ω_T=8.65 rad/sec and the corresponding time constant value, T=0.125 sec produced the following method for determining J:

$$\frac{0.081}{J} = \frac{1}{T} = \frac{1}{0.125\text{sec}} \Rightarrow J = 0.010 kg \cdot m^2 \tag{31}$$

D. BAND BRAKE MATERIALS

1. Overview

As mentioned earlier, the three band brake materials are a 1/8 inch synthetic nylon band (Material 1), a 1/8 inch leather band (Material 2), and a 1/16 inch, 6 strand

steel wire (Material 3). These materials were tested to evaluated their impact on the force feedback model's ability to control the speed of a joint on the master. Although other obvious characteristics of the three materials will be analyzed in the test results discussion, assessing each material's actual coefficient of friction was done as a means of further understanding the response of the system.

2. Coefficient of Friction (μ_k) Estimate

During the solenoid test runs for each material, two initial runs were completed; one with the motor apparatus rotating freely without any band brake material attached, and one with the solenoid configuration in the "off" position. These runs can be analyzed by the following two equations:

Without band brake:
$$J\dot{\omega} + C\omega = \tau \tag{32}$$

With band brake:
$$J\dot{\omega} + C\omega = \tau - T_1 r(e^{-\mu_k \beta}) \tag{33}$$

Thus it should be obvious that the difference in the torques of Equations 32 and 33 is the band brake term: $T_1 r(e^{-\mu_k \beta})$. The idea is two determine the difference in rotational speeds with and without the band brake for each material, convert this speed differential into a torque differential using an equation similar to those of Figure 36, and solve for the coefficient of friction (μ_k) using the band brake term. From the solenoid test runs (Section IV.F) the following data was accumulated:

CONDITION	MATERIAL 1	MATERIAL 2	MATERIAL 3
WITHOUT BRAKE	13.40 (rad/sec)	13.40 (rad/sec)	13.40 (rad/sec)
WITH BRAKE	13.26 (rad/sec)	12.85 (rad/sec)	12.88 (rad/sec)

Table 8: Test Apparatus Rotational Speeds Without and With the Band Brake Material (Solenoid Setup)

Next, by using Equation 23, a Rotational Speed versus Torque graph was produced for the operating condition of V_a=10.04 volts (Figure 38). Each rotational speed was converted to a corresponding torque, then a torque differential was determined for each material (Table 9). The torque differential was then utilized to solve for the coefficient of friction in the following manner:

$$\Delta\tau = T_1 r(e^{\mu_k \beta} - 1) \tag{34}$$

As an example of solving for μ_k for Material 1:

$$0.01Nm = (0.0657kg)(9.81\frac{m}{s^2})(.0254m)(e^{\mu_k \pi} - 1) \tag{35}$$

$$0.61 = e^{\mu_k \pi} - 1 \tag{36}$$

$$\ln(1.61) = \mu_k \pi \tag{37}$$

$$\mu_k = 0.15 \text{ for Material 1} \tag{38}$$

The results for each material are presented in Table 9.

	MATERIAL 1	MATERIAL 2	MATERIAL 3
ω=13.4 rad/sec and Torque τ=0.174 Nm for each run without the brake			
ω (RAD/SEC) WITH BRAKE	13.26	12.85	12.88
TORQUE (Fig 38)	0.184 Nm	0.210 Nm	0.208 Nm
TORQUE DIFFERENTIAL	0.010 Nm	0.036 Nm	0.034 Nm
μ_k	0.15	0.37	0.35

Table 9: Coefficient of Friction Data

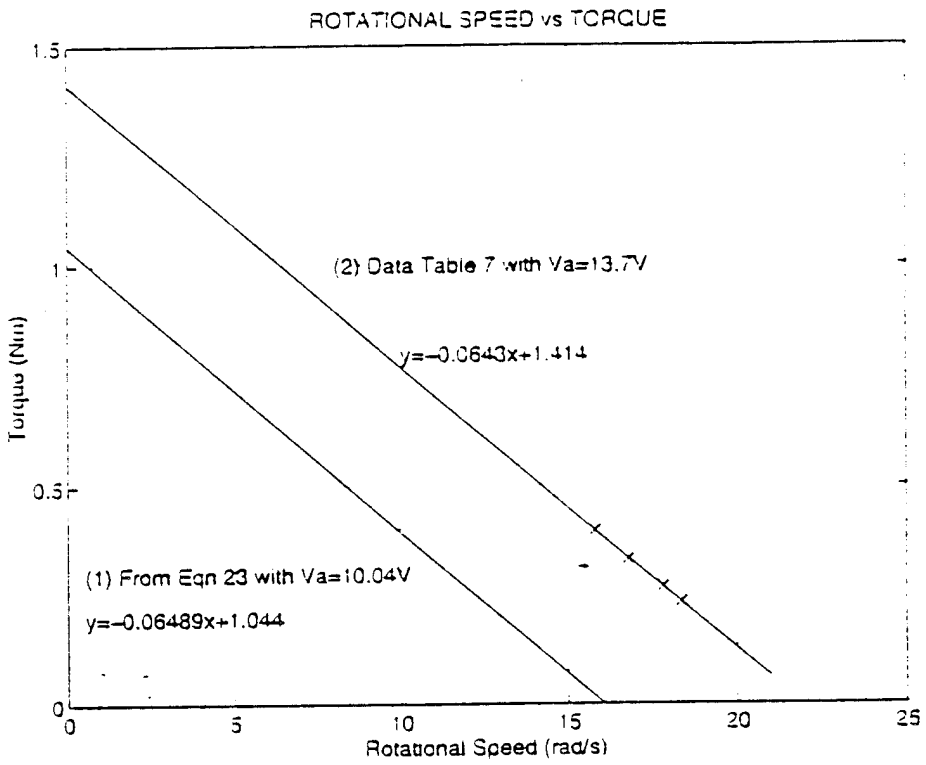

Figure 38: Rotational Speed versus Torque for Coefficient of Friction Estimation

The results of the coefficient of friction (COF) estimations show that the values obtained closely compare with the values obtained from Reference 4, as utilized in the Theoretical Model section (Section III.B). As one might expect, Material 1, the synthetic nylon band, had the lowest COF, and Material 2, the leather band, the highest. The impact of these values will be shown in analyzing the experimental test results.

E. SERVOMOTOR EXPERIMENTAL RUNS

1. Results

With the test apparatus configured in accordance with the servomotor setup of Figure 32 and 34, the six test runs were conducted for each band brake material under the provisions set forth in Section IV.A. The tests for each material will be presented in three sets of five separate graphs, one set for each band brake material. The first graph of each set will be an accumulation of all tests runs at various servomotor arm positions. Due to the nature of the black and white graphics in this print, dissemination of the data is difficult, but the graph does display the variance in speed control for each servomotor setting. The second graph provides a display of mean tachometer voltage from the test apparatus rotating freely without any band brake attached and tachometer voltage with the brake attached, but in the "off "position. The third and fourth figures are a collection of the initial and final mean tachometer voltages at the indicated servomotor arm positions. For each graph contained in these two figures, the system was allowed to reach an initial steady state speed (with the servomotor "on," and the arm at zero

degrees) for approximately two seconds, then the servomotor arm was immediately rotated to its ordered position. Data was extracted for approximately three seconds after arm rotation while the system reached a final steady state speed. The initial and final mean tachometer voltages are indicated on each graph, and can be converted to rotational speed (ω) by multiplying by the tachometer constant, K_T=25.97 rad/sec/volt. In the event of disk arrest due to band brake activation, the servomotor was rotated back to zero after about two seconds, allowing the system to regain its initial velocity. Additionally, the initial speed run data was collected for an extended five seconds and superimposed over the test data as a reference in measuring the speed (tachometer voltage) differential. The fifth and final graph for each material consist of an accumulation of the mean final speed versus servomotor position, which collectively demonstrates the range of speed controllability for the various servomotor positions. By fitting a second order curve to this data, a request for a mean speed can be correlated to a servomotor position. This is a necessary process in converting the strain gauge voltage from the slave (upon opposition to the intended motion) into a speed reduction or damping effect on the Master Control Apparatus. The results of each test run are represented in tabular form in Table 10, and graphically in the following order:

- Material 1: Figures 39-43
- Material 2: Figures 44-48
- Material 3: Figures 49-53

	MATERIAL 1		MATERIAL 2		MATERIAL 3	
RUN NUMBER	ARM POS (DEG)	TAC VOLTAGE (V)	ARM POS (DEG)	TAC VOLTAGE (V)	ARM POS (DEG)	TAC VOLTAGE (V)
INITIAL	0	0.5152	0	0.485	0	0.5043
Run 1	45	0.5072	20	0.4378	15	0.4637
Run 2	60	0.4725	45	0.2892	25	0.4544
Run 3	85	0.1794	60	0.0793	40	0.4018
Run 4	95	0.0002	80	0.0184	50	0.0154

Table 10: Summary of Servomotor Test Results

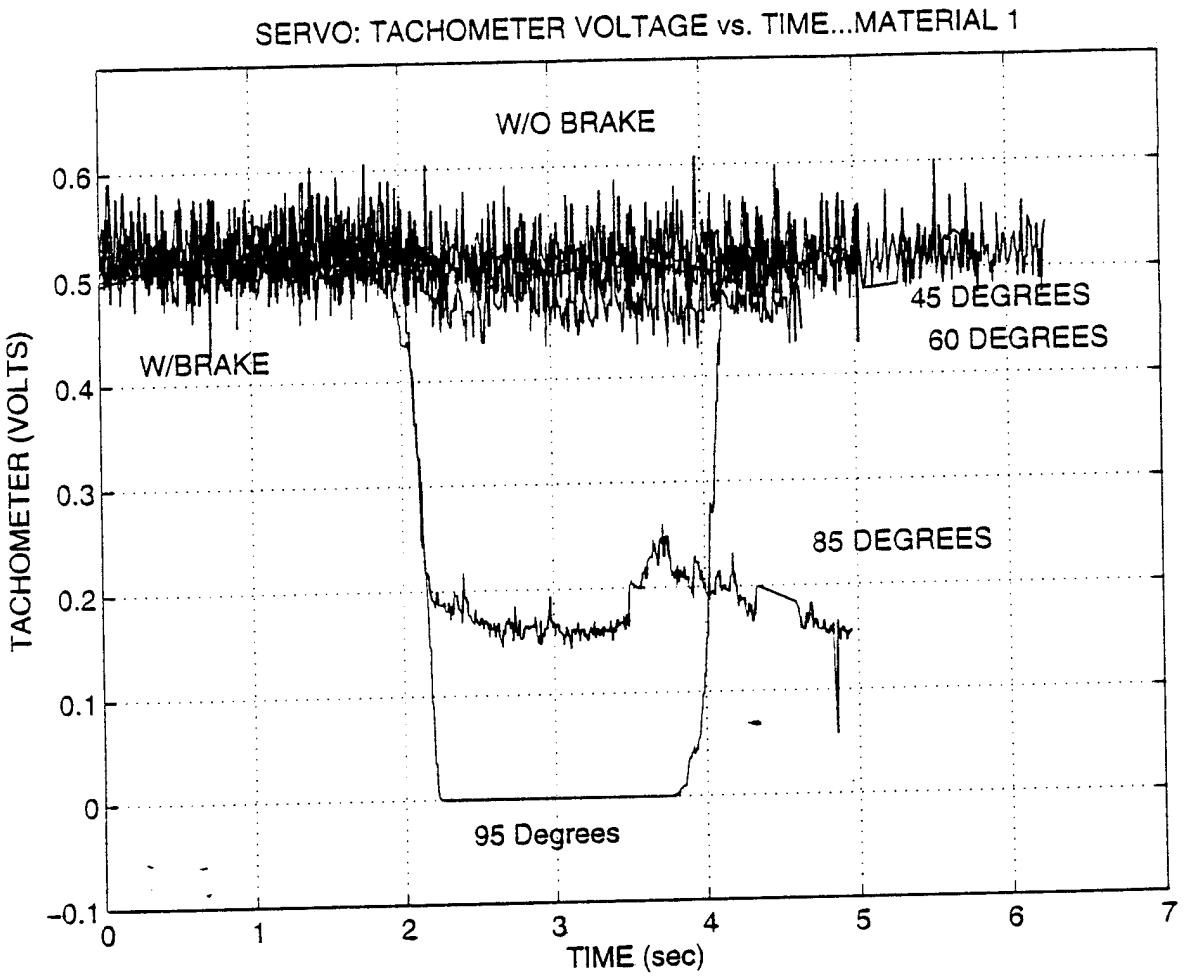

Figure 39: Material 1 - Tachometer Voltage versus Time for all Servomotor Positions

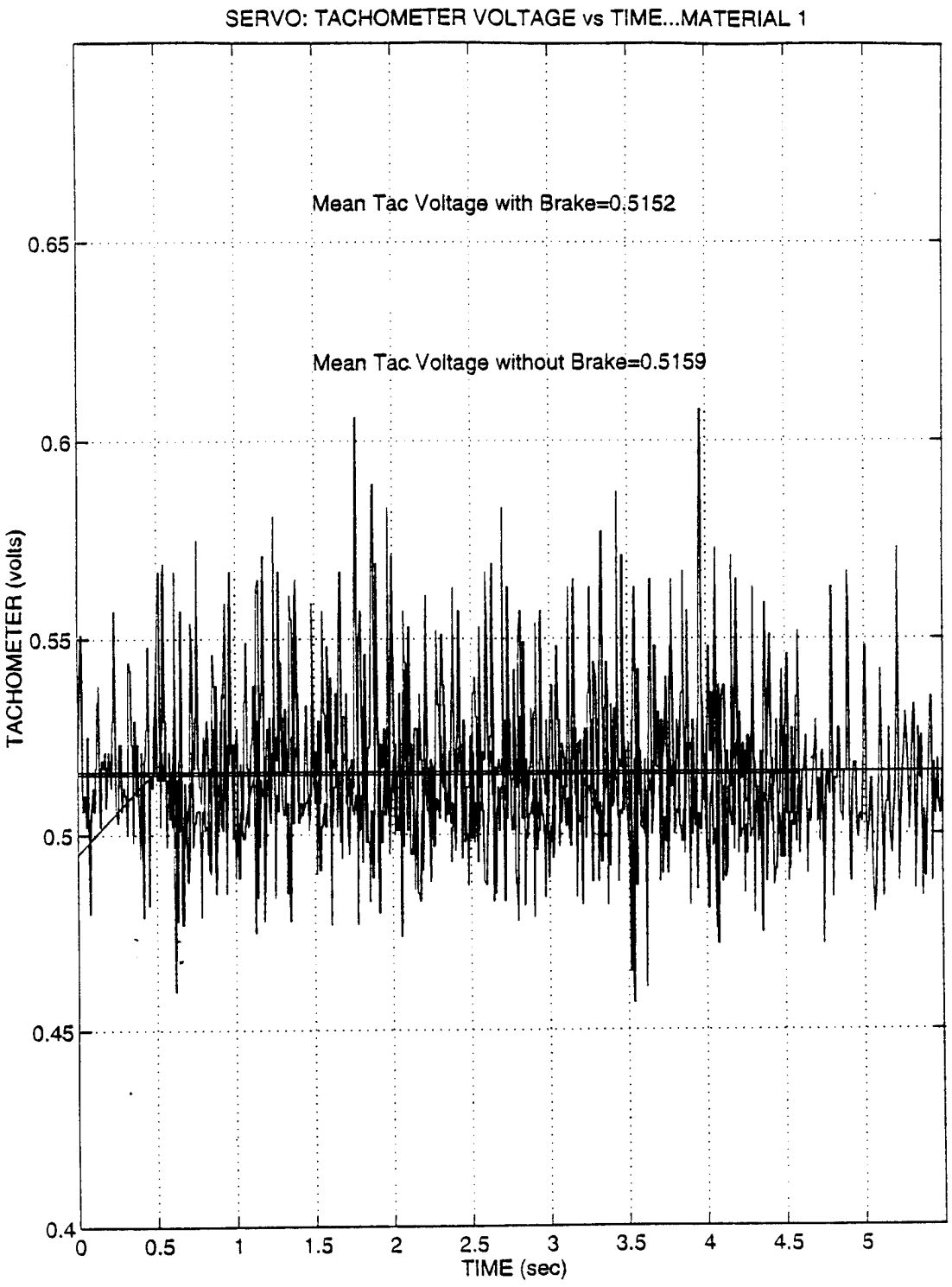

Figure 40: Material 1 - Mean Rotational Speed With and Without Band Brake (Servomotor)

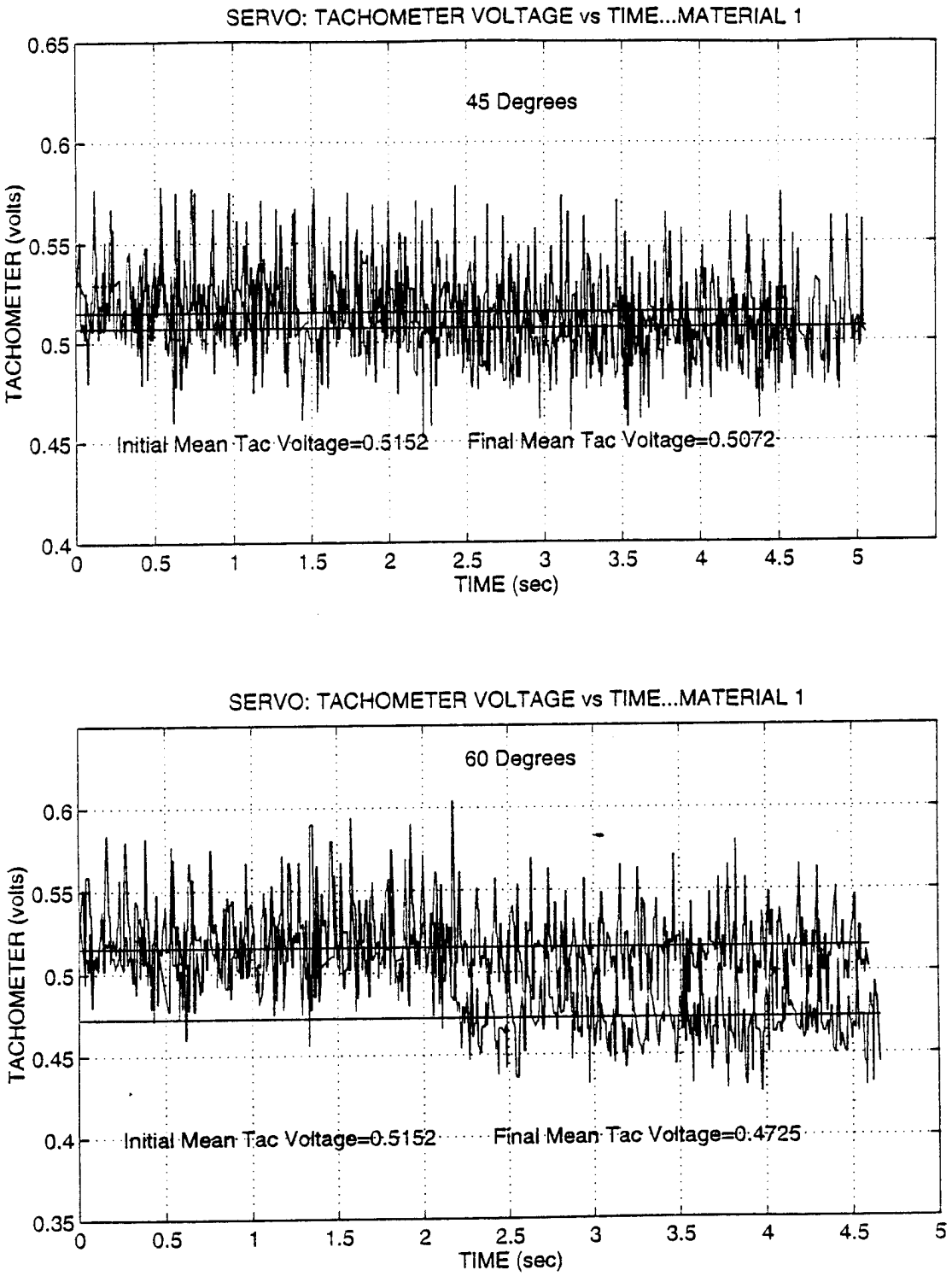

Figure 41: Material 1 - Tachometer Voltage Differential for Servomotor Positions of 45 and 60 Degrees, respectively

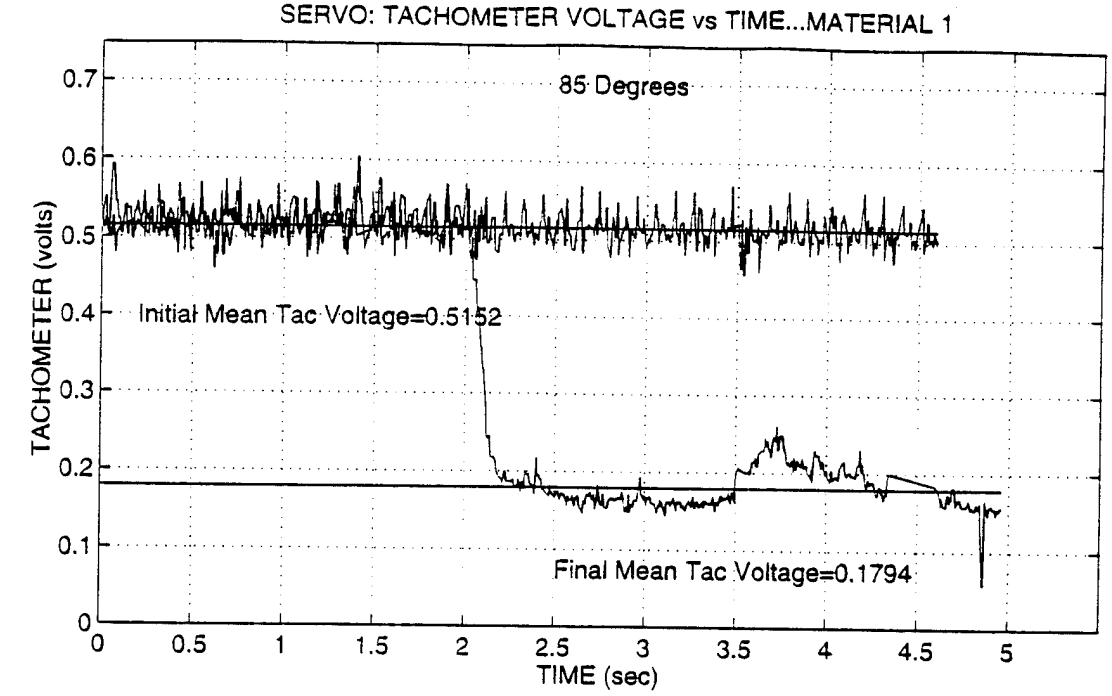

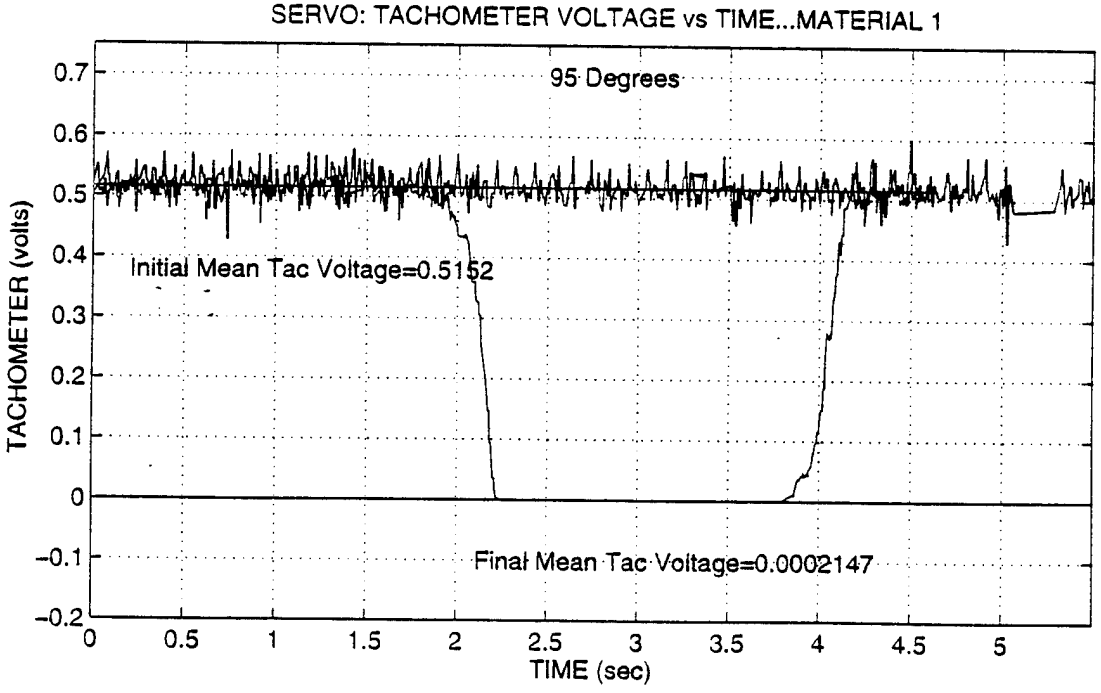

Figure 42: Material 1 - Tachometer Voltage Differential for Servomotor Positions of 85 and 95 Degrees, respectively

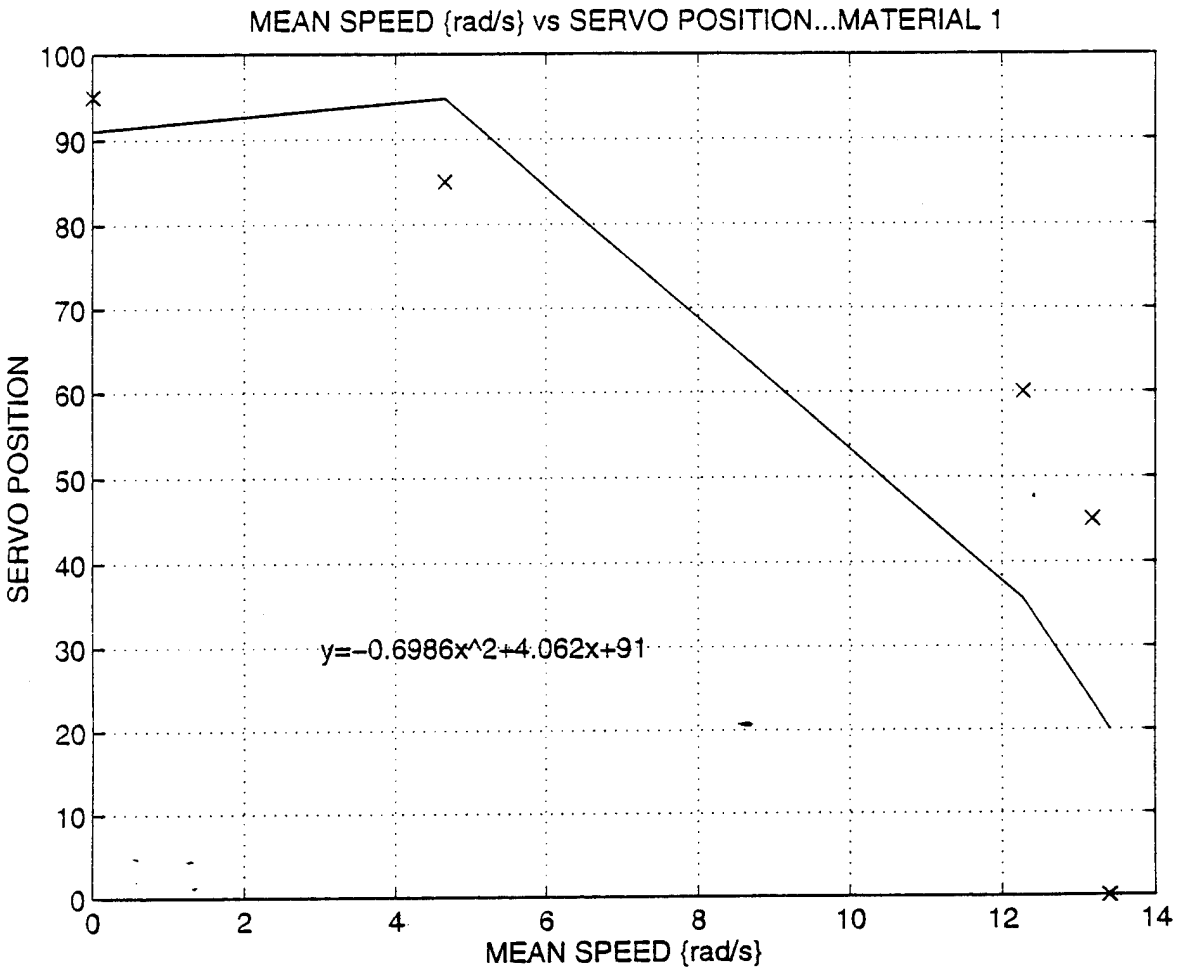

Figure 43: Material 1 - Mean Rotational Speed versus Servomotor Arm Position

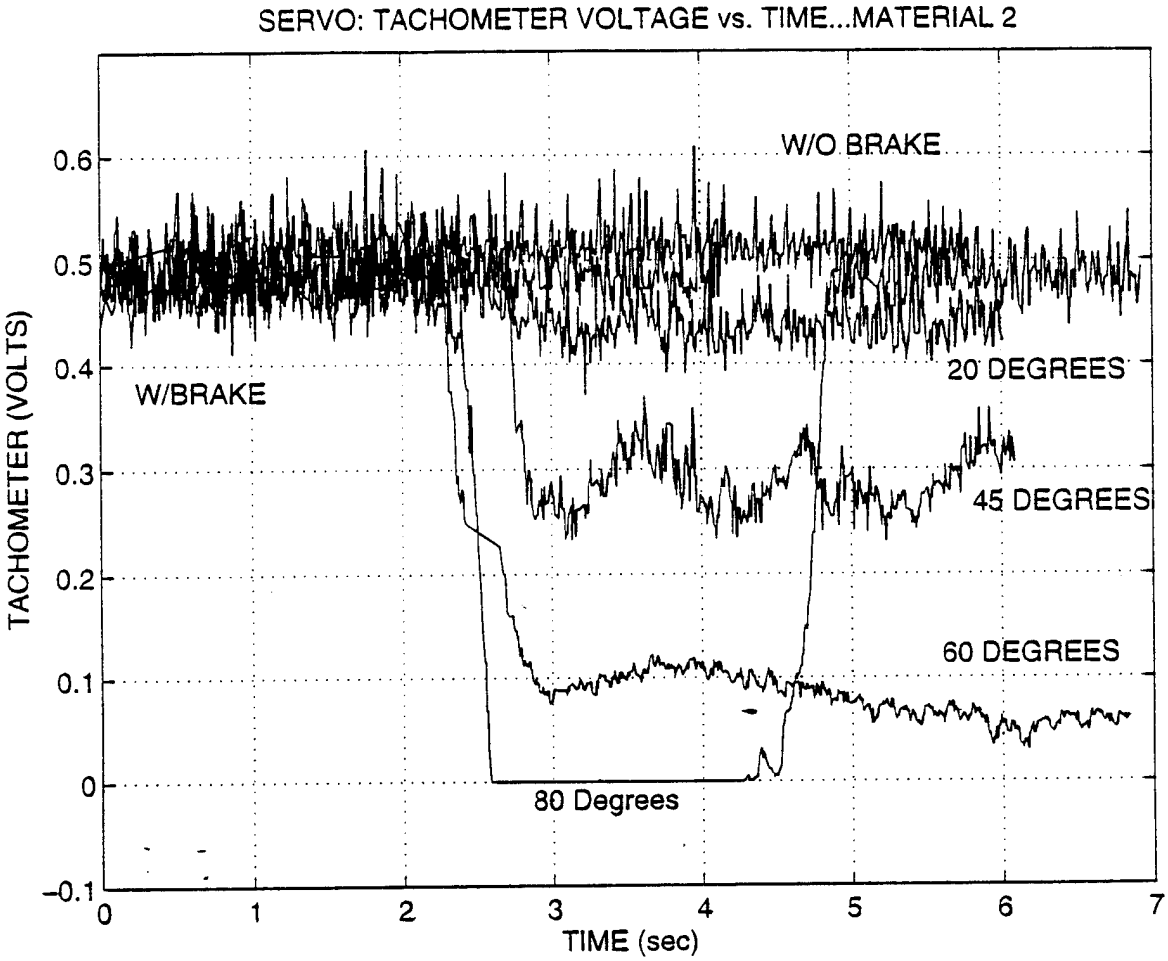

Figure 44: Material 2 - Tachometer Voltage versus Time for all Servomotor Positions

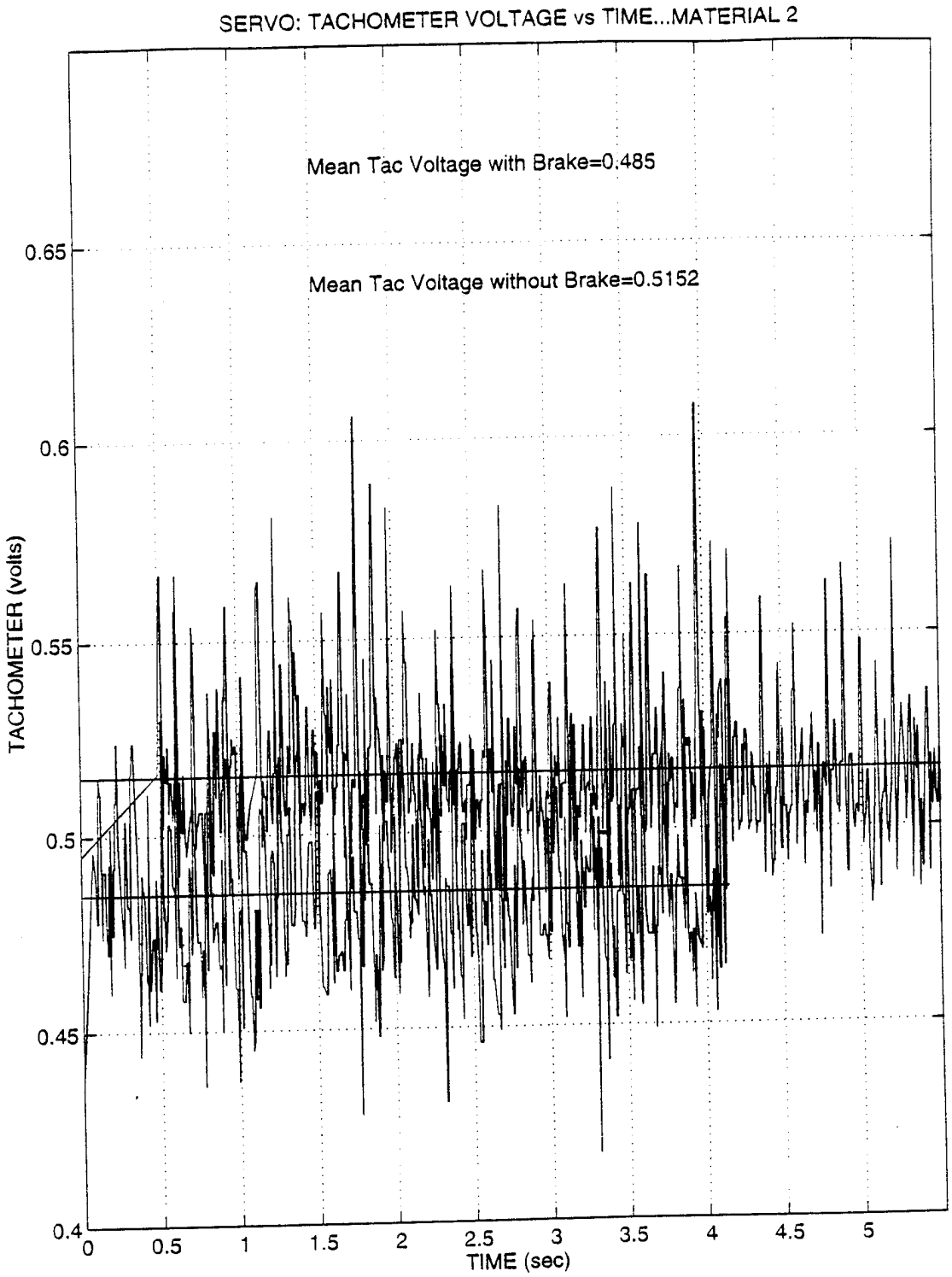

Figure 45: Material 2 - Mean Rotational Speed With and Without Band Brake (Servomotor)

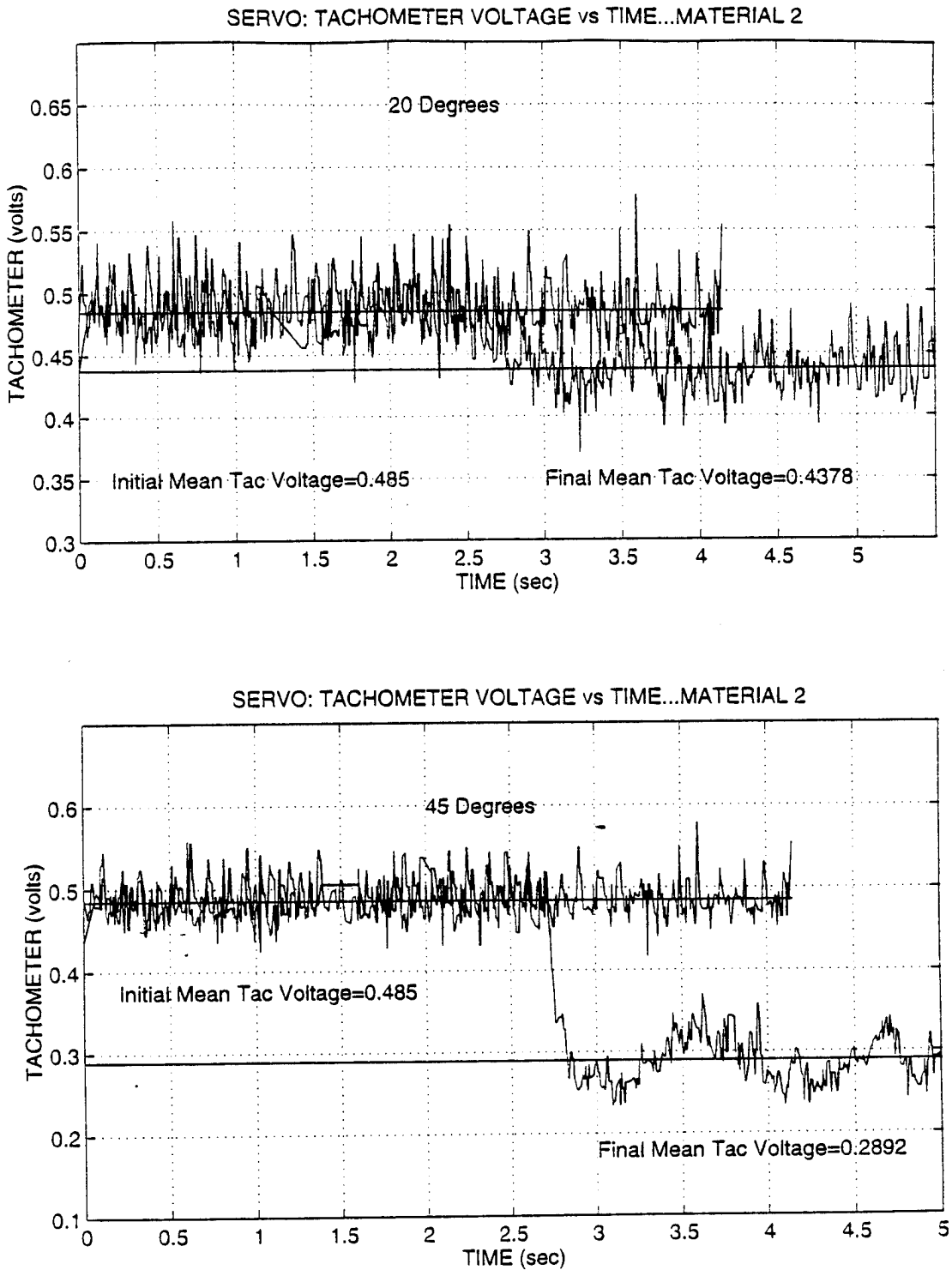

Figure 46: Material 2 - Tachometer Voltage Differential for Servomotor Positions of 20 and 45 Degrees, respectively

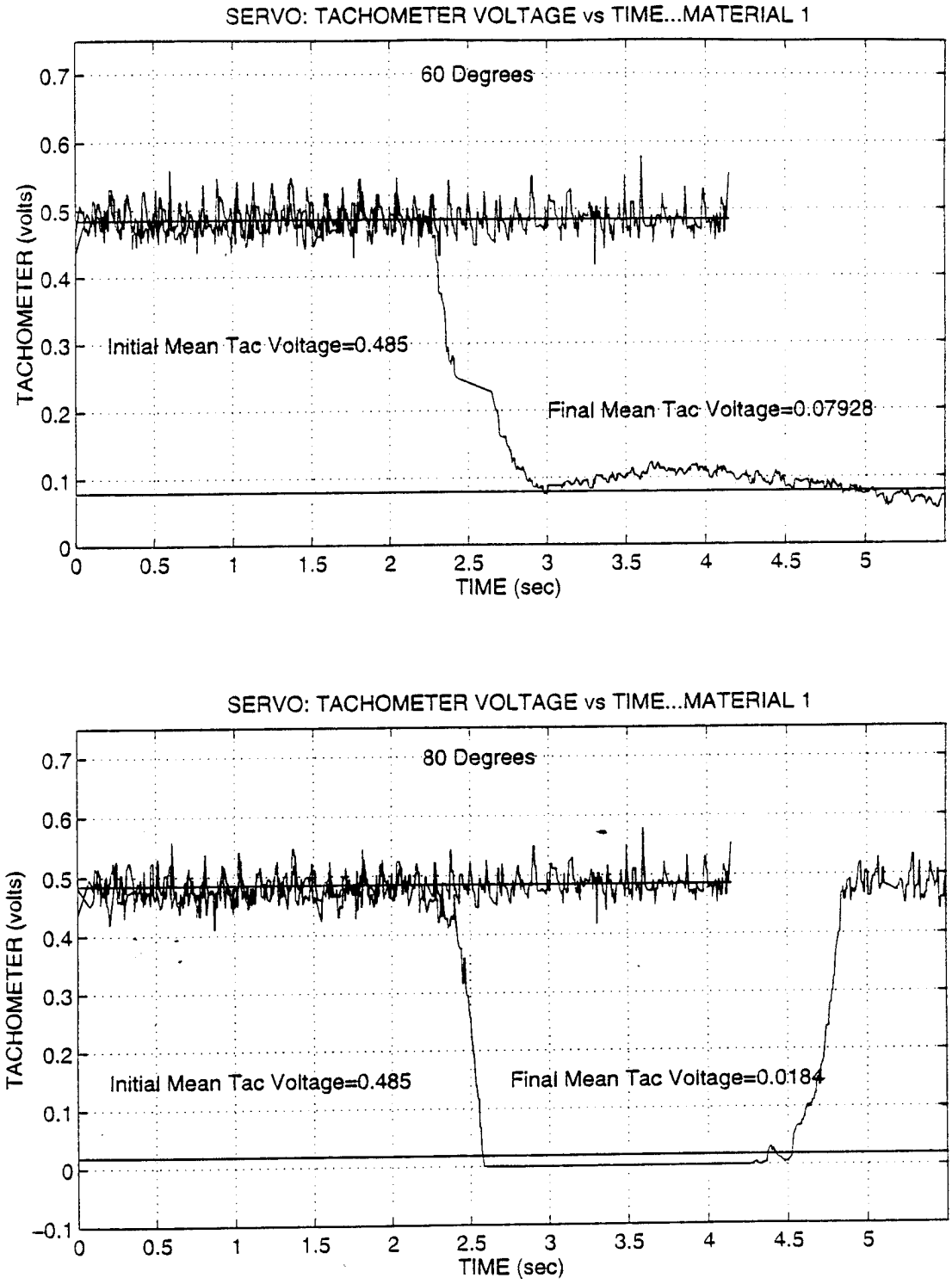

Figure 47: Material 2 - Tachometer Voltage Differential for Servomotor Positions of 60 and 80 Degrees, respectively

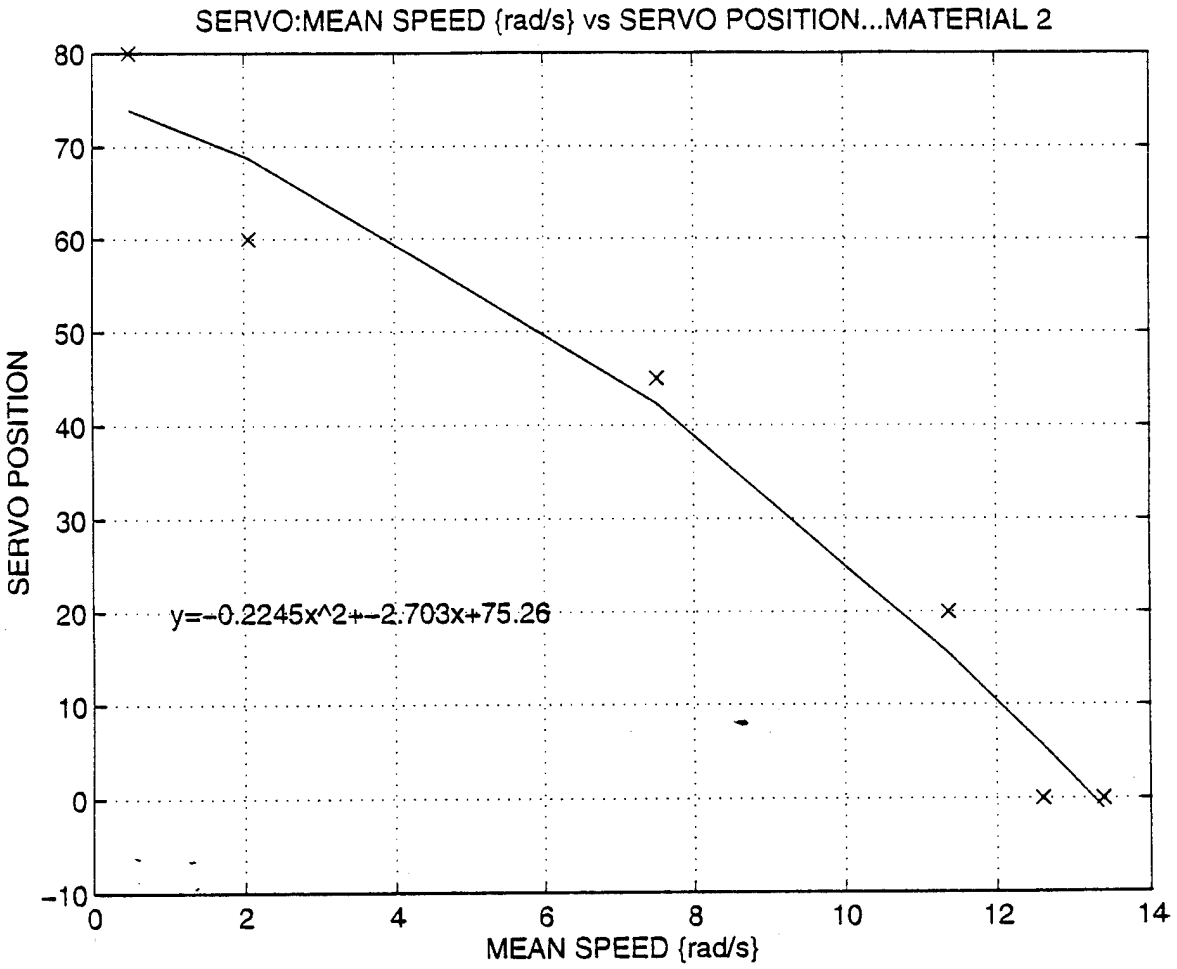

Figure 48: Material 2 - Mean Rotational Speed versus Servomotor Arm Position

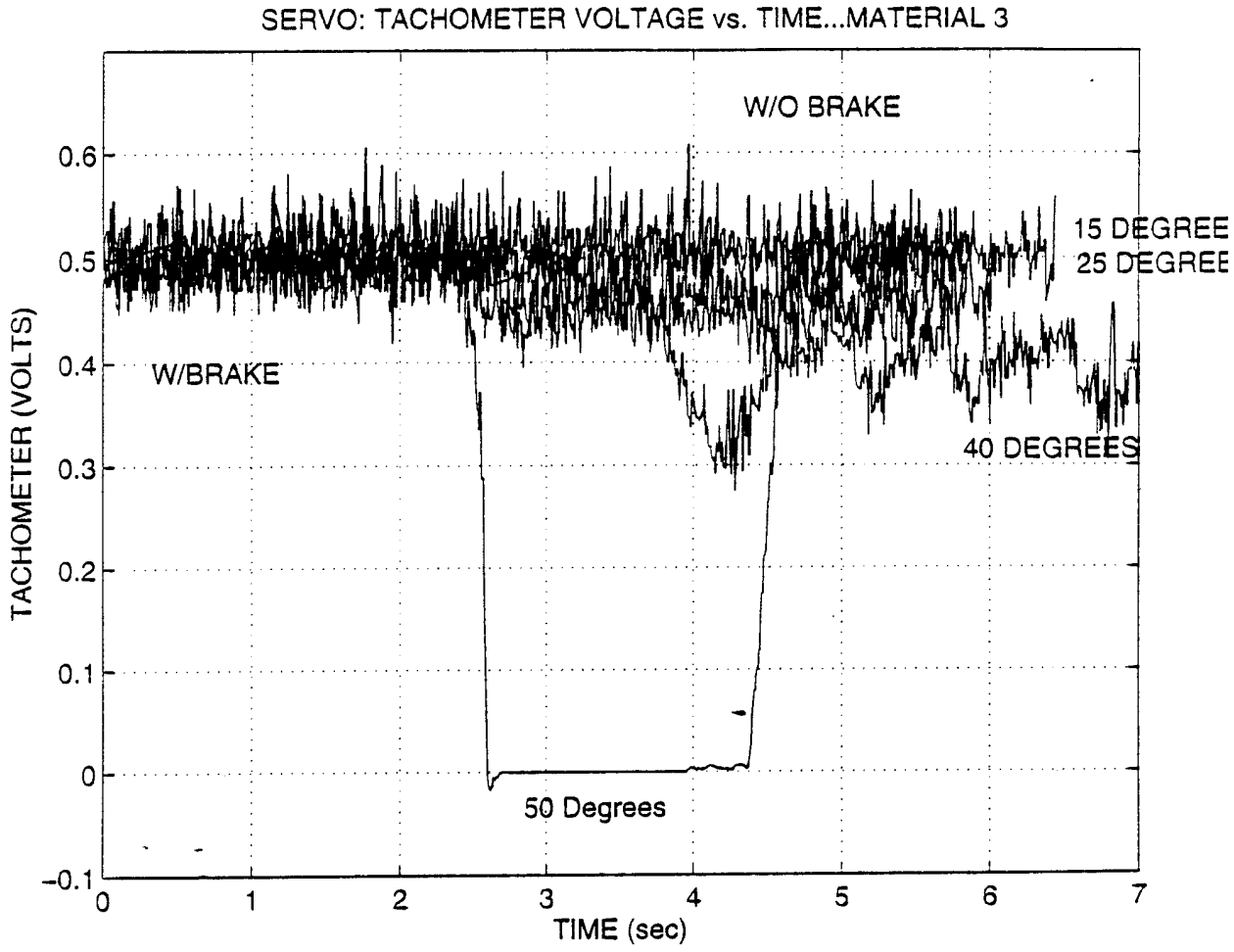

Figure 49: Material 3 - Tachometer Voltage versus Time for all Servomotor Positions

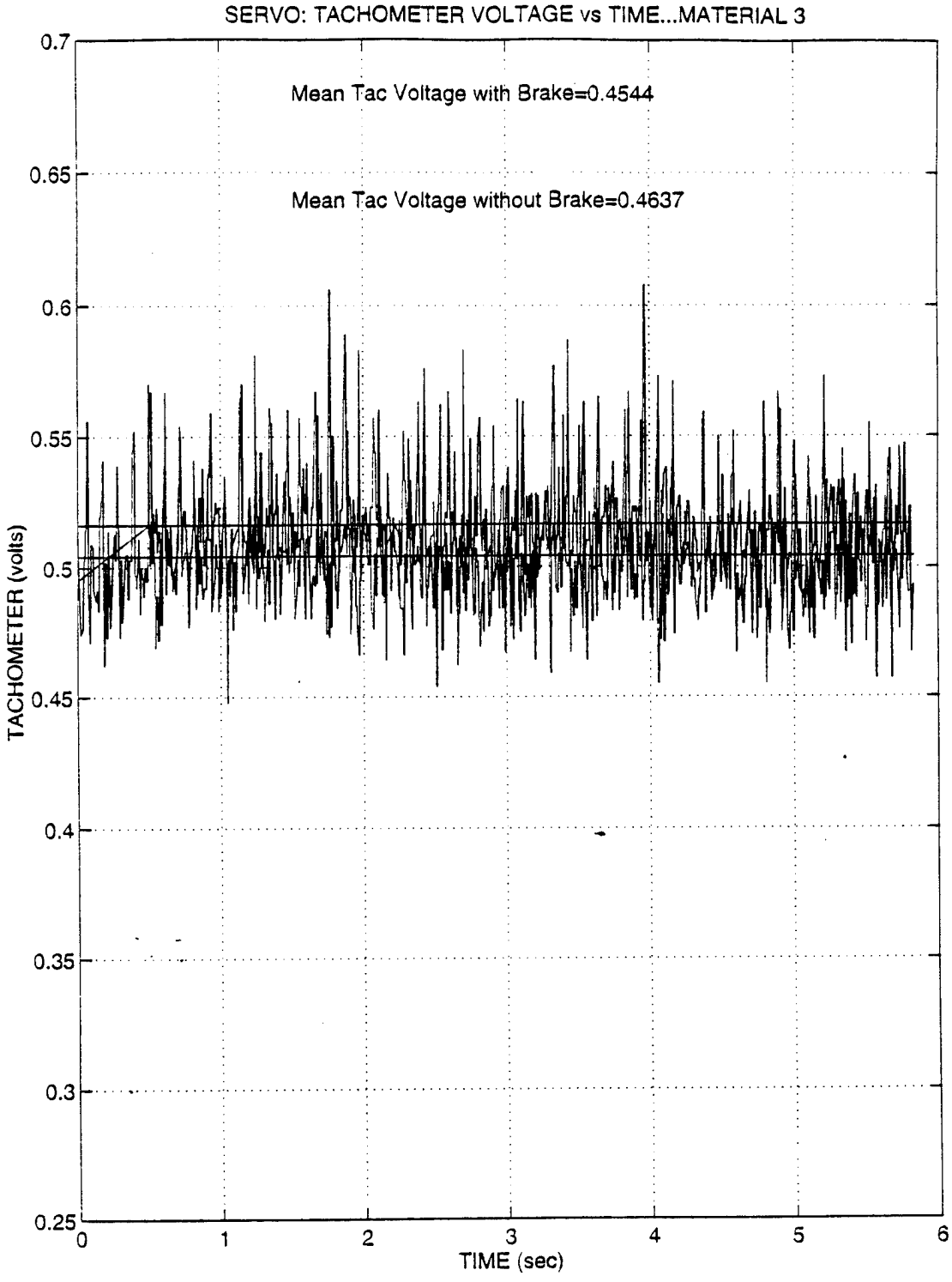

Figure 50: Material 3 - Mean Rotational Speed With and Without Band Brake (Servomotor)

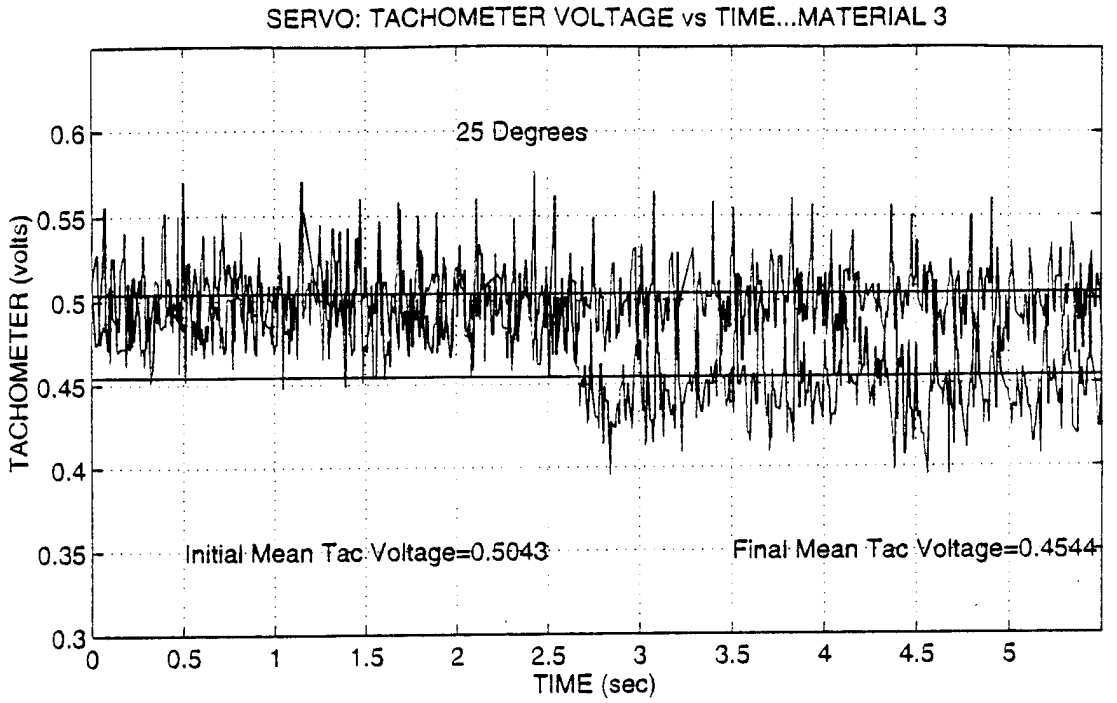

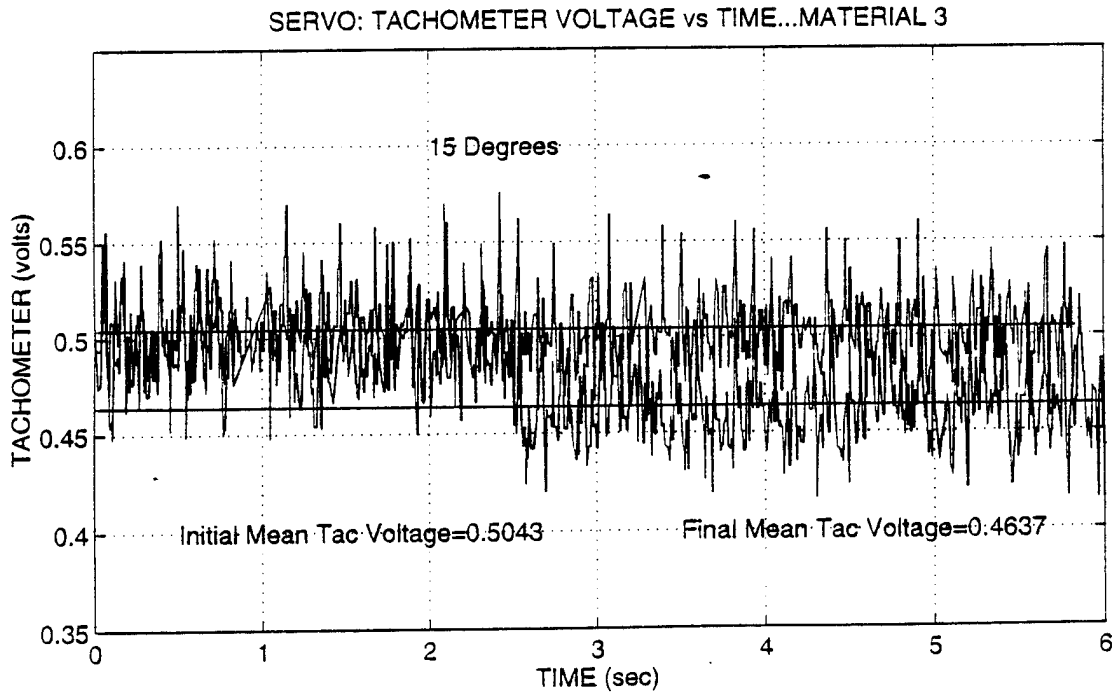

Figure 51: Material 3 - Tachometer Voltage Differential for Servomotor Positions of 25 and 15 Degrees, respectively

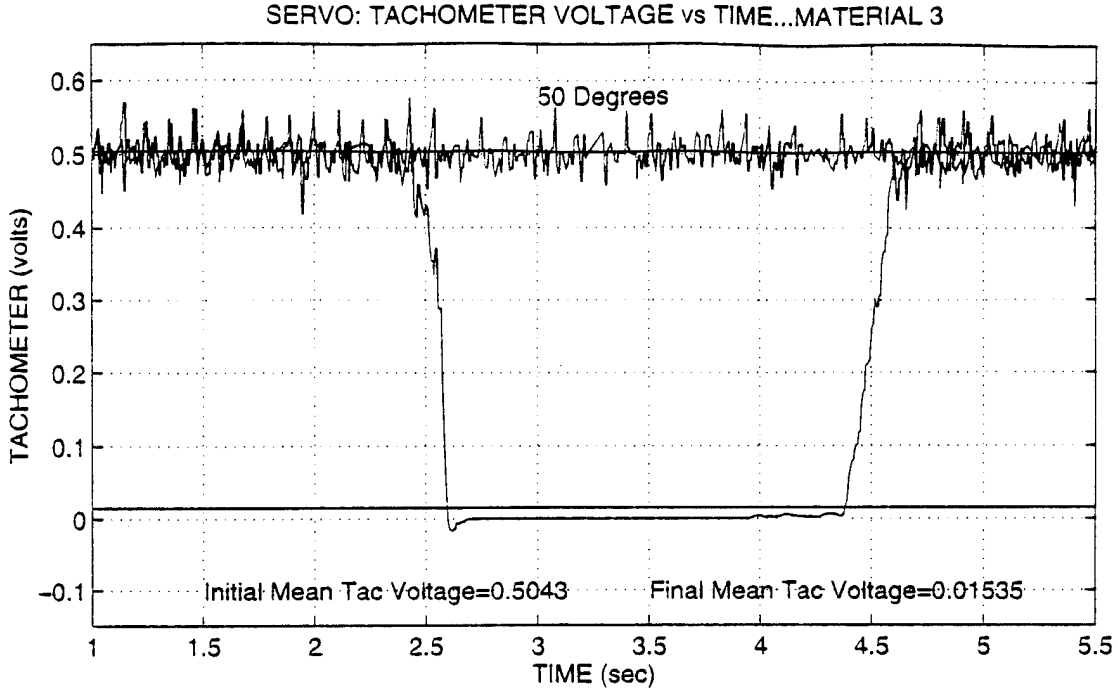

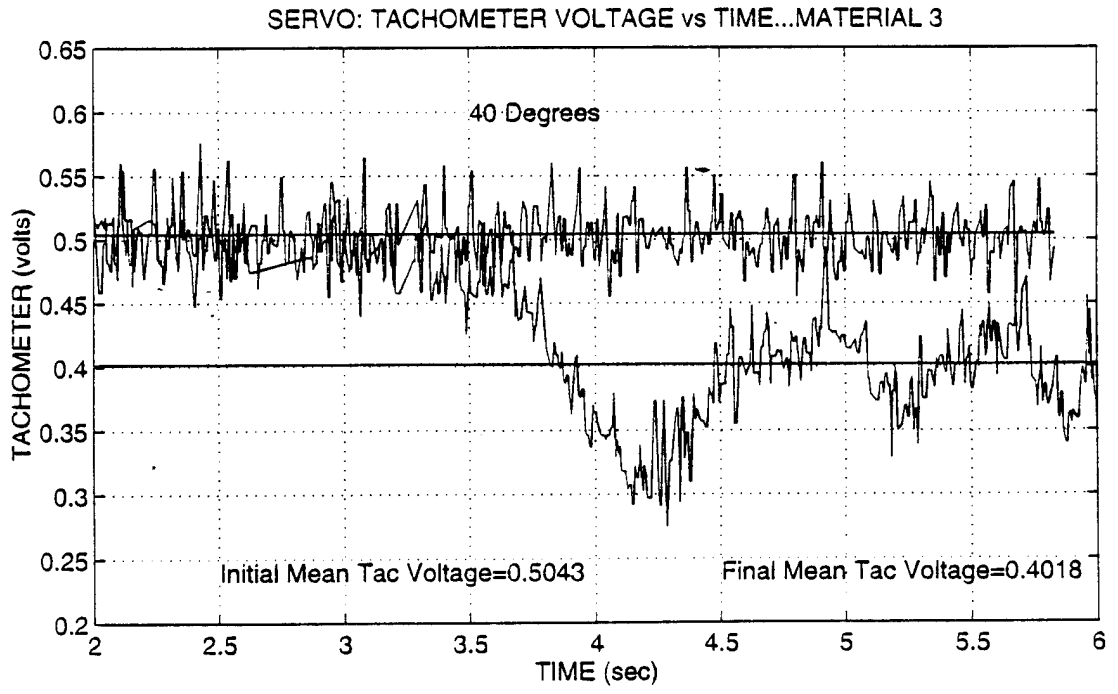

Figure 52: Material 3 - Tachometer Voltage Differential for Servomotor Positions of 50 and 40 Degrees, respectively

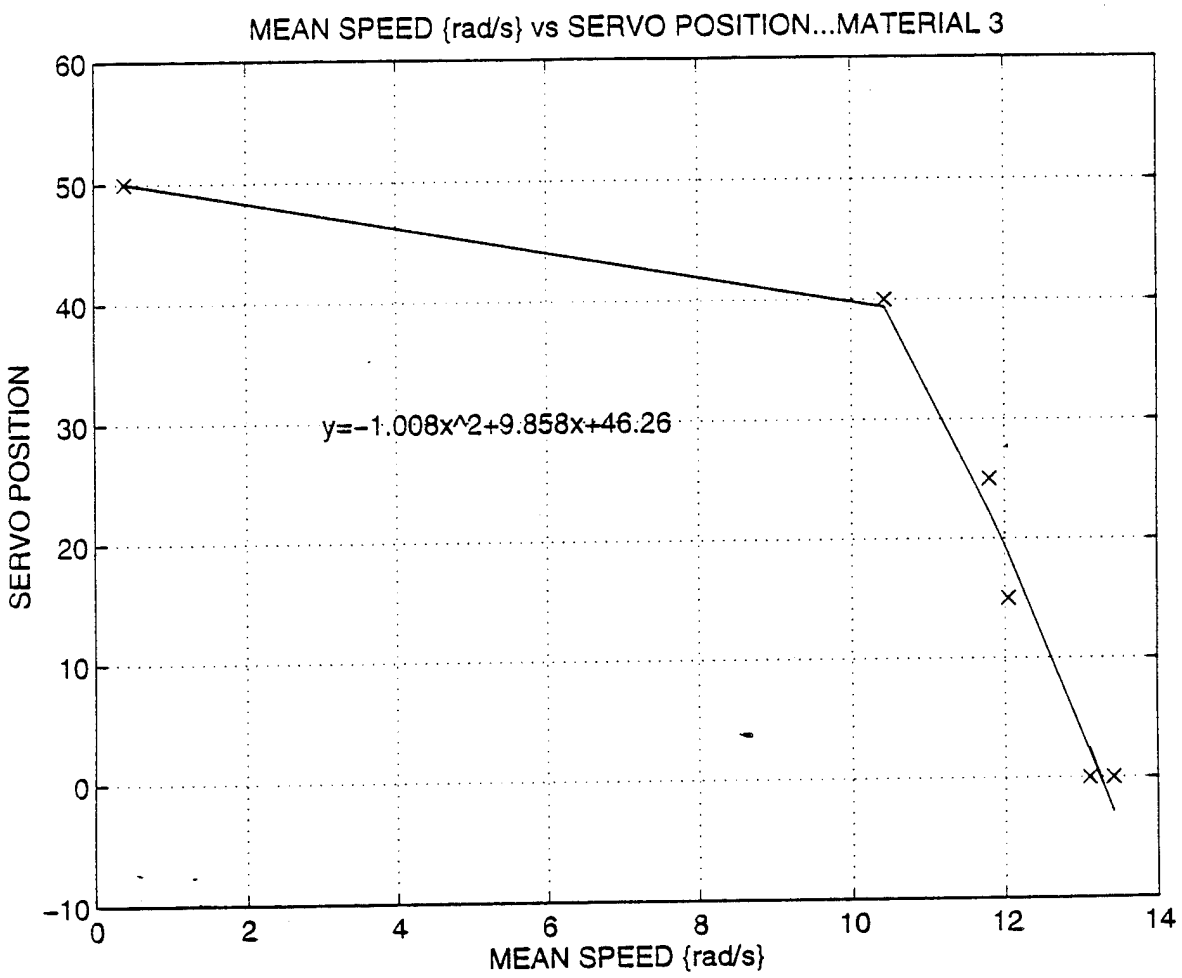

Figure 53: Material 3 - Mean Rotational Speed versus Servomotor Arm Position

F. SOLENOID EXPERIMENTAL RUNS

1. Results

With the test apparatus configured in accordance with the solenoid setup of Figure 32 and 33, the six test runs were conducted for each band brake material under the provisions set forth in Section IV.A. The results of these tests will be presented in three sets of four separate graphs, vice five, with the graph of the accumulation of test runs excluded due to the busy nature of the black and white print. Additionally, and extra set of graphs will be provided for experimental runs conducted with Material 3 wrapped twice around the disk, providing 540 degrees of wrap vice 180 degrees. Thus the first graph of each set provides a display of mean tachometer voltage from the test apparatus rotating freely without any band brake attached and tachometer voltage with the brake attached, but in the "off " position. The tachometer voltage, and corresponding speed differential between these two conditions was used to estimate the coefficient of friction for each material, as described in Section IV.D.2. The second and third figures are a collection of the initial and final mean tachometer voltages at the indicated solenoid activation duty cycle. For each graph contained in these two figures, solenoid activation duty cycle is superimposed above the test system tachometer response. Although the solenoid is receiving the PWM signal, the power to the solenoid is not supplied until the system has reached its steady state speed for approximately two seconds. Once at steady state, the solenoid is powered for approximately three to four seconds, allowing the effect

of the solenoid to steady out, then the solenoid power is disabled, and the system returns to its initial speed. The initial and final (actually the value during solenoid activation) mean tachometer voltages are again displayed on each graph. The fourth graph for each material consists of an accumulation of the mean final speed versus solenoid activation duty cycle, which demonstrates each materials ability to control the speed of the test apparatus over a range of duty cycles. As with the servomotor, a second order polynomial was fit to this data in order to provide a formula for converting the duty cycle of a PWM signal into a mean speed on the Master Control Apparatus. Thus a given strain gauge voltage can trigger a certain duty cycle, which will produce a corresponding speed reduction or damping effect on the Master Control Apparatus. The results of each test run are represented in tabular form in Tables 11 and 12, and graphically in the following order:

- Material 1: Figures 54-57
- Material 2: Figures 58-61
- Material 3: Figures 62-65

	MATERIAL 1		MATERIAL 2		MATERIAL 3	
RUN NUMBER	DUTY CYCLE (%)	TAC VOLTAGE (V)	DUTY CYCLE	TAC VOLTAGE (V)	DUTY CYCLE	TAC VOLTAGE (V)
INITIAL	0	0.5107	0	0.4957	0	0.4962
Run 1	25	0.4987	25	0.4790	25	0.4824
Run 2	50	0.4859	50	0.4418	50	0.4674
Run 3	83.3	0.4408	83.3	0.1206	83.3	0.1694
Run 4	91	0.2744	91	0.0810	91	0.1199

Table 11: Summary of Solenoid Test Results

	MATERIAL 3 DOUBLE WRAP	
RUN NUMBER	DUTY CYCLE (%)	TAC VOLTAGE (V)
INITIAL	0	0.5016
Run 1	25	0.4795
Run2	50	0.4441
Run 3	83.3	0.1558

TABLE 12: Summary of Solenoid Test Results for Material 3 Double Wrapped

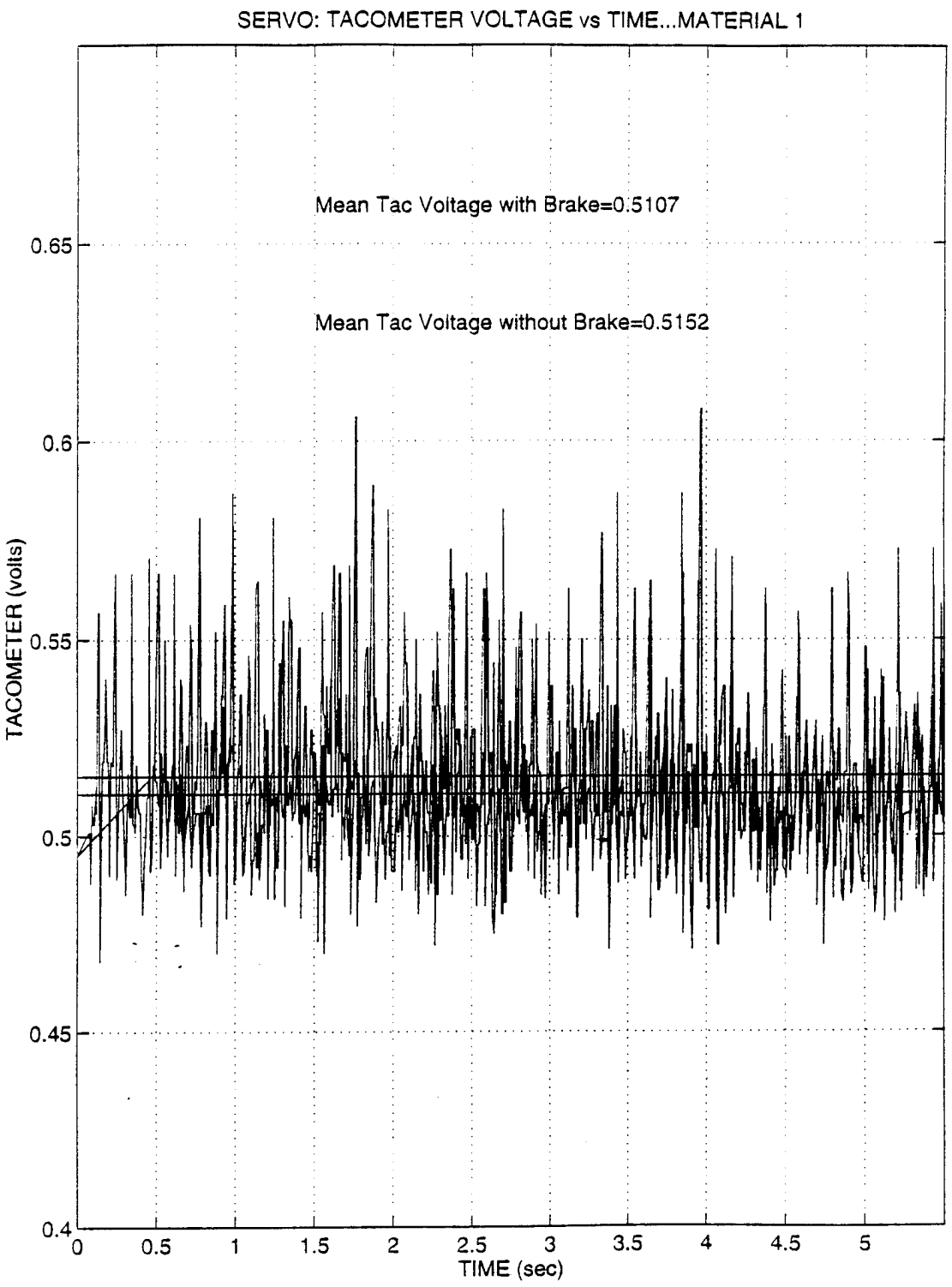

Figure 54: Material 1 - Mean Rotational Speed With and Without Band Brake (Solenoid)

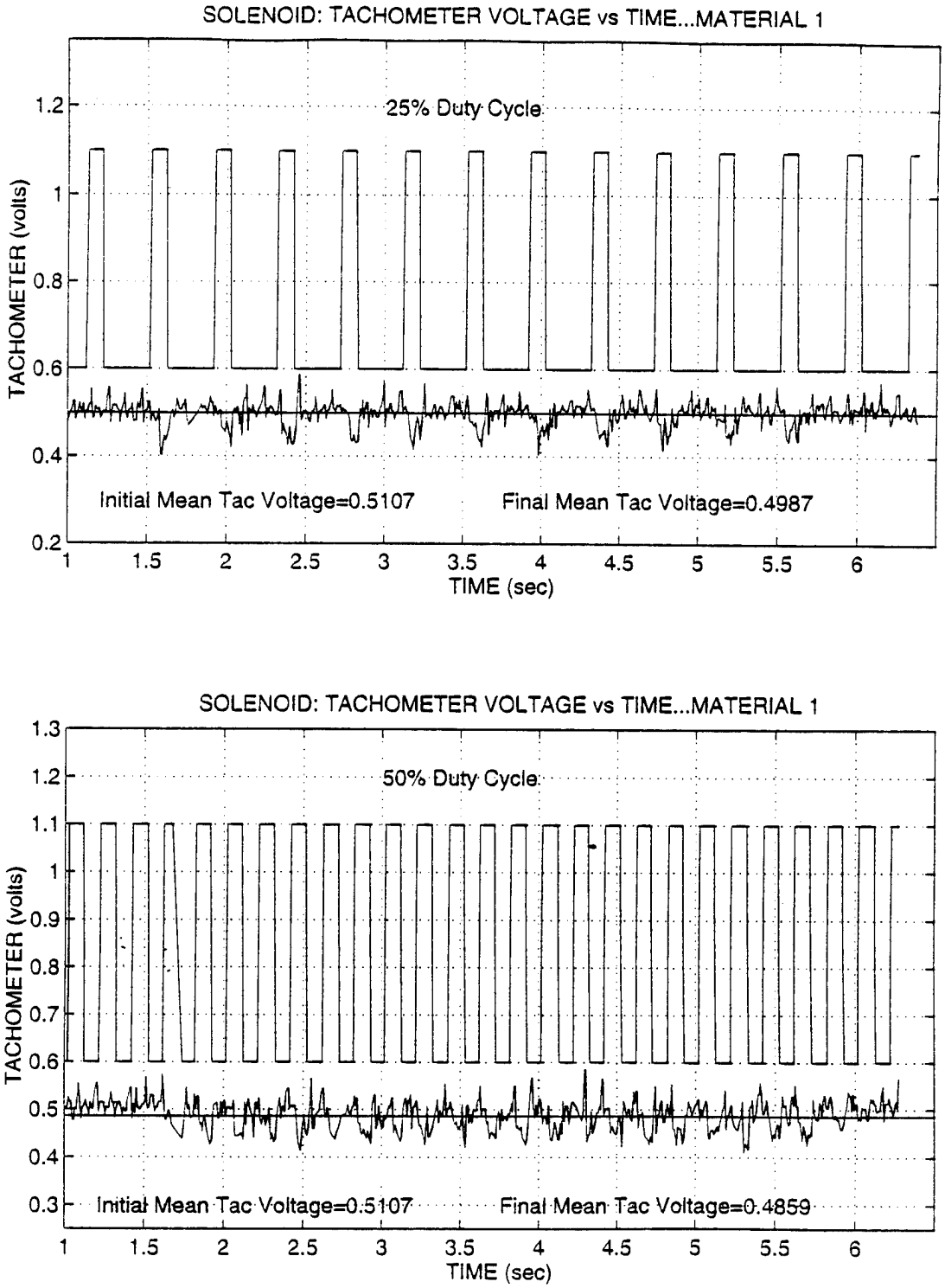

Figure 55: Material 1 - Tachometer Voltage Differential for Solenoid Activation Duty Cycles of 25 and 50 Percent, respectively

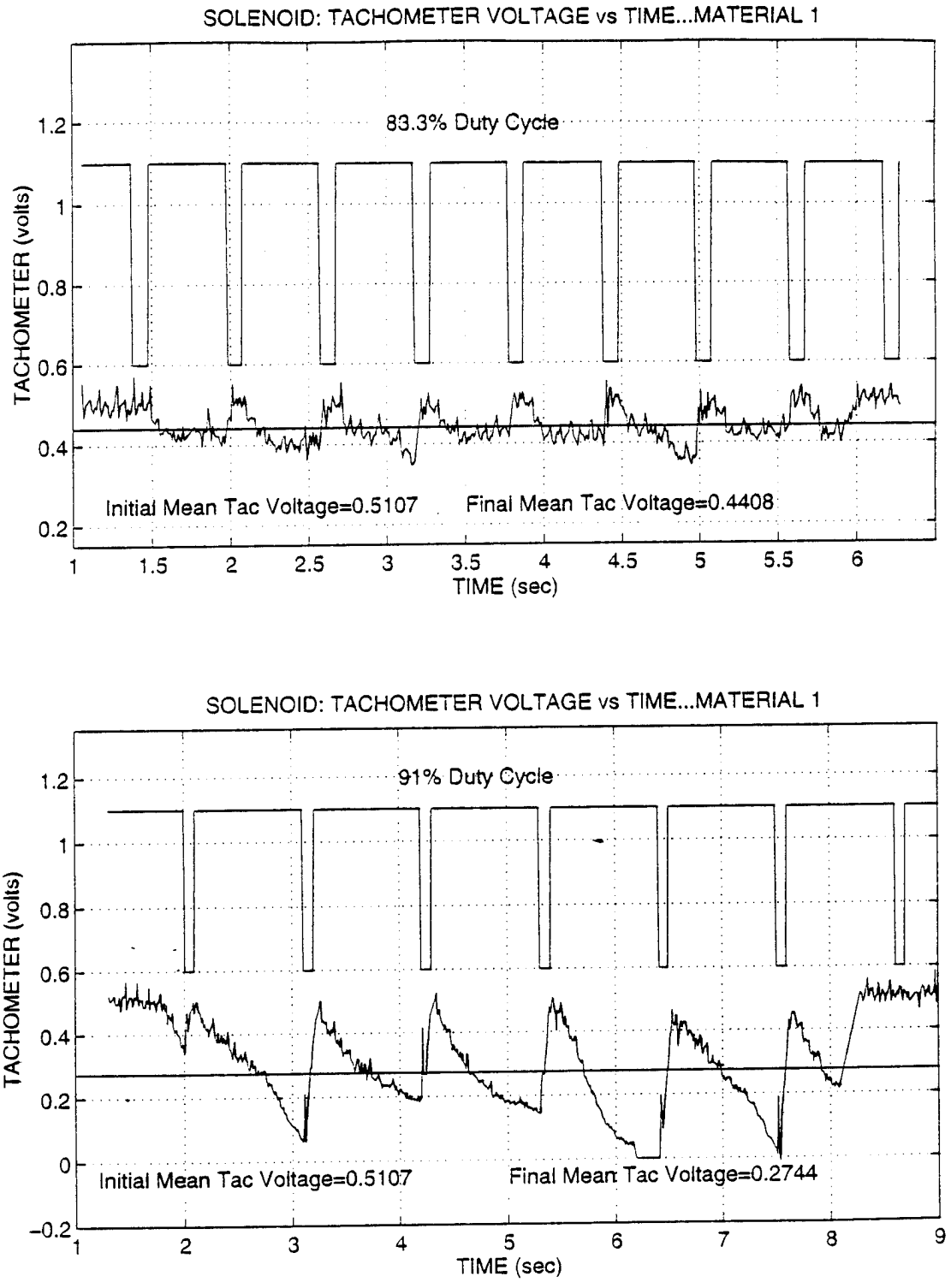

Figure 56: Material 1 - Tachometer Voltage Differential for Solenoid Activation Duty Cycles of 83.3 and 91 Percent, respectively

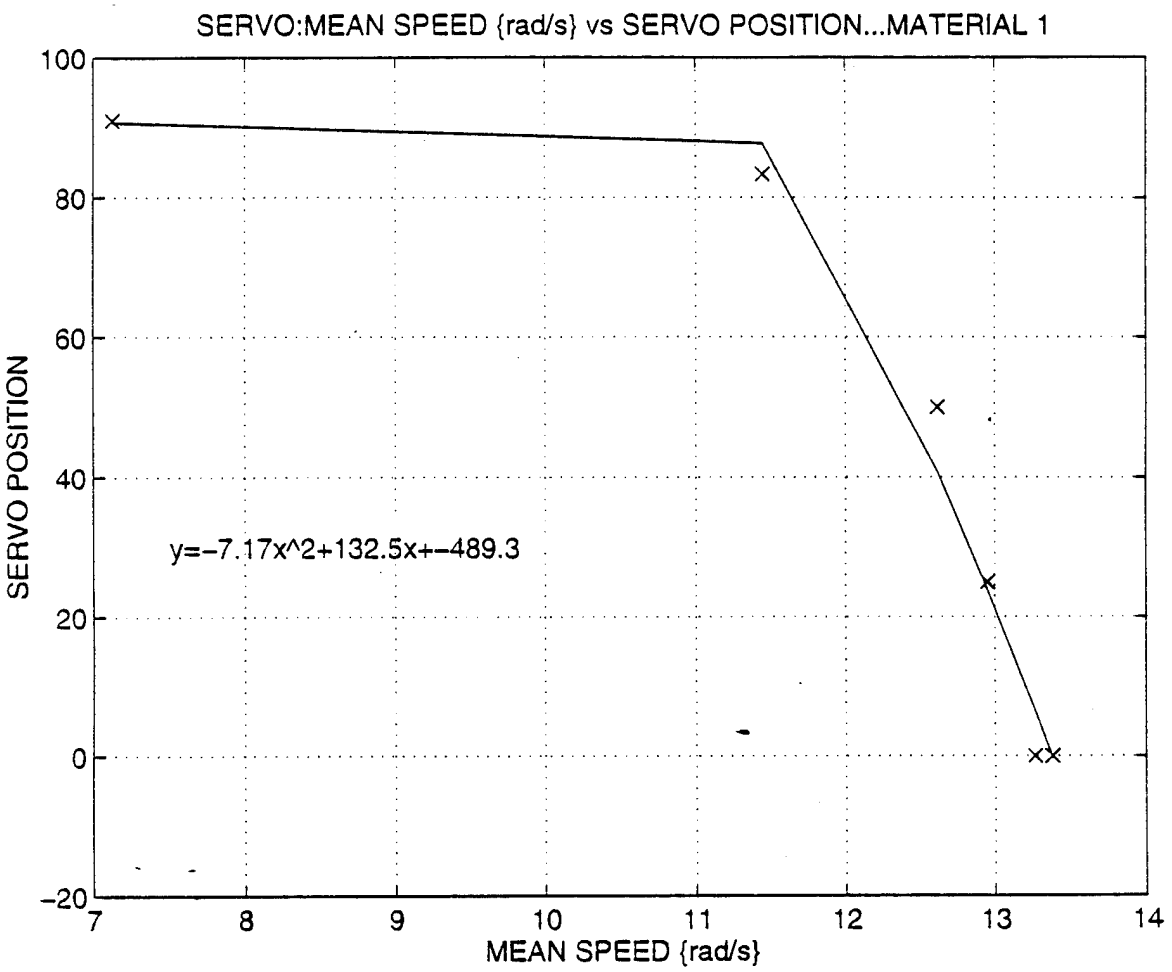

Figure 57: Material 1 - Mean Rotational Speed versus Duty Cycle

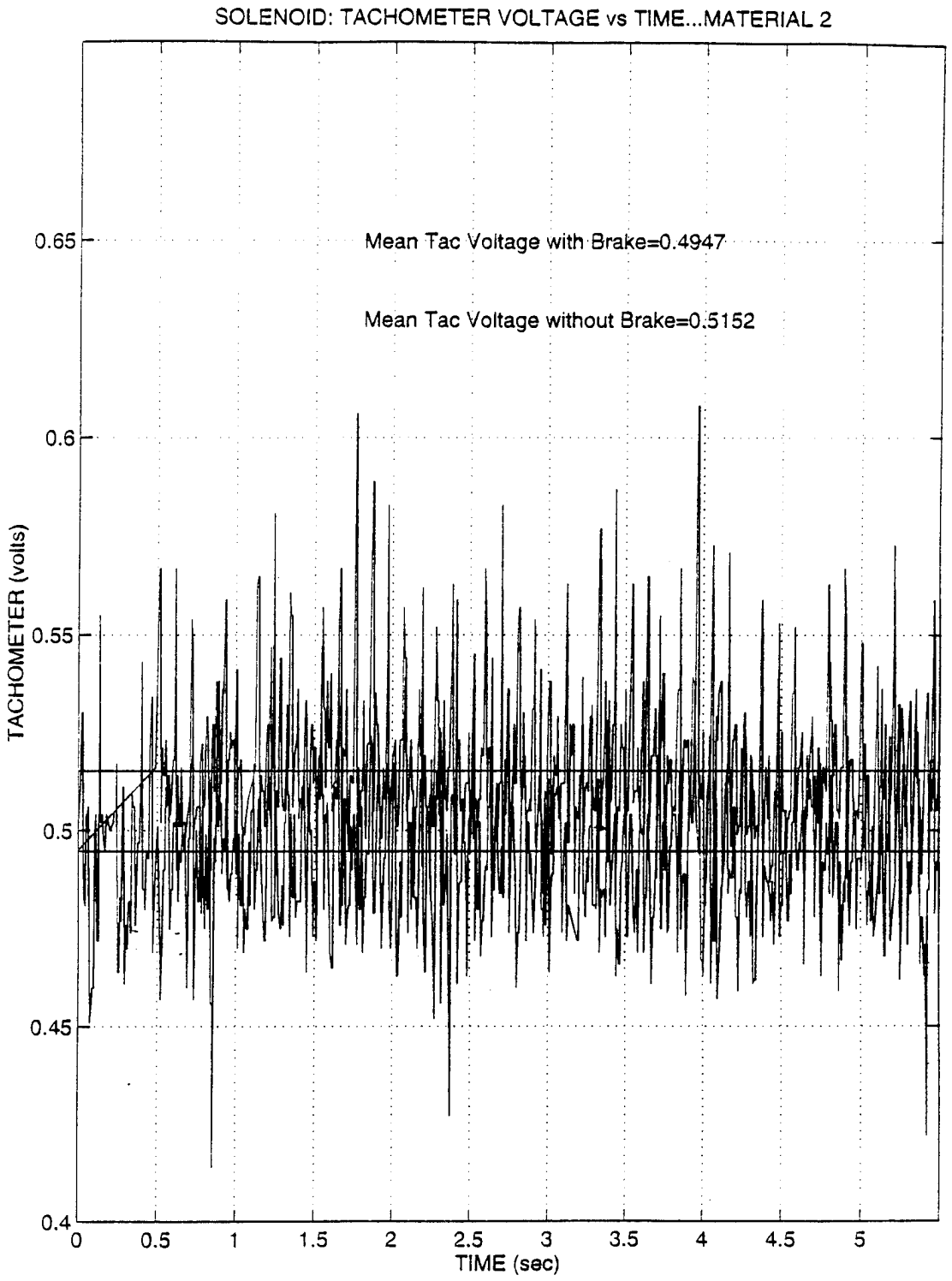

Figure 58: Material 2 - Mean Rotational Speed With and Without Band Brake (Solenoid)

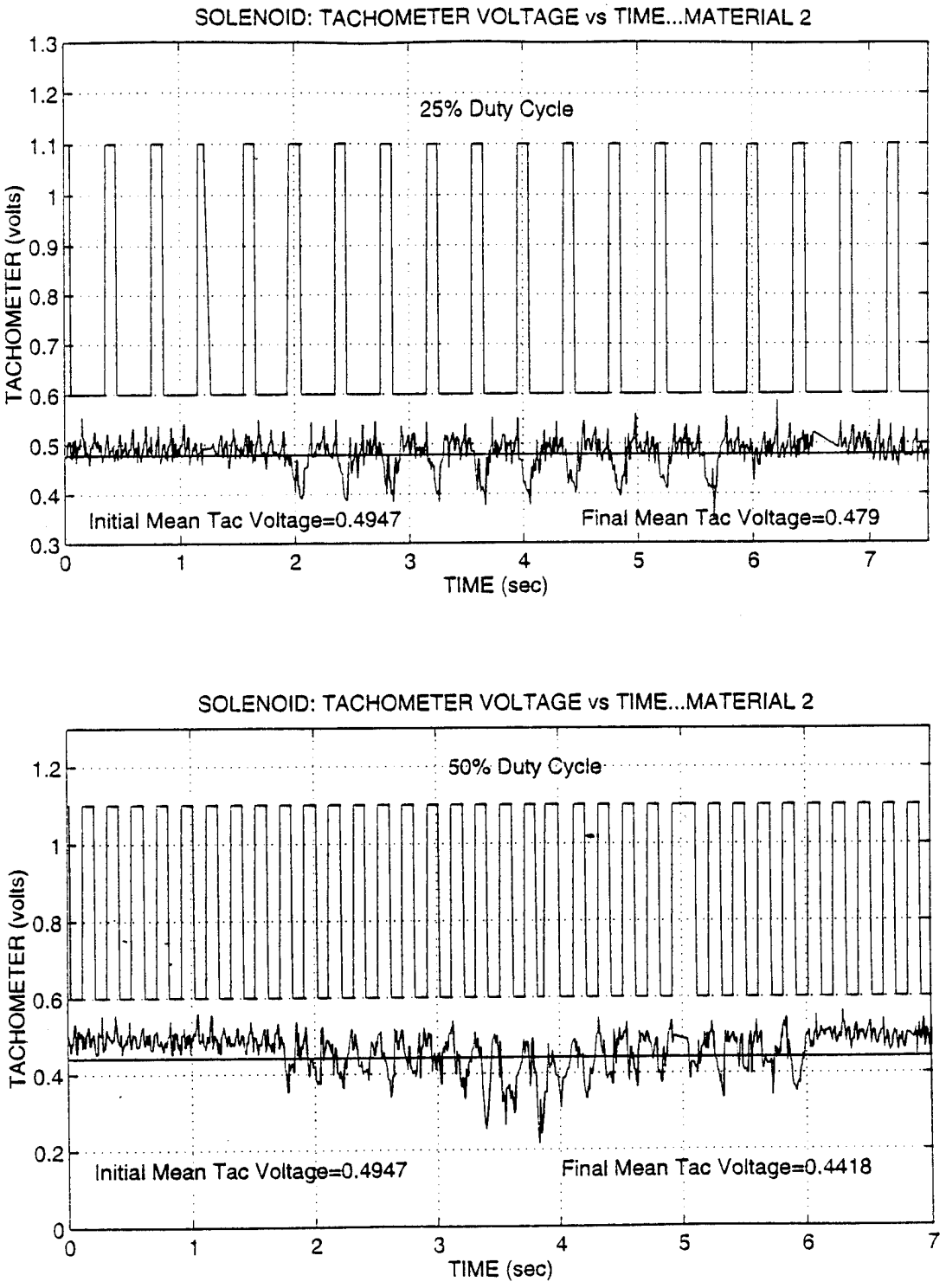

Figure 59: Material 2 - Tachometer Voltage Differential for Solenoid Activation Duty Cycles of 25 and 50 Percent, respectively

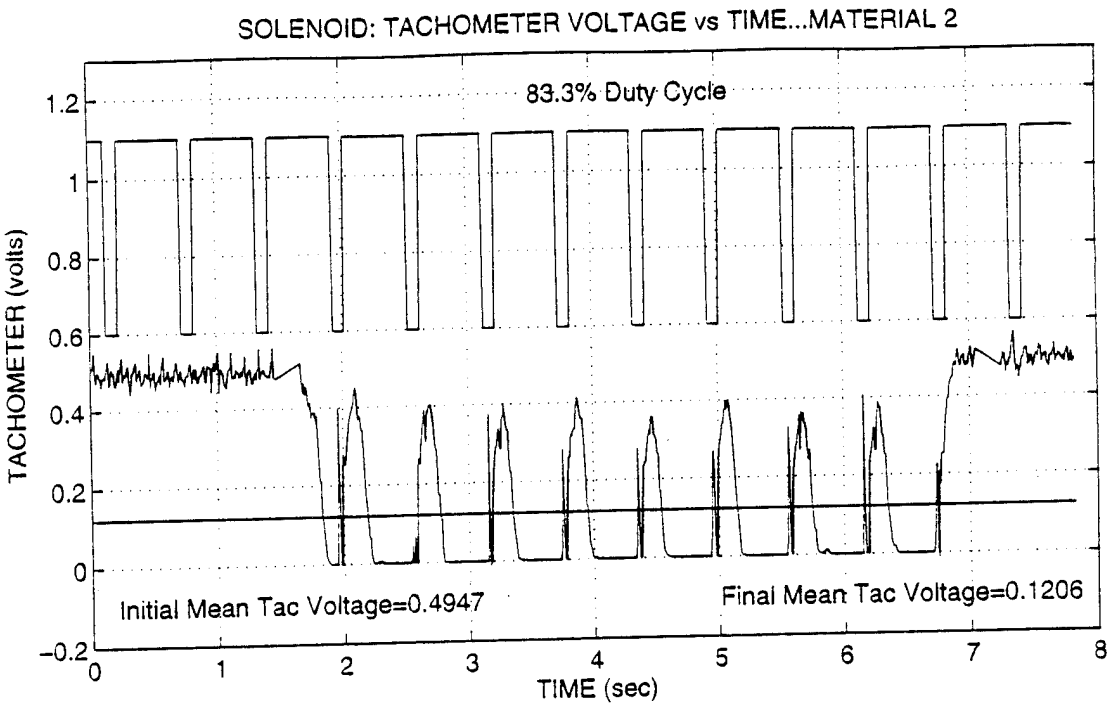

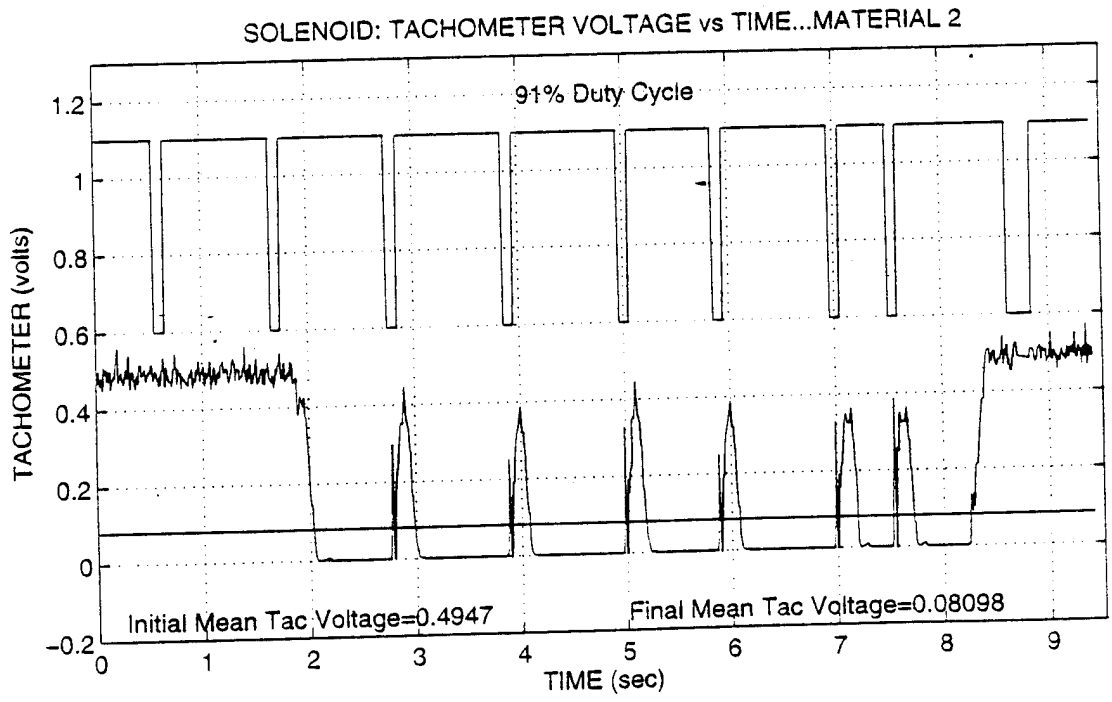

Figure 60: Material 2 - Tachometer Voltage Differential for Solenoid Activation Duty Cycles of 83.3 and 91 Percent, respectively

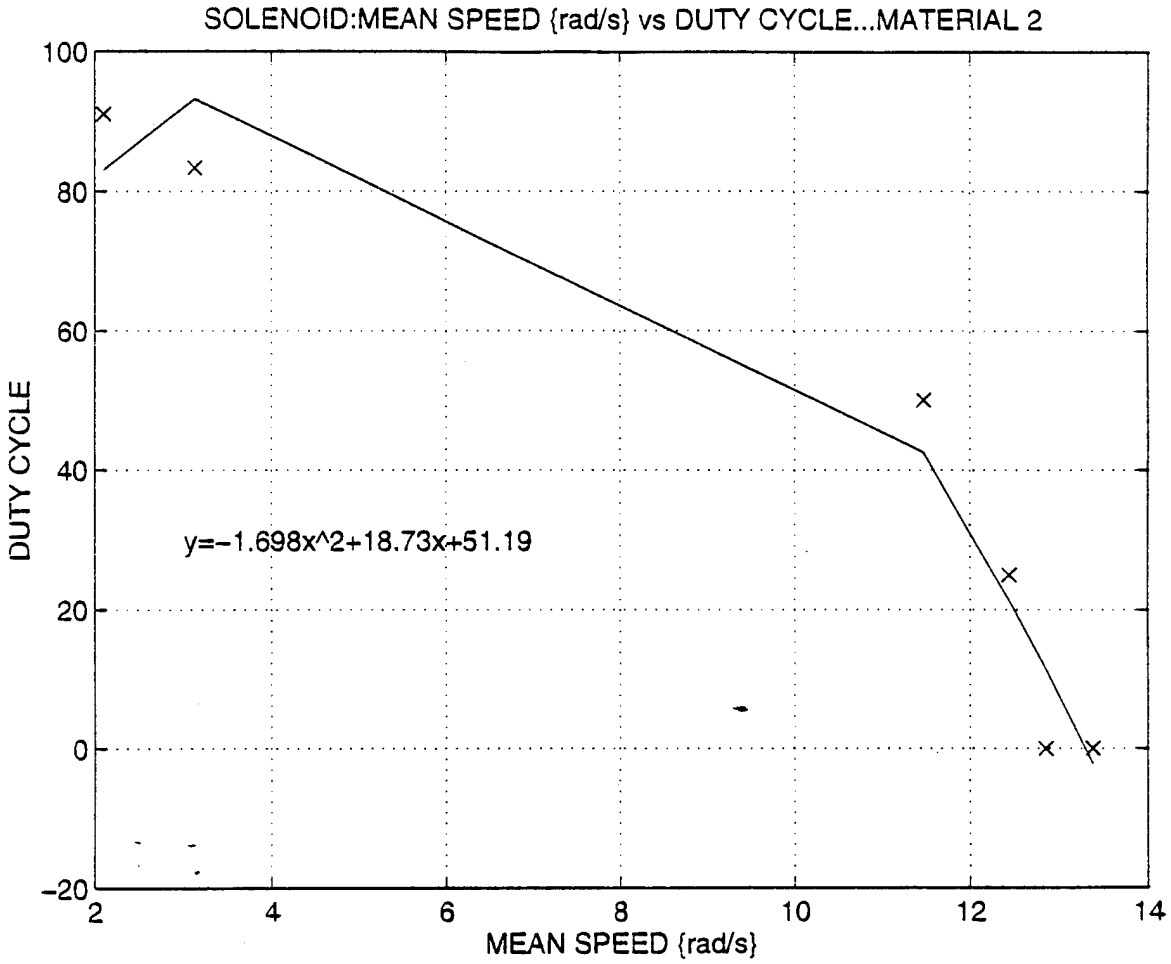

Figure 61: Material 2 - Mean Rotational Speed versus Duty Cycle

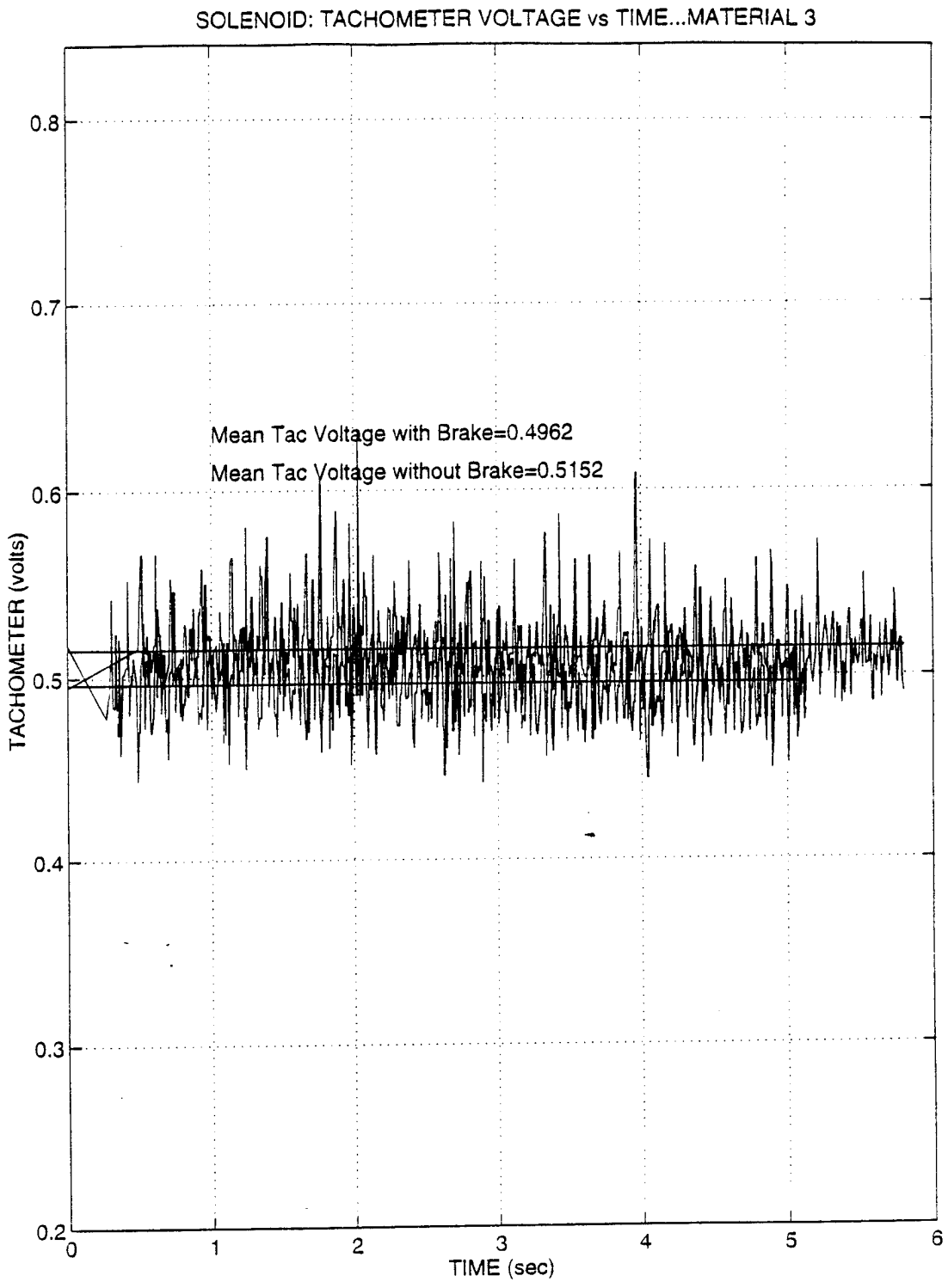

Figure 62: Material 3 - Mean Rotational Speed With and Without Band Brake (Solenoid)

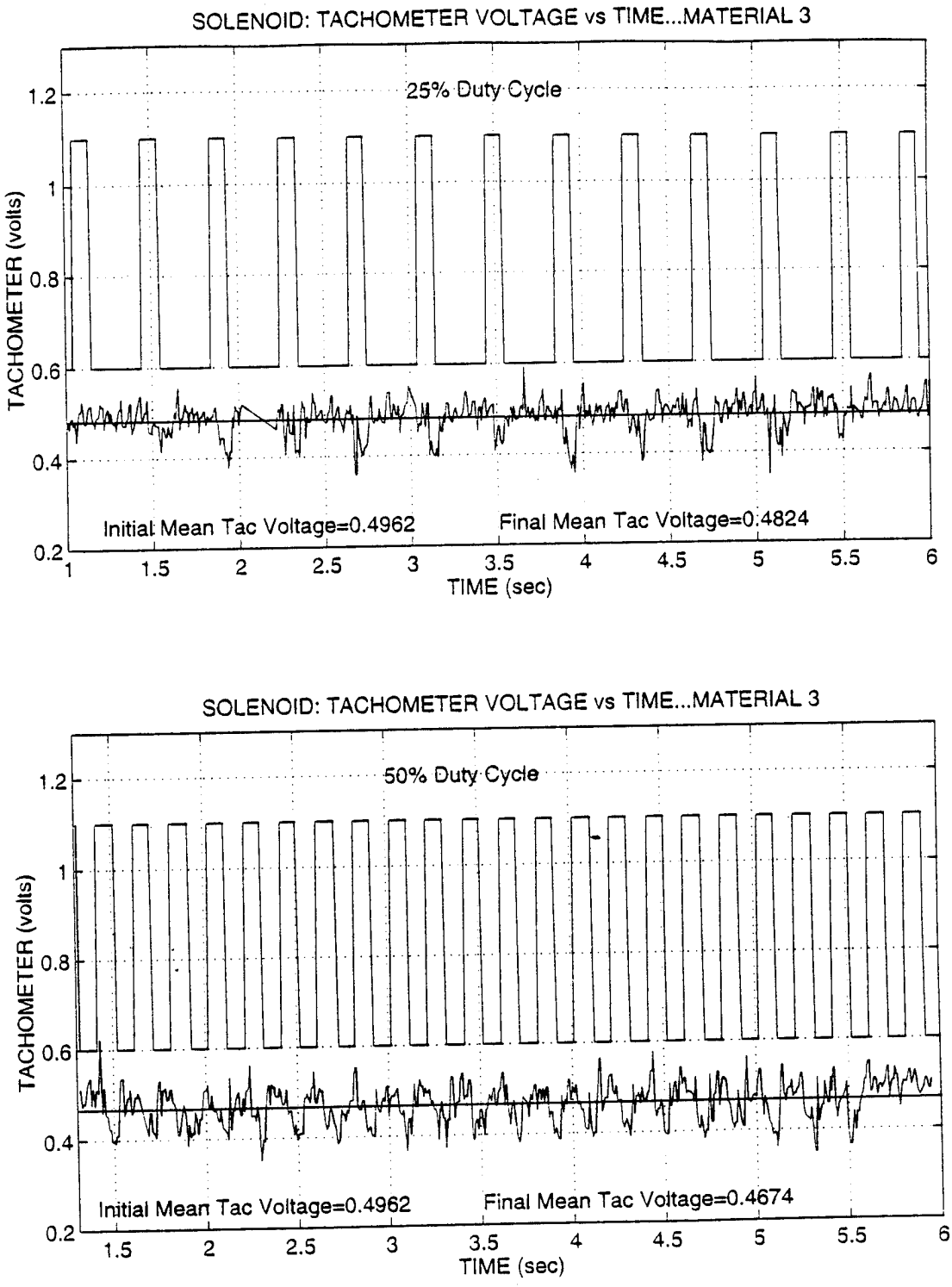

Figure 63: Material 3 - Tachometer Voltage Differential for Solenoid Activation Duty Cycles of 25 and 50 Percent, respectively

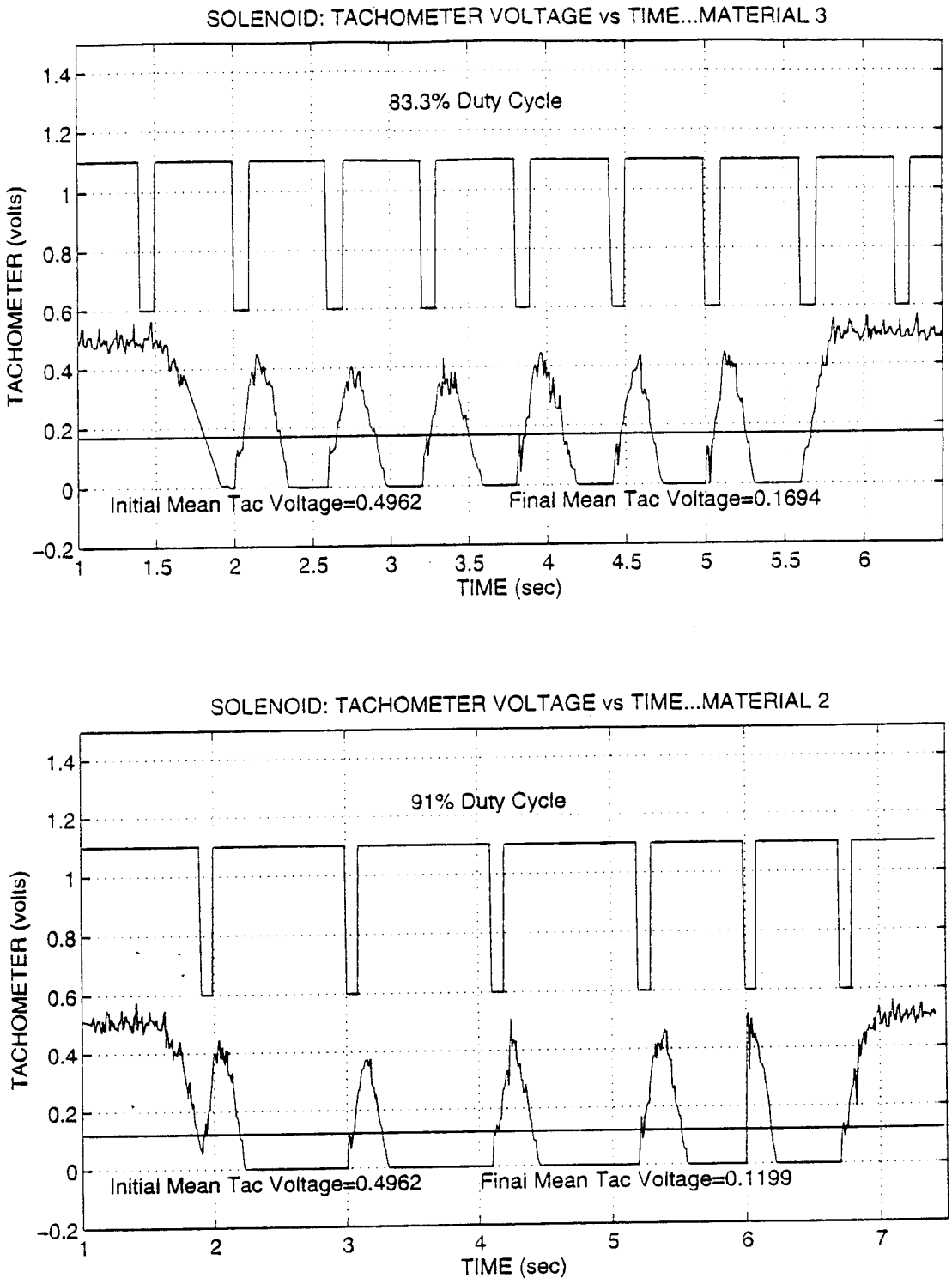

Figure 64: Material 3 - Tachometer Voltage Differential for Solenoid Activation Duty Cycles of 83.3 and 91 Percent, respectively

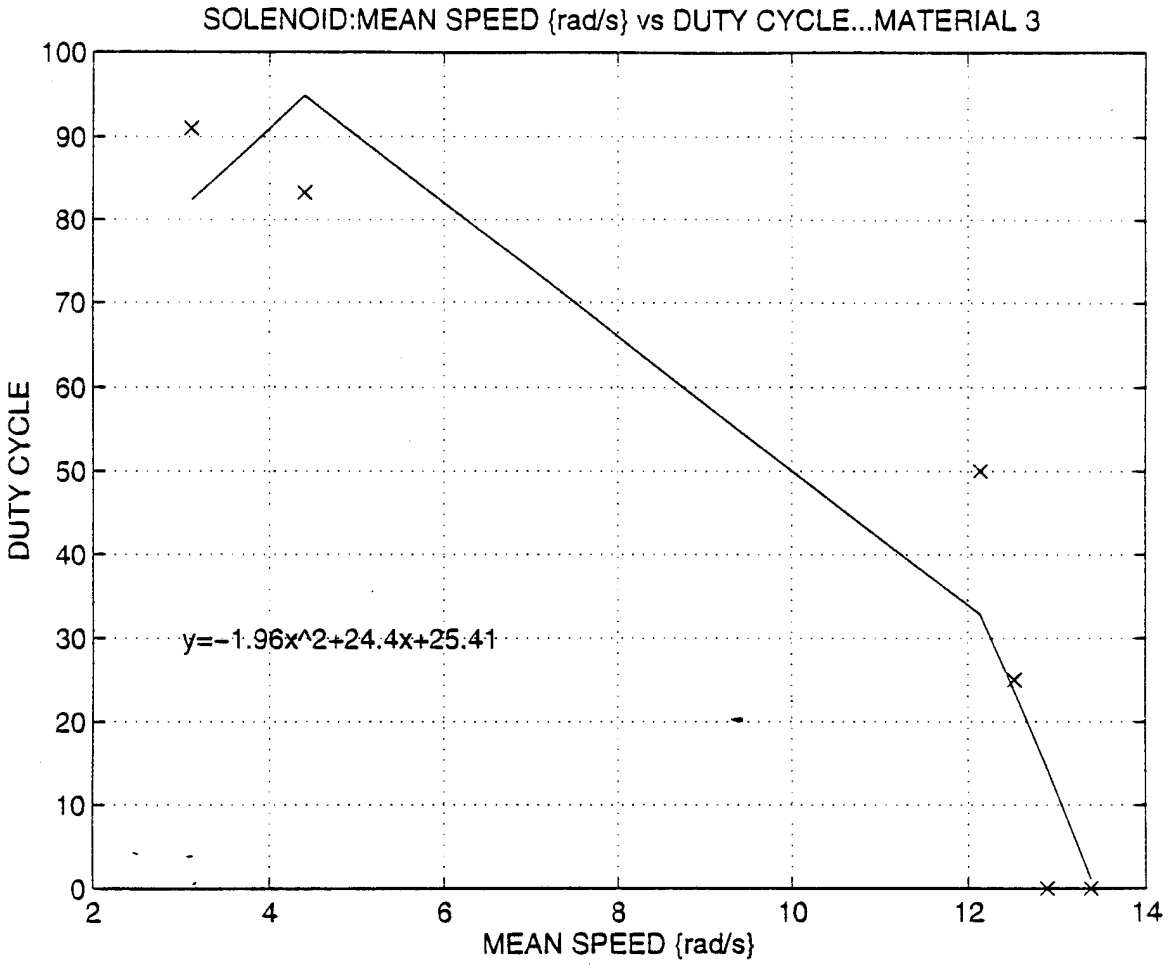

Figure 65: Material 3 - Mean Rotational Speed versus Duty Cycle

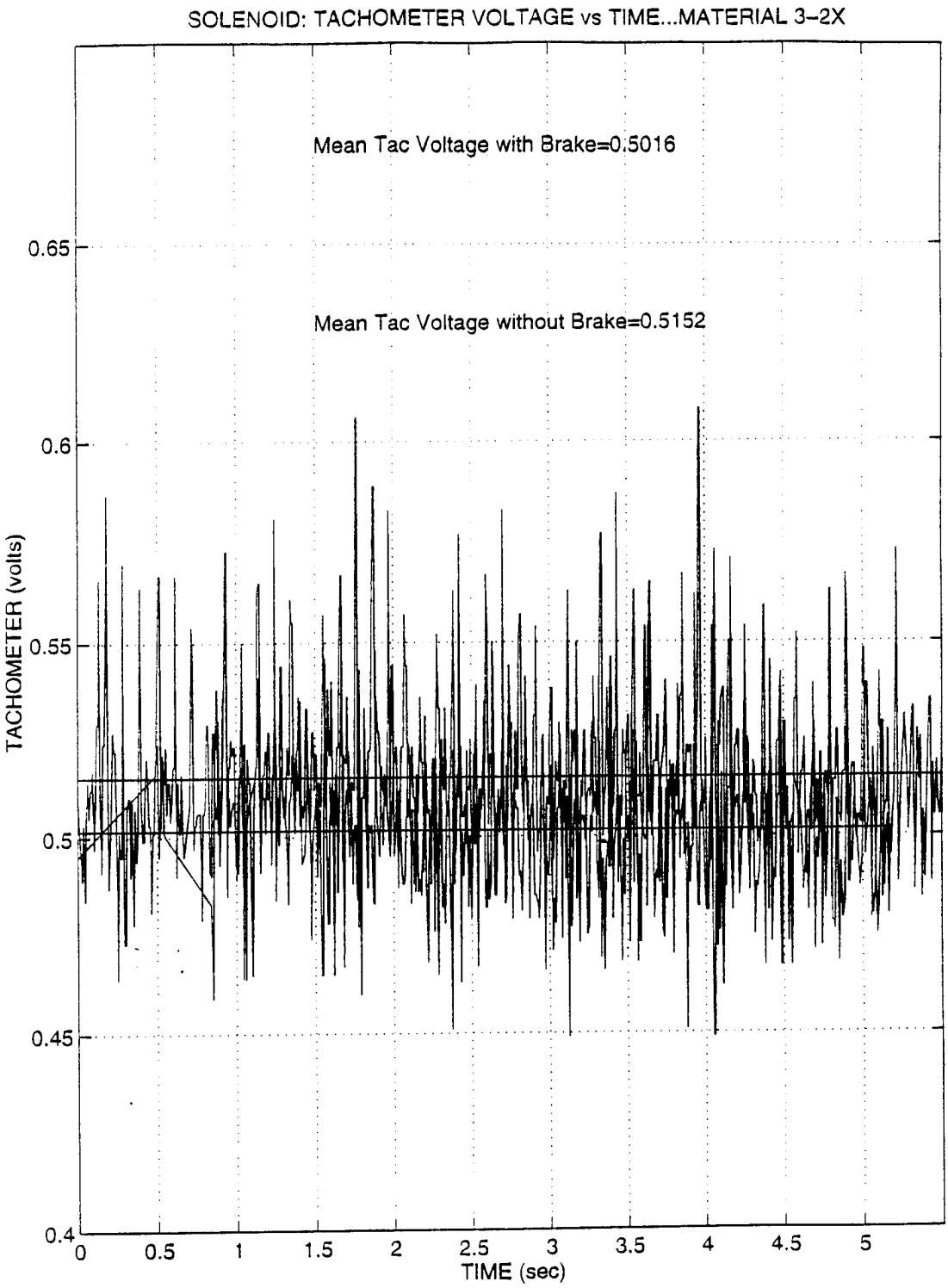

Figure 66: Material 3-2X - Mean Rotational Speed With and Without Band Brake (Solenoid)

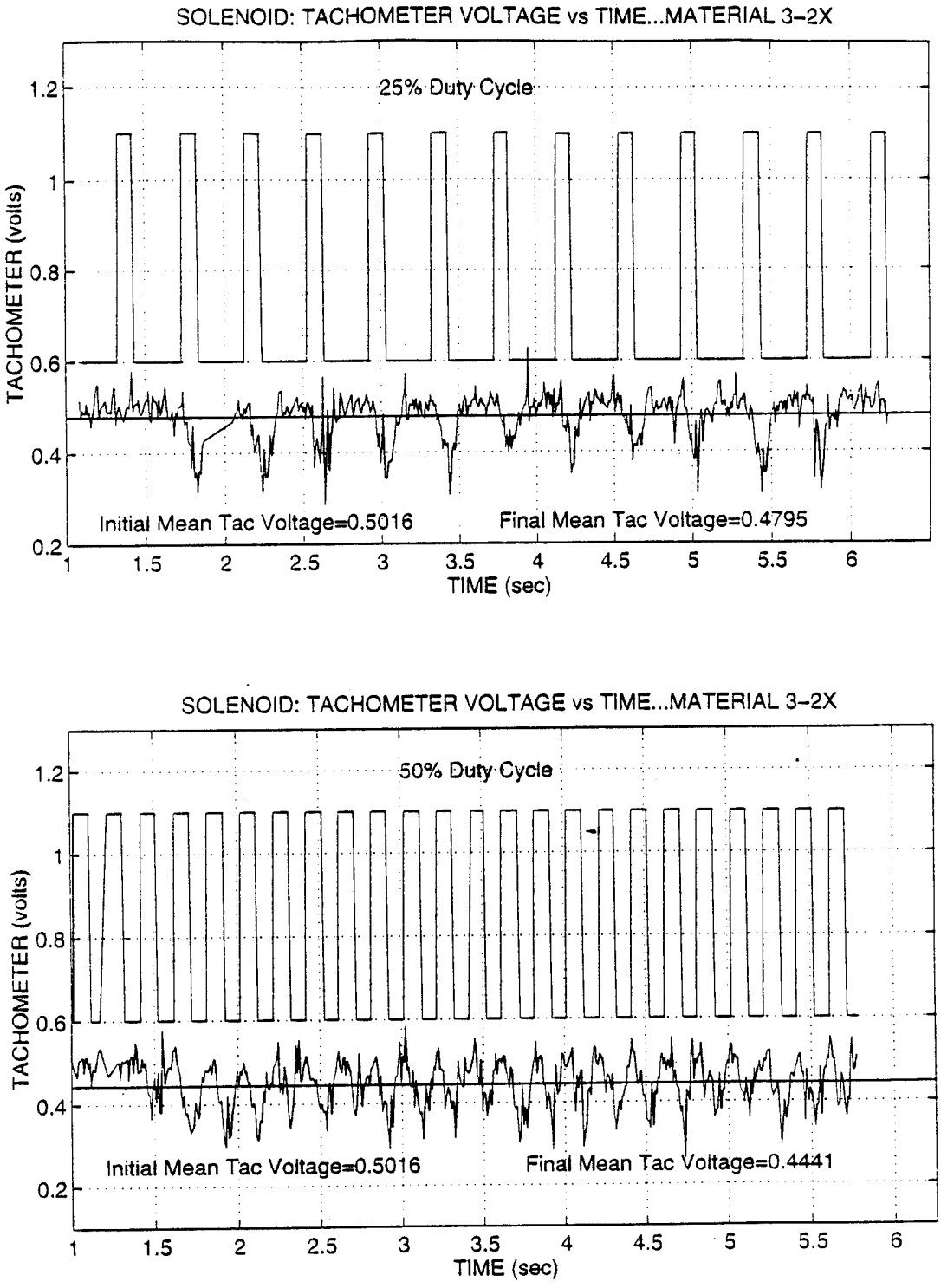

Figure 67: Material 3-2X - Tachometer Voltage Differential for Solenoid Activation Duty Cycles of 25 and 50 Percent, respectively

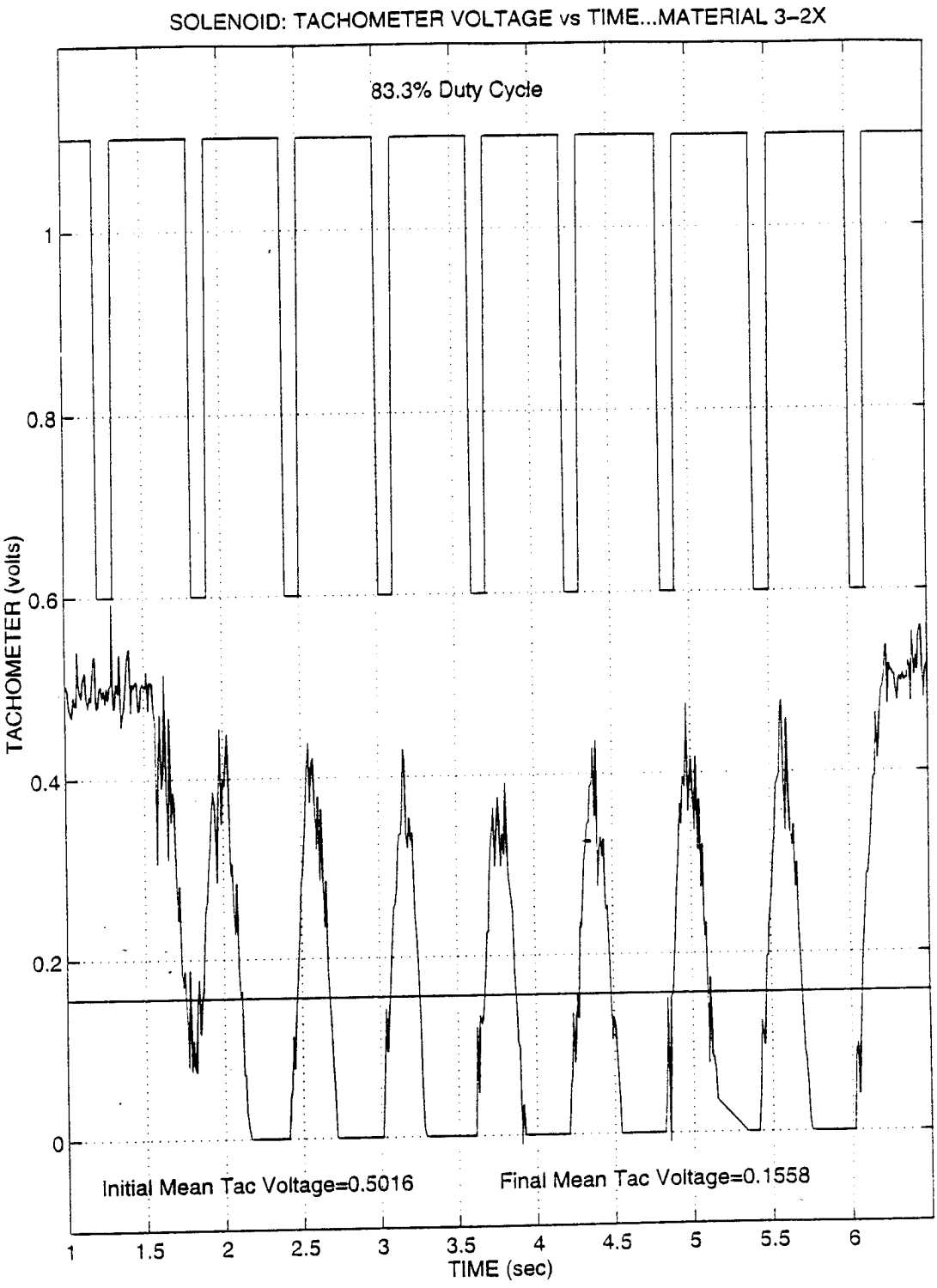

Figure 68: Material 3-2X - Tachometer Voltage Differential for Solenoid Activation Duty Cycle of 83.3 Percent

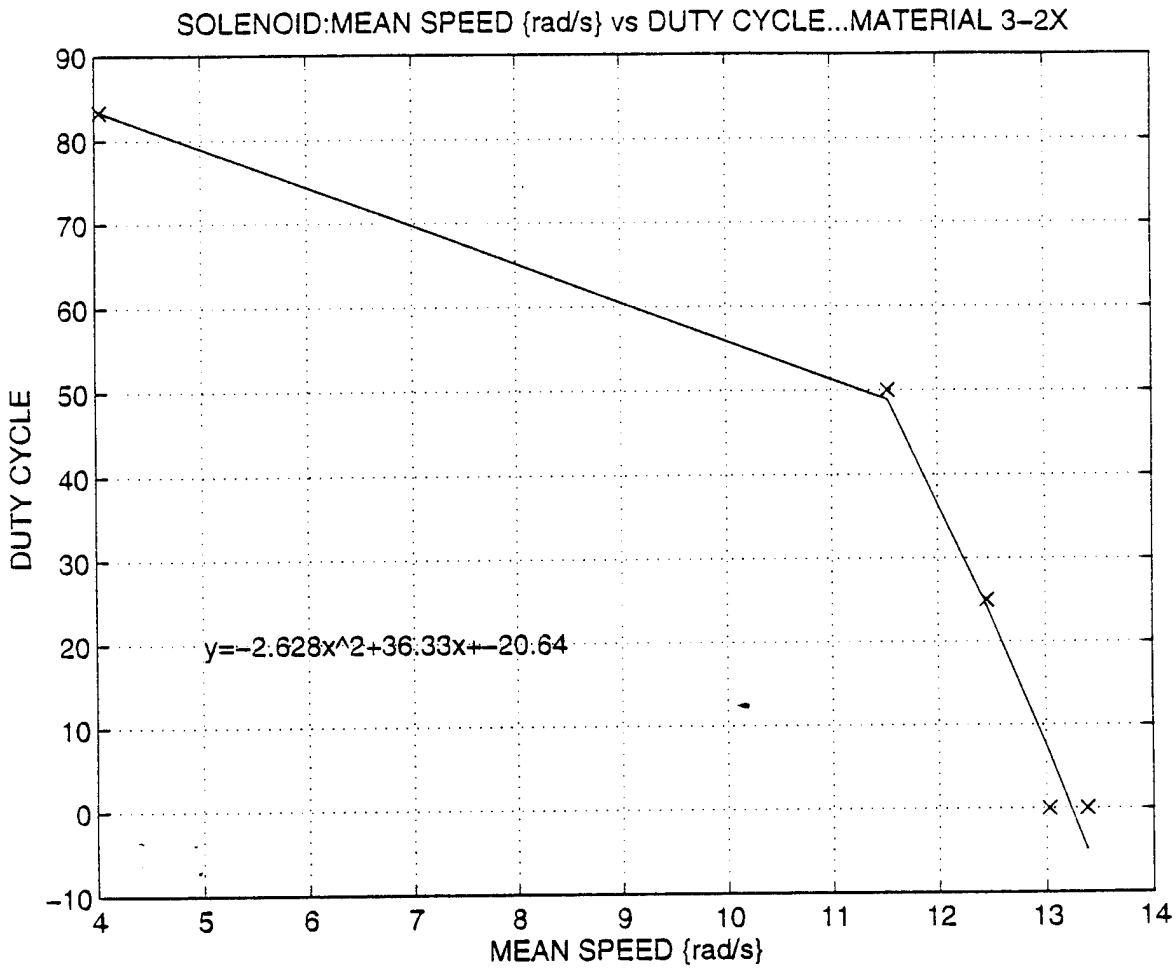

Figure 69: Material 3-2X - Mean Rotational Speed versus Duty Cycle

V. DISCUSSION

In analyzing the results of the solenoid and servomotor experimental tests it was found that the band brake activation system possesses the ability to control the rotational speed of the test apparatus, and could be implemented on the Master Control Apparatus as a viable means of bilateral force feedback. In making a recommendation as to which system fulfills the goals of low cost, efficiency, ease of implementation, and consistent positive control, each configuration has certain advantages and disadvantages.

The servomotor was very effective in controlling the speed of the test apparatus, with the added ability to stop rotation if necessary. Additionally because the servomotor arm quickly rotates to its designated position, the response was immediate, producing a steady speed differential that is detectable in less than one second as illustrated in Figures 41, 42, 46, 47, 51 and 52. However, the servomotor's ability to accurately and consistently dampen the movement of a Master Control Unit appendage depends greatly on a constant material coefficient of friction (COF). A material with a high COF can gain a positive, near linear control over the entire range of speed reductions, as illustrated with Material 2 (highest COF the of materials tested) in Figure 48. Although the servomotor can be ordered to rotate until the disk stops, the servomotor setup must be sensitive over all degrees of arm rotation, with ability to transmit even a slight dampening effect back to the operator. Materials 1 and 3 with a lower COF do not exhibit such control at smaller arm rotation (see Figures 43 and 50), as they rely on their

material stiffness to slow the disk only after greater servomotor arm rotation. A major disadvantage of the servomotor setup is that because the servomotor is more dependent on the band brake material's COF, over time, with wear and adverse working conditions, the performance of the servomotor activation system would vary.

The solenoid experimental tests showed that this setup was effective in controlling the rotational speed of the test apparatus. By varying the duty cycle of the pulse width modulated (PWM) signal, the solenoid activated band brake transmitted an overall damping effect on disk rotation that would effectively simulate an obstruction to slave movement like a spring or movement through water. This is shown in Figure 57, 61, 65, and 69 where it is obvious that the solenoid apparatus, for all materials, maintains tight control in small speed reductions. However the solenoid system does have difficulty in producing large speed reductions while operating within it's frequency range (1-12 Hz), in the "on/off" mode inherent to the solenoid. Thus, in conditions where stopping the disk (or particular joint) is necessary, i.e., if the slave has encountered a solid, immovable object, the solenoid must maintain an "on" posture with the plunger fully submerged in the cylinder. Due to the limited force of the solenoid, this could prove difficult, especially as the solenoid system is further miniaturized for implementation to the various joints of the Master Control Apparatus. As a possible solution to the stopping criteria, experimental runs were conducted utilizing Material 3, twice wrapped. As illustrated in Figures 66 through 69, this configuration did add sufficient resistance to

adequately dampen and/or stop the disk movement, however control over a range of speed differentials became difficult to achieve due to binding of the band brake material upon activation. Further turns would surely add to the resistance and stopping ability of the brake mechanism, but would cause increased binding problems. Additionally, because the solenoid plunger is only held in the cylinder by the electromagnetic field, each solenoid must be adapted with a mechanism that would prevent removal of the plunger from the cylinder, and complete failure of the feedback system for that particular joint. A further disadvantage of the solenoid system is that the damping effect is only felt after the solenoid proceeds through three or four "on/off" cycles. This makes the response somewhat sluggish and could cause the operator to constantly lag behind the actual movements available to the slave. The solenoid configuration does produce a damping effect that is less dependent on the COF of the material as shown by the similar distribution of data evident in Figures 57, 61, 65, and 69. This characteristic would produce more consistent results over extended period of operation, even with considerable wear on the band brake.

VI. CONCLUSIONS AND RECOMMENDATIONS

A. CONCLUSIONS

- Both the servomotor and solenoid are cost effective, with no appreciable price difference between the two.
- Solenoids are linear devices, largely homogeneous by nature, whereas there are a wide variety of servomotors available for procurement.
- Because of the variety of servomotors available, the servomotor system will be flexible in adapting to the various joints of the Master Control Apparatus (MCA). Solenoids have limited diversity that hampers their ability to effectively integrate into all MCA appendages.
- The servomotor activation apparatus could prove to be the optimal configuration provided the system utilized a band brake material with a constant coefficient of friction, that is resistant to wear and work environment, and has considerable strength and inelastisity.
- The solenoid activation could be optimal by utilizing a miniature solenoid with a maximum operating frequency of approximately 30 Hz, and a maximum force that could stop the rotation of the disk/joint. Although not as essential to proper operation, using a band brake material with considerable strength and inelastisity would be prudent.

B. RECOMMENDATIONS

Additional research and experimentation will be necessary to ensure that the system can be adapted to every joint, the most difficult joints being the upper and lower arm rotation devices and the end effectors (see Figure 9). Since the rotation controls revolve around a circular aluminum support on ball bearings, the band brake should adequately adapt to this subsystem. However, implementation on the end effectors will require absolute feedback control if the goal is life-like simulation of the hand movements and the sensitivity necessary to pick up objects.

Furthermore, because Green Man has the circuitry in place for audio and video transmission, the system could be further augmented for visual and audio feedback. Although largely untested, the torso, head, and neck movements of the slave unit promise to give the Green Man slave and teleoperator an outstanding view of any work environment should the slave head mount be outfitted with a camera.

A final area of further research and study would be updating and streamlining the Servo Electronics Circuit Card rack with a state of the art computer system that might allow operator interface in choosing various circuit configurations or for example, different amplifier gains. This could prove to be an excellent tool for control systems study.

Although much of the Green Man system may be outdated by today's industry standards, a great deal can be learned from understanding the operational capabilities and limitations of this anthropomorphic robot.

APPENDIX A. GREEN MAN POTENTIOMETERS

Single Turn Potentiometer

POT	MANUFACTURER	RESISTANCE	PART NUMBER	TOTAL
1	**NEI***	**5K**	**50BFA502**	**2**
2	**NEI**	**5K**	**F78BA502**	**3**
3	**NEI**	**5K**	**78ESA502**	**1**
4	**NEI**	**10K**	**50SFA103**	**5**
5	**NEI**	**10K**	**8221-50SFA103**	**2**
6	**NEI**	**10K**	**F78CA103**	**8**
7	**BOUNRE**	**10K**	**2051414120-.44/1274**	**2**

* indicates the New England Instrument Company

Helical Potentiometer

PART	MANUFACTURER	RESISTANCE	PART NUMBER	TOTAL
1	**BOURNE**	**20K**	**7223**	**1**
2	**BOURNE**	**5K**	**3551S-1-502**	**1**
3	**BOURNE**	**5K**	**3571S-1-501**	**2**
4	**BECKMAN INSTR Co**	**20K**	**65375-1-103**	**1**

Linear Potentiometer

PART	MANUFACTURER	RESISTANCE	PART NUMBER	TOTAL
1	**BOURNE**	**20K**	**2051414120-.44/1274**	**1**

APPENDIX B. FLOW CONTROL SERVO VALVES

CONTROL AREA	MANUFACTURER	PART INFO	TOTAL
TORSO	Parker Hannifin Corp Ogden Utah	PN:FC72-215C 1000PSI/12MA	3
SHOULDER	Parker Hannifin Corp Ogden Utah	PN:FC215B 1000PSI/8MA	6
LEFT & RIGHT BANKS	MOOG	PN:030A35010E022H4 MOD:305020	13
CENTER BANK	Dynamic Valve Inc. Palo Alto, CA 94303	Model:5 Serial #:5050 1000PSI/12MA	3

APPENDIX C. HYDRAULIC ACTUATORS

ACTUATOR	MANUFACTURER	PART INFO	TOTAL
ROTATION: LOWER ARM	Ex-Cell-O Corp Micro Precision Ops	ROTAC S-125-1V	2
SHOULDER PITCH	Automated Remotely Manned Systems(ARMS) MBAssociates San Ramon, CA 94583	PN:FC215B 1000PSI/8MA	2
TORSO	Compact Air Products Inc Westminster, SC 29693 (803)647-9521		4

APPENDIX D. MATLAB PROGRAMS FOR THEORETICAL MODEL

May 30 1995 08:46:32 — soltheo.m — Page 1

```
% JIM CHATFIELD
% THESIS
%
% EXPERIMENT TO CONTROL MOTOR SPEED BY PULSE
% WIDTH MODULATED BAND BRAKE USING A SOLENOID
%
% BRAKE "OFF"==> Jw(dot)+Cw=Q
% BRAKE "ON"==>  Jw(dot)+Cw=Q+r(T1-T2)....where T1/T2=exp(uk*B)
%
J=.076;                 % kgm^2         Motor inertia
c=0.54;                 % Nms           System Damping
g=9.81;                 % m/s^2         gravity
msol=.0657;             % kg            mass solenoid plunger
Kv=.624;                % V/r/s         Tacometer constant
Va=10.02;               % Volts         Motor voltage
ra=6;                   % Ohms          Motor resistance

Tenoff=msol*g;          % N             Tension w/sol off (weight of plunger)
Tenon=22.24;            % N             Tension w/sol on...max pull=80oz-->N
Q1=Kv*Va/ra             % Nm            Torque of motor
Qw=Kv^2/ra              % Nm
uk=.4;                  % kin coeff of friction SHOE LACE
r=.0254;                % m             pulley radius

brakeoff=(Q1+Tenoff*r*(exp(-uk*pi)-1))/J;       % combined effects of motor torque &
 brake off
brakeon=(Q1+Tenon*r*(exp(-uk*pi)-1))/J;         % combined effects of motor torque &
 brake on

B=(c+Qw)/J              % w(dot)+Bw=brake/J


ton=.1;                 % time pulse width "on"
toff=.2;                % time pulse width "off"
dc=ton/(ton+toff);      % duty cycle



%
ttotal=21;              % total time of experiment
n=ttotal/(ton+toff);    % number of cycles
t=zeros(1,2*n+1);
w=zeros(1,2*n+1);
%
t(1)=0;                 % initial time
w(1)=4;                 % rad/s         initial speed
%
for p=1:n

   w(2*p)=(w(2*p-1)-brakeoff/B).*exp(-B*toff)+brakeoff/B;     % "w" for brake off
   t(2*p)=t(2*p-1)+toff;

        if w(2*p)<0, w(2*p)=0;
        end

   w(2*p+1)=(w(2*p+1-1)-brakeon/(B*J)).*exp(-B*ton)+brakeon/B;    % "w" for brake on
   t(2*p+1)=t(2*p+1-1)+ton;

        if w(2*p+1)<0, w(2*p+1)=0;
        end

end

% ----mean speed calcs ------
[m,n]=size(w);
wm=ones(size(w));

sswm=w(:,3:n);
meen=mean(sswm);
wm=meen*wm;

plot(t,w,t,w,'+',t,wm),grid,title('THEORETICAL...SOLENOID'),xlabel('TIME (sec)'),...
ylabel('SPEED (rad/s)'),axis([0,21,-.50,7])
```

Program 1: Theoretical Model for Solenoid Activation

```
% JIM CHATFIELD
% THESIS---SERVO
%
% EXPERIMENT TO CONTROL MOTOR SPEED BY PULSE
% WIDTH MODULATED BAND BRAKE USING A SERVOMOTOR
%
% SERVO "ON"==>  Jw(dot)+Cw=Q+r(T1-T2)....where T1/T2=exp(uk*B)
%
uk=.25;                 % kin coeff of friction STEEL/LEATHER band

J=0.076                 % kgm^2         Motor inertia
c=0.540;                % Nms           System Damping

Kv=0.624;               % V/r/s         Tacometer constant
Va=10.02;               % Volts         Motor voltage
ra=6;                   % Ohms          Motor resistance

Tension=4;              % N             Tension w/servo at a position 20 degrees

Q1=Kv*Va/ra             % Nm            Torque of motor
Qw=Kv^2/ra              % Nm

r=.0254;                % m             pulley radius

servo=(Q1+Tension*r*(exp(-uk*pi)-1))/J; % combined effects of motor torque & brake o
ff

X=(c+Qw)/J              % w(dot)+Bw=brake/J

%
time=20;                % total time of experiment
step=.2;                % data every two seconds
n=time/.2;              % # data points

t=zeros(1,n);
w=zeros(1,n);
%
t(1)=0;                 % initial time
w(1)=4;                 % rad/s initial speed
%
x=0;

for p=0:.2:20

   x=x+1;

   w(x+1)=(w(x)-servo/X).*exp(-X*step)+servo/X;      % W w/servo on
   t(x+1)=t(x)+step;

end

% ----mean speed calcs ------
[m,n]=size(w);
wm=ones(size(w));

sswm=w(:,6:n);
meen=mean(sswm);
wm=meen*wm;

plot(t,w,t,w,'+'),grid,title('THEORETICAL...SERVOMOTOR WITH LEATHER BAND'),xlabel('T
IME (sec)'),...
ylabel('SPEED (rad/sec)'),%axis([0,20,0,4.5])
text(4,3.5,'Servo position...70 deg'),text(4,3,['Coefficent of Friction= ',num2str(u
k)]),...
text(4,2.5,['Mean Speed (rad/s)= ',num2str(meen)])

print -dps2 thesis5.ps
```

Program 2: Theoretical Model for Servomotor Activation

APPENDIX E. BAND BRAKE TENSION VALUES FOR SERVOMOTOR

In order to properly evaluate the tension(T_1) associated with each servomotor position for each band brake material, tests were conducted by substituting a spring of known constant k=50.5kg/s^2) into the test apparatus for the fixed anchor point (refer to Figure 24). By starting at position 0 degrees where the tension in the band was zero (Δx of the spring =0) and rotating the servomotor to four positions (20, 45, 75, 90 degrees) while observing the deflection of a spring required to bring the band back to it's anchor point, the tension was determined for each servomotor position using the simple relationship:

$$T_1 = k\Delta x \tag{1}$$

These values were plotted on a graph of Tension (Nm) versus Servo Position (degrees), with a linear least squares fitted line through the data providing any value any tension corresponding to a servomotor position for any of the three band materials. The tension values for each material are formulated below in 10 degree increments.

POSITION (deg)	MATERIAL 1 TENSION (Nm)	MATERIAL 2 TENSION (Nm)	MATERIAL 3 TENSION (Nm)
0	0	0	0
10	0.20	0.25	0.73
20	0.75	0.95	1.35
30	1.35	1.65	2.00
40	2.10	2.30	2.70
50	2.70	2.95	3.33
60	3.33	3.60	4.00
70	3.95	4.25	4.65
80	4.55	4.95	5.40
90	5.20	5.60	6.00

Table 1: Band Brake Tensions for Servomotor Positions

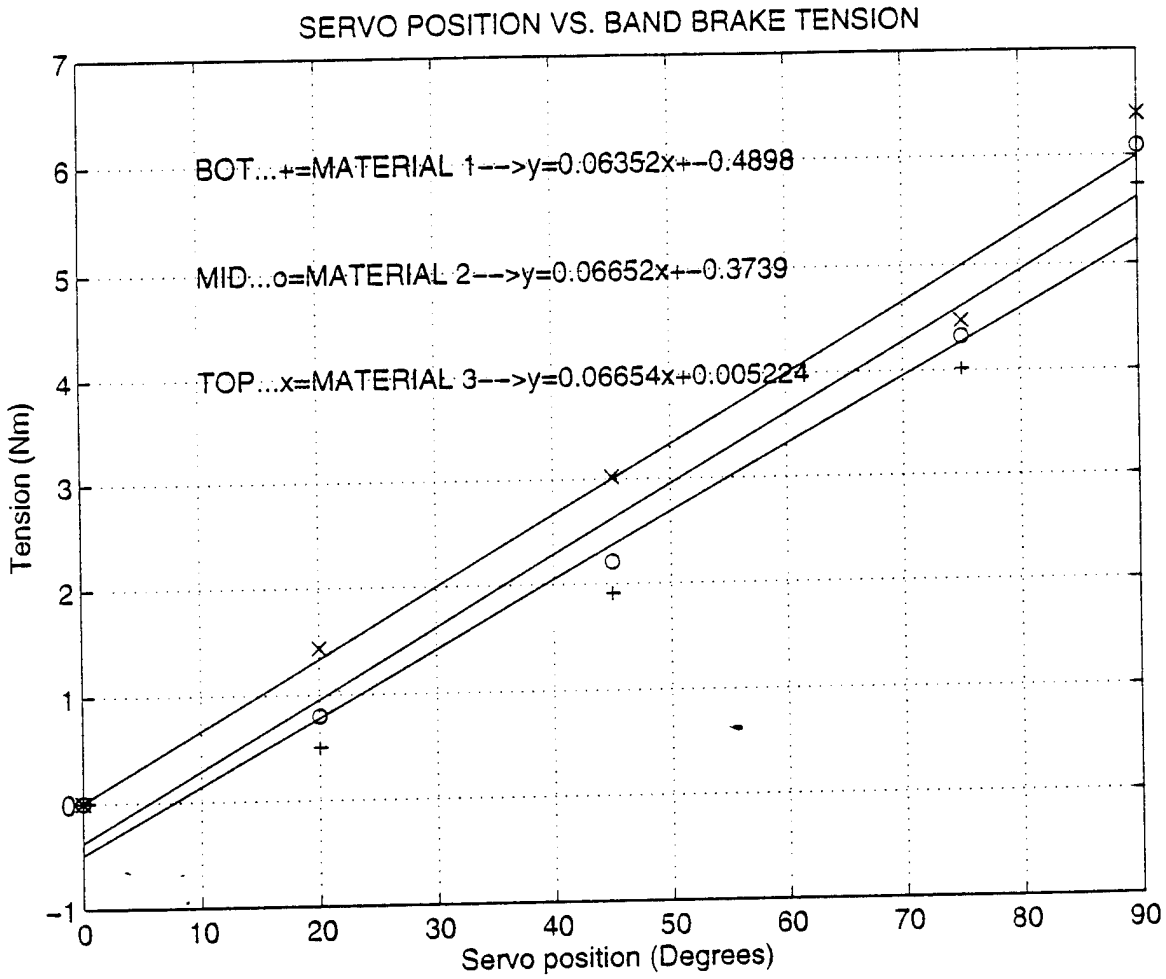

Figure1: Graph of Tension versus Servomotor Arm Position

APPENDIX F. SOLENOID INFORMATION

from Allied Electronics Pub

16F6815

GUARDIAN ELECTRIC — AC and DC Sol

T and TP Series Tubular Solenoids

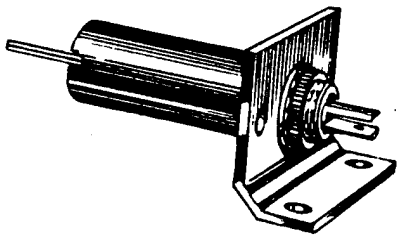

Tubular solenoids are available in either pull (T series) or push (TP series). TP series dimensions are identical to T series. Notched assembly of shell and bushing permits tightening of mounting nut without damaging coil. **Insulation Material:** Class "A" (110°C). **Termination:** 6" leads. Mounting hardware included. T and TP series recognized under the Component Program of Underwriters' Laboratories, Inc.

T3.5x9: L—1 1/8"; D—7/16"; Mounting thread size—5/16-32 UNEF; Bracket W—1 1/8". **T4x7:** L—7/8"; D—1/2"; Mounting thread size—3/8-32 UNEF; Bracket W—1 1/8". **T4x12:** L—1 1/2"; D 1/2"; Mounting thread size—3/8-32 UNEF; Bracket W—1 1/8". **T4x16:** L—2"; D—1/2"; Mounting thread size—3/8-32 UNEF; Bracket W—1 1/8". **T6x12:** L—1 1/2"; D—3/4"; Mounting thread size—5/32-32 UNEF; Bracket W—1 3/8". **T8x9:** L—1 1/8"; D—1"; Mounting thread size—3/4-24 UNS; Bracket W—2". **T8x16:** L—2"; D—1"; Mounting thread size—3/4-24 UNS; Bracket W—2". **T12x13:** L—1 3/8"; D—1 1/2"; Mounting thread size—1-27 UNS; Bracket W—2 1/2". **T12x19:** L—2 3/8"; D—1 1/2"; Mounting thread size—1-27 UNS; Bracket W—2 1/2".

Stock No.	Mfr.'s Type	Duty	Coil Voltage	Ohms	Watts	Typical Lifts and Strokes		EACH	
						Minimum	Maximum	1-24	25-48
802-1151	T3.5x9*	Inter.	24DC	57.0	10.0	8.5 oz. at 1/32"	1 oz. at 1/2"	9.85	9.14
802-1152	T3.5x9*	Cont.	24DC	260.0	2.0	5.5 oz. at 1/32"	.75 oz. at 1/16"	9.85	9.14
802-1153	T3.5x9*	Inter.	12DC	14.0	10.0	8.5 oz. at 1/32"	1 oz. at 1/2"	9.85	9.14
802-1154	T3.5x9*	Cont.	12DC	80.0	2.0	5.5 oz. at 1/32"	.75 oz. at 5/16"	9.85	9.14
802-1155	TP3.5x9	Inter.	24DC	57.0	10.0	6.8 oz. at 1/32"	.96 oz. at 1/2"	14.61	13.57
802-1156	T4x7*	Inter.	24DC	80.0	7.0	12 oz. at 1/32"	6 oz. at 1/4"	10.83	9.51
802-1190	T4x7*	Cont.	24DC	240.0	2.4	6 oz. at 1/32"	1 oz. at 3/16"	10.83	9.51
802-1157	TP4x7	Cont.	24DC	240.0	2.4	4.8 oz. at 1/32"	.8 oz. at 3/16"	17.25	16.01
802-1158	T4x12*	Inter.	24DC	38.0	15.0	14 oz. at 1/32"	1.5 oz. at 1/8"	10.83	9.51
802-1159	T4x12*	Cont.	24DC	160.0	3.5	7 oz. at 1/32"	1.5 oz. at 1/4"	10.98	10.13
802-1160	TP4x12	Inter.	24DC	38.0	15.0	12 oz. at 1/32"	1.2 oz. at 1/8"	14.59	13.54
802-1161	TP4x12	Cont.	24DC	160.0	3.5	6 oz. at 1/32"	1.2 oz. at 1/4"	14.59	13.54
802-1162	T4x16*	Inter.	24DC	24.0	20.0	7 oz. at 1/32"	4 oz. at 1"	11.68	10.84
802-1163	T4x16*	Inter.	12DC	6.0	20.0	7 oz. at 1/32"	4 oz. at 1"	11.68	10.84
802-1191	T4x16*	Cont.	12DC	36.0	4.0	6.5 oz. at 1/32"	1.5 oz. at 1/8"	11.68	10.84
802-1192	TP4x16*	Inter.	24DC	24.0	20.0	5.6 oz. at 1/32"	3.2 oz. at 1"	13.16	12.21
802-1164	TP4x16	Cont.	24DC	145.0	4.0	5.2 oz. at 1/32"	1.2 oz. at 1/8"	13.16	12.21
802-1165	T6x12*	Inter.	24DC	25.0	22.0	30 oz. at 1/16"	4 oz. at 1/16"	11.84	10.26
802-1166	T6x12*	Cont.	24DC	165.0	3.5	12 oz. at 1/16"	1 oz. at 3/16"	11.84	10.26
802-1167	T6x12*	Inter.	12DC	6.5	22.0	30 oz. at 1/16"	4 oz. at 1/16"	11.84	10.26
802-0585	T6x12*	Cont.	12DC	41.0	3.5	12 oz. at 1/16"	1 oz. at 3/16"	11.84	10.26
802-1193	TP6x12*	Inter.	24DC	25.0	22.0	24 oz. at 1/16"	3.2 oz. at 3/16"	12.93	12.01
802-1194	TP6x12*	Cont.	24DC	165.0	3.5	9.6 oz. at 1/16"	.8 oz. at 3/16"	12.93	12.01
802-1168	T8x9*	Inter.	24DC	145.0	4.0	23 oz. at 1/16"	3 oz. at 1/16"	11.24	10.43
802-1195	TP8x9	Inter.	24DC	44.0	14.0	42 oz. at 1/16"	4.8 oz. at 1/16"	15.23	14.14
802-1169	TP8x9	Cont.	24DC	145.0	4.0	18.4 oz. at 1/16"	2.4 oz. at 1/16"	15.23	14.14
802-1170	T8x16*	Inter.	24DC	15.0	38.0	80 oz. at 1/16"	14 oz. at 1/8"	10.48	9.88
802-0574	T8x16*	Cont.	24DC	105.0	5.5	35 oz. at 5/16"	5.5 oz. at 1/8"	10.48	9.88
802-1171	T8x16*	Inter.	12DC	2.7	38.0	80 oz. at 1/16"	14 oz. at 1/8"	10.48	9.88
802-0573	T8x16*	Cont.	12DC	26.0	5.5	35 oz. at 1/16"	5.5 oz. at 1/8"	10.48	9.88
802-1172	T12x13*	Inter.	24DC	14.0	40.0	150 oz. at 1/8"	14 oz. at 3/16"	19.66	18.26
802-1173	T12x13*	Cont.	24DC	85.0	6.6	50 oz. at 1/8"	4 oz. at 3/16"	19.66	18.26
802-1178	TP12x13	Inter.	24DC	14.0	40.0	120 oz. at 1/8"	11.2 oz. at 3/16"	19.57	18.26
802-1179	TP12x13	Cont.	24DC	85.0	7.0	40 oz. at 1/8"	3.2 oz. at 3/16"	19.57	18.26
802-1174	T12x19*	Inter.	24DC	9.5	60.0	150 oz. at 1/8"	12 oz. at 1 1/2"	18.38	17.07
802-1175	T12x19*	Cont.	24DC	59.0	10.0	80 oz. at 1/8"	5 oz. at 1 1/2"	18.38	17.07
802-1176	TP12x19	Inter.	24DC	9.5	60.0	120 oz. at 1/8"	9.6 oz. at 1 1/2"	20.40	18.94
802-1177	TP12x19	Cont.	24DC	59.0	10.0	64 oz. at 1/8"	4 oz. at 1 1/2"	20.40	18.94

*U.L. Model.

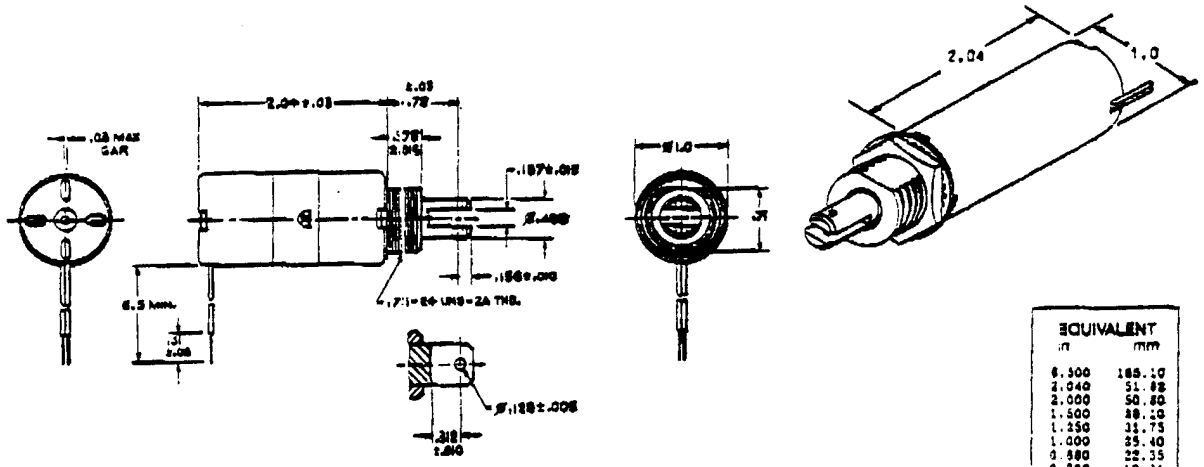

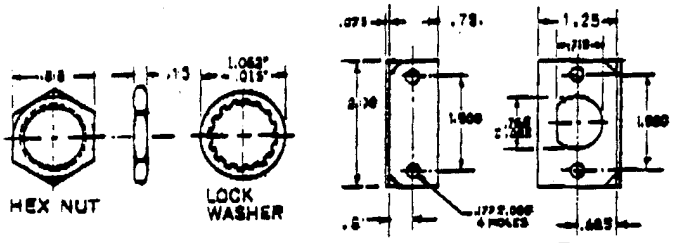

EQUIVALENT in	mm
6.500	165.10
2.040	51.82
2.000	50.80
1.500	38.10
1.250	31.75
1.000	25.40
0.880	22.35
0.750	19.81
0.765	19.43
0.750	19.05
0.718	18.24
0.710	18.03
0.688	18.48
0.500	12.70
0.438	11.13
0.375	9.53
0.312	7.92
0.310	7.87
0.187	4.75
0.177	4.50
0.158	3.96
0.130	3.30
0.125	3.25
0.075	1.91
0.060	1.52
0.030	0.76
0.015	0.38
0.010	0.25
0.005	0.13

DATA AND SPECIFICATIONS

VOLTAGE	TYPICAL COILS CONTINUOUS 5.5 Watts			INTERMITTENT 16 Watts		
	COIL No	OHMS	MI	COIL No	OHMS	MI
6 DC	13	7.5	806	6	2.34	1446
12 DC	19	28.2	814	14	9.3	1434
24 DC	25	110	818	20	38.1	1432
120 AC 60	38	2358	788	33	808	1402

TYPICAL OPERATE TIME 62 Deg Plunger Cone Angle	N I (Ampere Turns) 500	1000	1500
P U L L I N (Maximum)	120 ms	55 ms	40 ms
D R O P O U T (Maximum)	65 ms	70 ms	75 ms

Position = Plunger Down
Stroke = .200 in (5.1 mm)
Load = 3.5 oz (71 gms)

POWER INPUT RANGE:
Minimum ..... 1.1 Watts
Maximum ..... (Continuous Duty) .. 5.5 Watts
1 Sec on.... (Pulse Duty) ..... 110 Watts
10 Sec on ... (10% Duty Cycle) ... 40 Watts
100 Sec on ... (25% Duty Cycle) ... 16 Watts

U/L RECOGNITION:
Recognized under the Component Recognition Program of Underwriters Laboratories Inc.

MAJOR DIMENSIONS:

Length	2	in	(51 mm)
Body Diameter.....	1	in	(25.4 mm)
Height		in	(mm)
Plunger Diameter	.437	in	(11.1 mm)
Maximum Stroke	1	in	(25.4 mm)

Available in push type action. See page 8.

DIELECTRIC WITHSTAND: ..... 1500 Volts 60 Hz.

COIL LEADS:
Standard 22 ga. 6.5 in (165 mm) PVC insulation
Also available ... Other size wire and insulation or leads with terminals.

INSULATING MATERIALS: (Class "105" Standard)
Coil Bobbin ..... Polyester
Coil Cover (Standard) ..... Polyester Tape
Also available ....Special Hi-Temp Materials

WEIGHT:
Plunger ..... 1.57 oz (44.5 gms)
Total ..... 5.8 oz (164 gms)

PLUNGER CONE ANGLE:
Standard ..... 62 Degrees
Also available ..... Flat, 92 Deg. Custom

LIST OF REFERENCES

1. Sheridan, Thomas B., *Teletobotics, Automation, and Human Supervisory Control*, The MIT Press, 1992.

2. Green Man Operational Pamphlet

3. Shigley, J. E. and Mitchell, L. D., *Mechanical Engineering Design*, McGraw-Hill Book Company, 1983.

4. Gieck, Kurt and Gieck, Reiner, *Engineering Formulas, 6th Edition*, McGraw-Hill Inc., 1990

5. Kraus, A. D., "Course Notes for EC2270," Naval Postgraduate School, Monterey, California, Fall 1994

INITIAL DISTRIBUTION LIST

1.	Defense Technical Information Center Cameron Station Alexandria, VA 22304-6145	2
2.	Dudley Knox Library, Code 052 Naval Postgraduate School Monterey, CA 93943-5101	2
3.	Department Chairman, Code ME Department of Mechanical Engineering Naval Postgraduate School Monterey, CA 93943-5002	1
4.	Professor Morris Driels, Code ME/DR Department of Mechanical Engineering Naval Postgraduate School Monterey, CA 93943-5000	3
5.	Naval Engineering Curricular Office (Code 34) Naval Postgraduate School Monterey, CA 93943-5002	1
6.	Director, Training and Education MCCDC, Code C46 1019 Elliot Rd Quantico, Virginia 22134-5027	1
7.	Kathryn A. Chatfield 104 Woodbridge Dr Pittsburgh, PA 15237	1
8.	James A. Chatfield 104 Carriage Dr Pittsburgh, PA 15229	1
9.	LT James A. Chatfield II 504 1/2 Van Buren Str Monterey, CA 93940	1